How to scale clearance from adults to children for drugs undergoing hepatic metabolism? Insights from advanced PBPK modelling and simulation

Calvier, E.A.M.

Chapter 5

Drugs being eliminated via the same pathway will not always require similar pediatric dose adjustments

Elisa A. M. Calvier, Elke H. J. Krekels, Huixin Yu, Pyry A. J. Välitalo, Trevor N. Johnson, Amin Rostami-Hodjegan, Dick Tibboel, Piet H. van der Graaf, Meindert Danhof, Catherijne A. J. Knibbe

CPT Pharmacometrics Syst Pharmacol (2018) 7: 175

Abstract

For scaling drug plasma clearance (CLp) from adults to children, extrapolations of population pharmacokinetic covariate models between drugs sharing an elimination pathway have enabled accelerated development of pediatric models and dosing recommendations. This study aims at identifying conditions for which this approach consistently leads to accurate pathway-specific CLp scaling from adults to children for drugs undergoing hepatic metabolism. A physiologically-based pharmacokinetic simulation workflow utilizing mechanistic equations defining hepatic metabolism was developed. We found that drugs eliminated via the same pathway require similar pediatric dose adjustments only in specific cases, depending on drugs extraction ratio (ER), fraction unbound, type of binding plasma protein and the fraction metabolized by the isoenzyme pathway for which CLp is scaled. Overall, between-drug extrapolation of pediatric covariate functions for CLp is mostly applicable to low and intermediate ER drugs eliminated by one isoenzyme and binding to human serum albumin, in children older than 1 month.

Study Highlights

What is the current knowledge on the topic?

Proofs of concept for extrapolation of pediatric covariate functions for plasma clearance (CLp) between drugs sharing the same elimination pathway have been published for a limited number of drugs eliminated through glucuronidation and renal excretion.

What question did the study address?

The study identifies the conditions upon which between-drug extrapolation of isoenzyme specific pediatric covariate functions consistently leads to accurate CLp scaling from adults to pediatric ages, for drugs metabolized by one or multiple hepatic isoenzymes.

What this study adds to our knowledge?

Between-drug extrapolation of pediatric covariate functions for CLp is mostly applicable to low and intermediate extraction ratio drugs eliminated by one isoenzyme and binding to human serum albumin in children older than 1 month.

How might this change drug discovery?

We now have a tool available that can establish *a priori* whether two drugs metabolized by the same isoenzyme will require the same or different dose adjustments in pediatrics.

5.1 Introduction

Accurate scaling of plasma clearance (CLp) of drugs from adults to the pediatric population is crucial for the definition of first-in-child doses and for the development of pediatric dose recommendations [1–4]. As illustrated in Figure 1, for drugs undergoing hepatic metabolism, CLp values are driven by the complex interplay between drug-specific and system-specific properties. Relevant parameters to describe hepatic clearance are hepatic blood flow (Qh), the unbound drug fraction in plasma (fu), the blood to plasma ratio (B:P), and the intrinsic metabolic clearance in the liver based on unbound drug concentration (CLint) [5]. Qh is a purely system-specific parameter, whereas unbound fraction, B:P and CLint are derived from both system-specific and drug-specific parameters. Moreover, in children, system-specific parameters vary with age due to ontogenic processes, which in turn drive CLp changes across the pediatric age range (Figure 1) [6]. Because physiologically-based pharmacokinetic (PBPK) modeling integrates all the above-mentioned information [6,7], it can provide a yard-stick for scaling drug CLp from adults to various pediatric ages in the absence of pediatric clinical data [6,8–11], which is relevant for first-in-child dose definition. In addition to PBPK modeling, there is a need for model-based scaling methods that aggregate the influence of ontogeny of the system-specific parameters in a smaller set of equations, thereby facilitating scaling of pediatric CLp in drug development and clinical practice.

In pediatric population pharmacokinetic (popPK) models, the net influence of ontogeny of system-specific parameters on CLp of a drug is described using empirical covariate models derived from clinical data (i.e., concentration-time profiles). Although these covariate models can be directly used as the basis for pediatric dose adjustments [12–14], this approach requires clinical data obtained upon the administration of every single drug of interest in every pediatric sub-population.

Semimechanistic or semiphysiological popPK pediatric scaling approaches have been proposed to bridge the gap between PBPK and popPK methodologies, allowing for accelerated development of pediatric popPK models and subsequent dosing recommendations. One of these approaches relies on extrapolations of popPK covariate models between drugs that share an elimination pathway [15–19]. Because popPK covariate models are the basis of dose recommendations, this approach would also allow for extrapolation of pediatric dosing recommendation from a drug of which the changes in clearance have been quantified to other drugs for which no pediatric pharmacokinetic (PK) studies have been undertaken, provided

these drugs share the same elimination pathway. To date, proofs of concept for this method have been published for a limited number of drugs eliminated through glucuronidation or renal excretion [15–19]. However, as illustrated in Figure 2, with this method, between drug differences in CLp of drugs sharing the same elimination pathway are solely accounted for by the absolute value of the scaled CLp (e.g., adult CLp values), whereas CLp ontogeny is assumed to be purely system-specific and, therefore, drug-independent. This assumption is challenged by the fact that CLp of drugs with different properties might be impacted differently by the various ontogenic changes in system-specific parameters (Figure 1).

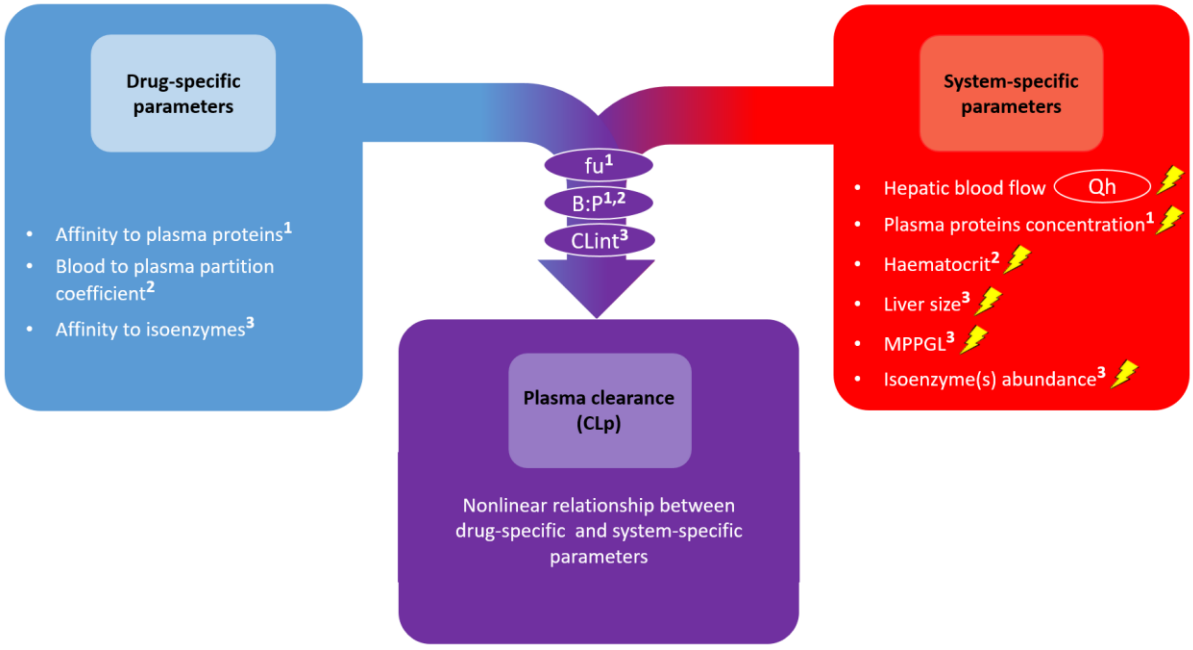

Figure 1 *Schematic representation of the complex interplay between drug-specific and system-specific parameters driving hepatic CLp values. Parameters within circles are directly used in the PBPK hepatic clearance model (e.g., dispersion model). Parameters in the purple circles represent composite parameters that are derived from the system-specific parameters and the drug-specific parameters indicated by the numbers in the superscripts. In children each of the system-specific parameters change with age, each represented by a lightning bolt. MPPGL stands for microsomal protein per gram of liver, fu stands for the unbound drug fraction in plasma, CLint stands for the intrinsic metabolic clearance in the liver based on unbound drug concentrations and B:P stands for the blood to plasma ratio.*

Therefore, the aim of the current study is to identify the conditions for which between-drug extrapolation of pediatric covariate functions for hepatic metabolic CLp consistently leads to accurate pathway-specific CLp scaling from adults to children of various ages (absolute prediction error ≤ 30%). We developed a PBPK-based simulation workflow utilizing mechanistic equations defining hepatic metabolism to systematically screen a wide parameter

space for both system-specific and drug-specific variables impacting hepatic CLp by one specific isoenzyme. Additionally, we investigated the impact of multiple elimination pathways on the between-drug extrapolation potential of pediatric covariate functions for hepatic metabolic CLp. This allowed us to define a decision tree to identify the conditions leading to consistently accurate pediatric CLp scaling using between-drug extrapolations of pathway-specific pediatric covariate models.

5.2 Methods

5.2.1 Model drug and test drug

Total (i.e., bound and unbound) hepatic metabolic plasma clearance will be referred to as CLp in this paper. We investigate the extrapolation potential of pediatric covariate functions scaling CLp from adults to pediatric patients between a model drug and a test drug both exclusively eliminated by the same hepatic isoenzyme. This method is illustrated in Figure 2. The impact of elimination by multiple isoenzymes is investigated as described under the section "Multiple elimination pathways".

- Model drug and determination of the pediatric covariate function: A pediatric covariate function is developed to describe the ontogeny of CLp of what will be referred to as the model drug (M).
- Test drug and between-drug extrapolation of the pediatric covariate function: The pediatric covariate function developed based on the model drug (M) is used to scale CLp for what will be referred to as the test drug (T) from adult to various pediatric ages.

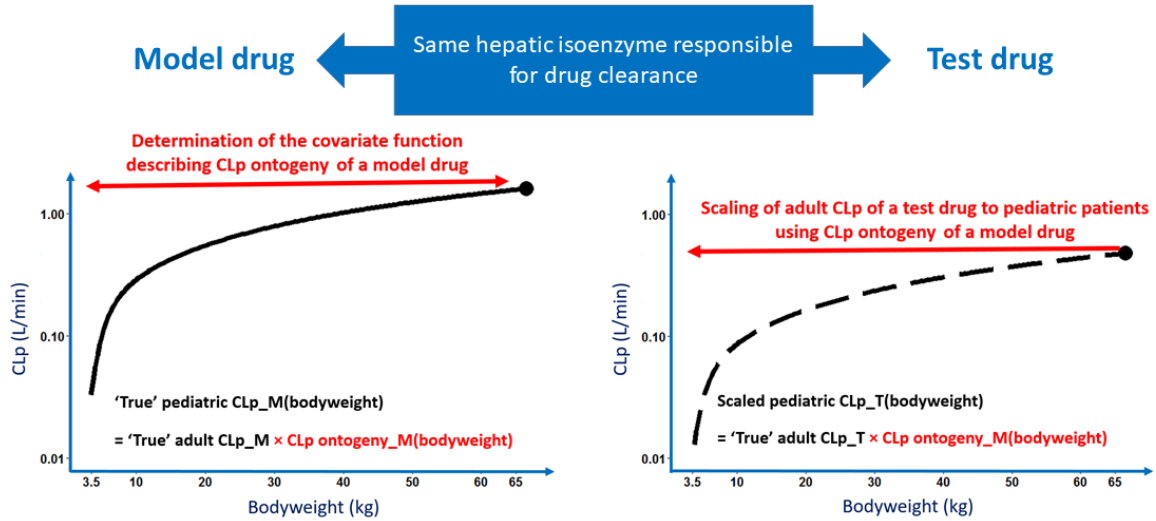

Figure 2 *Illustration of between-drug extrapolation of pediatric covariate functions to scale hepatic plasma clearance (CLp) from adults to pediatric patients for drugs eliminated by the same isoenzyme. The black dot in both graphs shows the adult hepatic CLp value for the model drug ('True' adult CLp_M) and the test drug ('True' adult CLp_T). The solid black line represents the change in CLp of the model drug throughout the pediatric age range, which is described by a pediatric covariate function based, in this example, on bodyweight (CLp ontogeny_M(bodyweight)). The dashed black line represents the scaled pediatric CLp predicted for the test drug by between-drug extrapolation of the pediatric covariate function obtained for the model drug (CLp ontogeny_M(bodyweight)).*

5.2.2 PBPK-based simulation workflow

A four steps PBPK-based simulation workflow (Figure 3) was developed in R software [20] version 3.3.1 with R studio interface version 0.99.902 following a similar approach, as previously published [21]. This workflow investigates the impact of two main variables on the accuracy of pediatric CLp predictions based on extrapolation of pediatric covariate functions from a model drug to a test drug. These variables are the drug-specific parameters of both the model drug and test drug and the ontogeny of the system-specific parameters (Figure 1). This investigation was undertaken for 15 different elimination pathways. These elimination pathways correspond to elimination by the following isoenzymes: CYP1A2, CYP2A6, CYP2B6, CYP2C8, CYP2C9, CYP2C18_19, CYP2D6, CYP2E1, CYP3A4, UGT1A1, UGT1A4, UGT1A6, UGT1A9, UGT2B7 and SULT1A1. Ultimately, conditions for which extrapolations consistently led to accurate CLp predictions were identified.

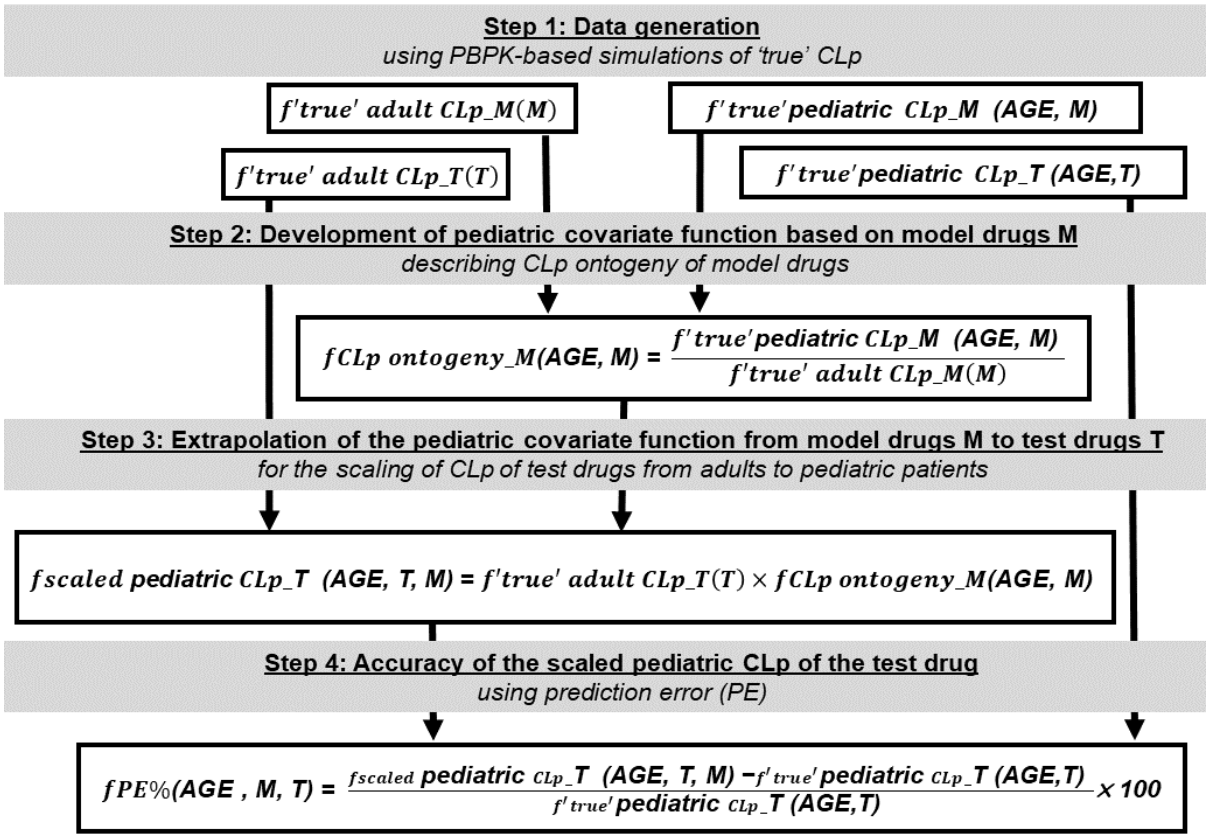

Figure 3 *PBPK-based simulation workflow used to investigate the between-drug extrapolation potential of pediatric covariate models when scaling total plasma clearance (CLp) from adults to pediatric patients. The model drug is denoted with M and the test drug with T. AGE stands for pediatric postnatal age. All steps are performed for model drugs and test drugs binding to the same plasma proteins and eliminated by the same isoenzyme and repeated for each of the 15 isoenzymes and each of the 2 binding plasma proteins investigated.*

5.2.3 Variables in the PBPK-based simulation workflow

For a systematic investigation of the impact of each variable, we chose a factorial design (i.e., a global sensitivity analysis approach) with a wide yet realistic parameter space for each individual variable. For this purpose, continuous variables were transformed into categorical variables using a number of intermediate values within the defined parameter space allowing for the generation of single point estimates of the different functions of the PBPK-based simulation workflow. To enable the computation across a wide parameter space and interpretability of the results, variability and uncertainty in both demographics and model parameters were not accounted for.

5.2.3.1 Ontogeny of system-specific parameters

To unravel the impact of ontogeny of the system-specific parameters (see Figure 1) on the extrapolation potential of pediatric covariate functions between drugs sharing the same elimination pathway, simulations were performed for 8 typical individuals for whom demographic characteristics and system-specific parameters are specified in Table 1. The PBPK model parameters for typical individuals were computed as average values of men and women. Ontogeny functions for each system-specific model parameter were taken from the Simcyp® software (Simcyp Ltd, Sheffield, UK) V15.R1 library, except for the isoenzyme ontogeny of SULT1A1. For SULT1A1 maturity was taken to have been reached at birth [22], and, therefore, isoenzyme ontogeny of SULT1A1, defined as the pediatric to adult ratio of microsomal intrinsic clearance, was set to 1. More information can be found in Supplementary Material 1.

5.2.3.2 Drug-specific properties of the model drugs and test drugs

To unravel the impact of drug-specific properties on the between-drug extrapolation potential of pediatric covariate functions, a total of 7,560 hypothetical drugs with unique combinations of drug-specific properties were generated and used as model drugs, as well as test drugs. This set of hypothetical drugs was generated using all possible combinations of different values of the following three drug-specific properties: adult unbound fraction in plasma (range: 0.01-1, n=10), blood-to-plasma partition coefficient or Kp (range: 0.35-40, n=9), and adult total unbound intrinsic clearance value of one microgram of liver microsomes or adult $CL_{int,mic,total}$ (range: $0.56 \cdot 10^{-6}$ - $0.209 \cdot 10^{-3}$ L. $min^{-1}.mg^{-1}$ microsomal protein, n=42). The hypothetical drugs were assumed to be exclusively bound to either human serum albumin (HSA) or alpha-1 acid glycoprotein (AAG). More details can be found in Supplementary Material 1.

Table 1 *Demographic characteristics of the 8 typical individuals implemented in the PBPK-based simulation workflow and their corresponding system-specific parameters values*

Demographic values								
Age	1 day	1 month	6 months	1 year	2 years	5 years	15 years	25 years
Bodyweight, kg	3.45	4.30	7.55	9.90	12.35	18.25	54.25	72.65
Height, cm	49.75	54.25	66.00	74.75	86.00	108.25	166.00	172.30
BSA, m^2	0.22	0.26	0.38	0.46	0.55	0.74	1.60	1.86
System-specific parameters								
Qh, L/h	6.55	7.83	12.95	17.65	24.65	41.14	89.75	87.92
HSA, g/L	35.78	39.94	42.07	42.90	43.73	44.82	44.68	43.94
AAG, g/L	0.2678	0.5497	0.6774	0.7172	0.7512	0.7877	0.6711	0.6847
Hematocrit, %	51.93	38.14	35.11	35.78	36.79	38.29	40.01	40.74
Liver size, g	133	159	249	313	385	544	1351	1614
MPPGL	25.53	25.60	25.99	26.45	27.36	29.97	36.80	39.79
IO CYP1A2, %	24	35	118	150	164	161	126	100
IO CYP2A6, %	2.10^{-9}	0.48	99	100	100	100	100	100
IO CYP2B6, %	15	19	34	47	62	83	99	100
IO CYP2C8, %	38	86	97	99	99	100	100	100
IO CYP2C9, %	40	74	87	90	92	100	100	100
IO CYP2C18-19, %	30	33	84	95	97	98	100	100
IO CYP2D6, %	6	47	84	91	95	98	100	100
IO CYP2E1, %	10	37	59	67	74	82	88	100
IO CYP3A4, %	11	13	48	78	96	104	106	100
IO UGT1A1, %	0.2	23	98	104	100	100	100	100
IO UGT1A4, %	74	74	74	75	77	81	97	100
IO UGT1A6, %	15	30	63	76	87	95	100	100
IO UGT1A9, %	9	12	34	52	71	90	100	100
IO UGT2B7, %	8	9	11	13	18	32	79	100
IO SULT1A1, %	100	100	100	100	100	100	100	100

AAG, alpha-1 acid glycoprotein; BSA, body surface area; HSA, human serum albumin; MPPGL, milligram microsomal protein per gram of liver; IO, isoenzyme ontogeny expressed as percentage of adult microsomal intrinsic clearance; Qh, hepatic blood flow.

5.2.4 Steps of the PBPK-based simulation workflow

Between-drug extrapolation of covariate models was studied for model and test drugs sharing the same elimination pathway and binding to the same plasma protein. For each of the 15 elimination pathways investigated and each type of binding plasma protein, the following steps were undertaken as also illustrated in Figure 3.

5.2.4.1 Step 1: Data generation

Using the dispersion model (Equations 1 to 6), PBPK-based simulations of 'true' CLp were performed for all hypothetical model drugs M and test drugs T in adults ('true' adult CLp_M and 'true' adult CLp_T respectively) as well as in each investigated pediatric age ('true' pediatric CLp_M and 'true' pediatric CLp_T respectively).

$$\mathrm{CLp} = \mathrm{CL_B} \times \mathrm{B{:}P} \quad (1)$$

$$\mathrm{CL_B} = \mathrm{Qh} \times \mathrm{ER} \quad (2)$$

$$\mathrm{ER} = 1 - \mathrm{F_H} \quad (3)$$

$$\mathrm{F_H} = \frac{4a}{(1+a)^2 \exp\{(a-1)/2D_N\} - (1-a)^2 \exp\{-(a+1)/2D_N\}} \quad (4)$$

$$a = (1 + 4R_N \times D_N)^{1/2} \quad (5)$$

$$R_N = (\mathrm{fu/B{:}P}) \times \mathrm{CLint/Qh} \quad (6)$$

In these equations, CLp is the overall total (i.e., bound and unbound) hepatic plasma clearance, CL_B is the total whole blood clearance, B:P is the blood to plasma ratio, Qh is the hepatic blood flow, ER is the hepatic extraction ratio, fu is the unbound drug fraction in plasma, CLint is the total hepatic intrinsic clearance, R_N is the efficiency number and D_N is the axial dispersion number. For the axial dispersion number (D_N) a value of 0.17 was used [23]. See Supplementary Material 1 for more details.

5.2.4.2 Step 2: Development of pediatric covariate function based on model drugs M

The pediatric covariate function (*f* CLp ontogeny_M) describes the ontogenic changes in 'true' CLp from adults to pediatric patients and is derived from the model drug M. For each model drug M and investigated pediatric postnatal age (AGE), single point estimates of *f* CLp ontogeny_M were computed (see equation in Figure 3).

5.2.4.3 Step 3: Extrapolation of the pediatric covariate function from model drugs M to test drugs T

Analogous to Figure 2, scaled pediatric CLp of the test drugs (*f* scaled pediatric CLp_T) was computed by scaling the 'true' adult CLp of each test drug T ('true' adult CLp_T) to each pediatric age. This scaling was performed by extrapolating the pediatric covariate function (*f* CLp ontogeny_M) from all model drugs to each test drug, following the equation in Figure 3. This led, for each pediatric age and test drug, to as many scaled pediatric CLps as the number of model drugs.

5.2.4.4 Step 4: Accuracy of the scaled pediatric CLp of the test drug

The prediction errors (PEs) of scaled pediatric CLps obtained in step 3 was calculated by comparing, for each test drug and each age, the scaled pediatric CLps with the 'true' CLp value obtained in step 1. This led, for each pediatric age and test drug, to as many PEs as the number of model drugs. Predictions were considered to be accurate when the absolute prediction error was 30% or lower.

5.2.5 Conditions leading to accurate CLp predictions

First, for the diversity of investigated ages and isoenzymes, trends in prediction errors (PEs) with all drug properties of the model and the test drug were separately assessed. These drug properties were the type of binding plasma protein, Kp, and fraction unbound in plasma, B:P, CLint, and ER in adults, as well as the difference in the latter parameters between the model drug and test drug.

In order to define scenarios consistently leading to accurate CLp scaling from adults to the different pediatric ages using between-drug extrapolation of pediatric covariate functions, drug properties allowing to best discriminate between accurate and inaccurate scaled pediatric CLp were identified by a hierarchical tree analysis (see Supplementary Material 1) [24].

All model-test drug combinations were grouped into scenarios based on the most discriminative drug properties. Within each of these scenarios, multiple model-test drug combinations are included and for all combinations, both model and test drug are eliminated

by the same isoenzyme and binding to the same plasma protein. Overall accuracy of the test drug CLp predictions for each model-test drug scenario was summarized per pediatric age group as follow:

- Model-test drug scenario systematically leading to accurate CLp scaling of the test drug: all CLp predictions within the defined scenario are accurate (absolute PE ≤ 30%).
- Model-test drug scenario not systematically leading to accurate CLp scaling of the test drug: at least one of the CLp predictions within the defined scenario is inaccurate (absolute PE > 30%).

5.2.6 Multiple elimination pathways

Because many drugs are metabolized by multiple isoenzymes, we also evaluated the situation in which the model drug and/or the test drug are metabolized by two isoenzymes, namely I_A and I_{NA}. I_A is the isoenzyme representing the elimination pathway accounted for by the covariate function, whereas I_{NA} is the isoenzyme representing the elimination pathway not accounted for by the covariate function. In order to include model drugs and/or test drugs undergoing metabolism through multiple hepatic isoenzymes, adaptations of the PBPK-based simulation workflow earlier described were performed. Details on these alterations can be found in Supplementary Material 1.

5.3 Results

5.3.1 Results for scenarios in which model and test drugs are metabolized by one isoenzyme

Visual inspection of the PEs revealed trends with age, type of metabolizing isoenzyme, the type of binding plasma protein and extraction ratio in adults of the model drug and test drug. Figure 4 displays these trends in PEs for all hypothetical drugs that are exclusively metabolized by one isoenzyme and that are either exclusively binding to HSA (Figure 4A) or to AAG (Figure 4B). Results are categorized by age and by adult extraction ratio category of the model and test drug, with increasing absolute PE values indicating increasing between-drug differences in CLp ontogeny, with CLp standing for total (i.e., bound and unbound) hepatic metabolic plasma clearance. For each age, results are reported for the lowest,

intermediate and highest isoenzyme ontogeny values of the 15 isoenzymes included in the analysis.

Figure 4 shows similar trends in PEs between drugs binding to HSA and drugs binding to AAG, except in neonates of 1 day of age. However, for AAG bound drugs, the ranges in PE were either similar or higher than PE ranges for HSA bound drugs. For both HSA and AAG bound drugs, the range of absolute PE values tend to decrease with increasing age. Decreased isoenzyme ontogeny value tends to increase the range of the absolute PEs, with the highest absolute PEs being > 1000% in neonates of one day (for isoenzyme ontogeny ≈ 0%) and the highest absolute PE value in adolescents being only about 70% (for isoenzyme ontogeny = 79%).

Generally, within each age category and isoenzyme ontogeny category, the median PE can be seen to be closest to 0 when extrapolating pediatric covariate models between drugs of the same extraction ratio category, although even for these drugs the range in PE values shows a number of scenarios in which absolute PE values are higher than 30%. The absolute median PE was the highest when model and test drugs belonged to extreme extraction ratio categories. Except for drugs binding to AAG in neonates of one day, extrapolating pediatric covariate functions to a test drug of a lower extraction ratio category than the model drug systematically yields a positive median PE, indicating a bias towards overprediction of CLp of the test drug. The reverse trend is observed when extrapolating pediatric covariate functions to a test drug of a higher extraction ratio category than the model drug. These trends increase as the isoenzyme ontogeny decreases to values below 100%.

Overall, the hierarchical tree analysis revealed that the most discriminating drug properties for identifying systematically accurate CLp predictions across the pediatric age range were the extraction ratio of the test drug and/or the model drug, and the difference in extraction ratio and in unbound fraction in plasma between model drug and test drug, (extraction ratio and fu defined in adults, see Supplementary Material 1). The additional influence of the difference in fraction unbound between the model drug and test drug on the PEs was not observed upon visual inspection of the trends in PEs, likely because trends in PE with fu are smaller than trends with extraction ratio and they depend on the extraction ratio of the model drug and test drug. As the extrapolations to the test drug require the use of a pediatric covariate model that is defined for the model drug, scenarios leading to accurate between-drug extrapolations were defined using the extraction ratio of the model drug.

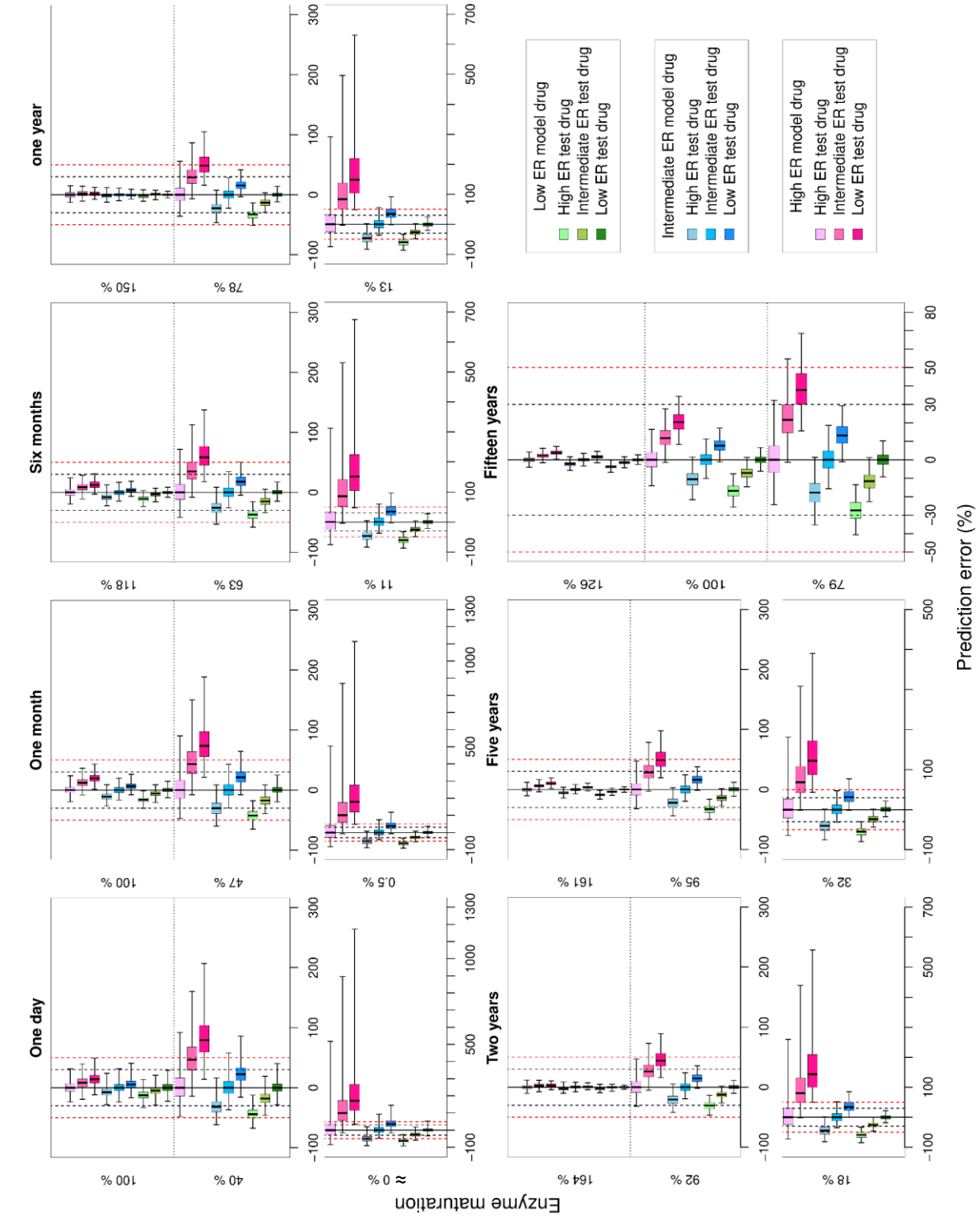
4A
Enzyme maturation
Prediction error (%)
One day
One month
Six months
one year
Two years
Five years
Fifteen years
≈ 0 %
0.5 %
11 %
13 %
18 %
32 %
79 %
40 %
47 %
63 %
78 %
92 %
95 %
100 %
100 %
118 %
150 %
164 %
161 %
126 %
Low ER model drug
High ER test drug
Intermediate ER test drug
Low ER test drug
Intermediate ER model drug
High ER test drug
Intermediate ER test drug
Low ER test drug
High ER model drug
High ER test drug
Intermediate ER test drug
Low ER test drug

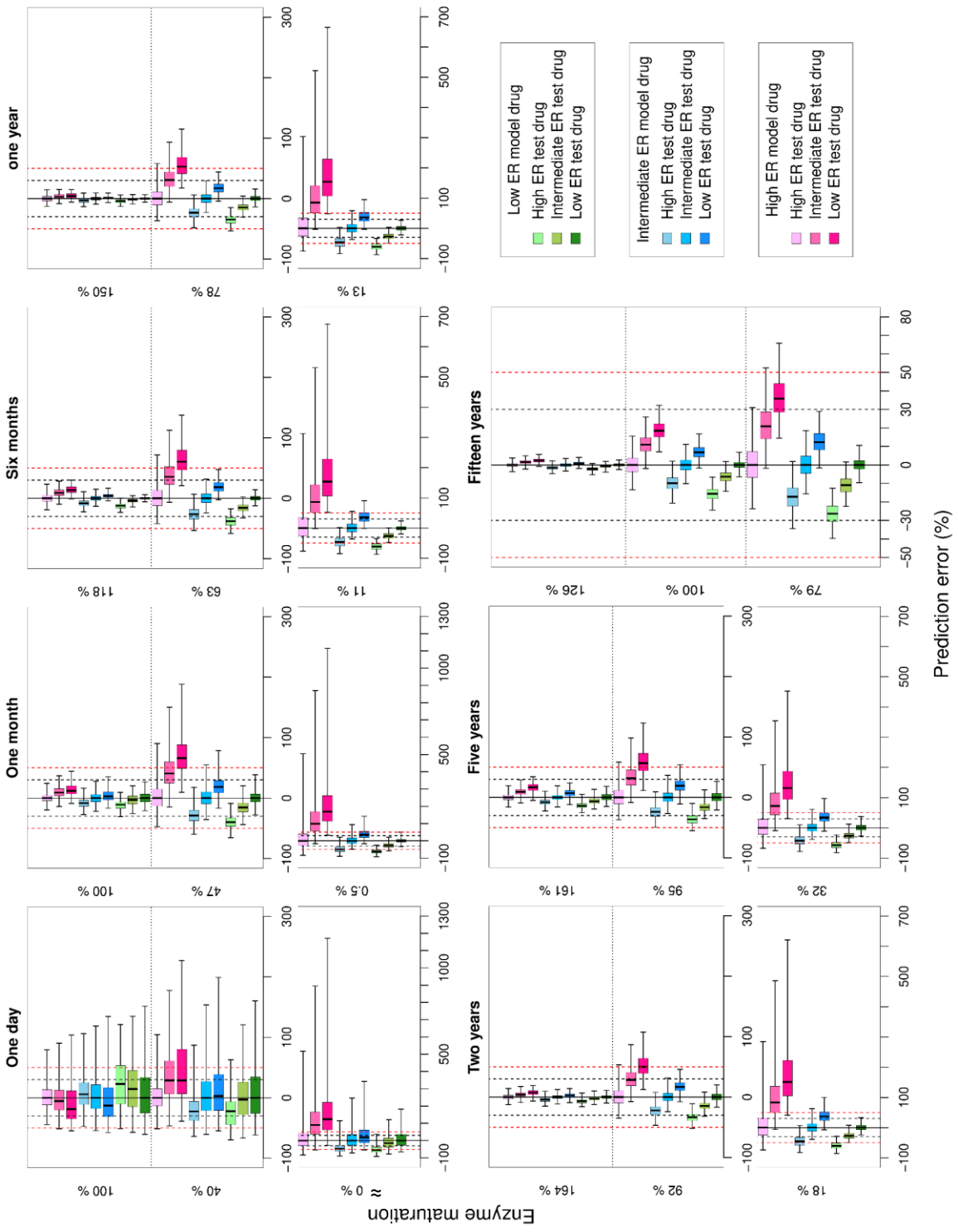
4B
Enzyme maturation
≈ 0 %
40 %
100 %
0.5 %
47 %
100 %
11 %
63 %
118 %
13 %
78 %
150 %
18 %
32 %
79 %
92 %
95 %
100 %
164 %
161 %
126 %
One day
One month
Six months
one year
Two years
Five years
Fifteen years
Low ER model drug
High ER test drug
Intermediate ER test drug
Low ER test drug
Intermediate ER model drug
High ER test drug
Intermediate ER test drug
Low ER test drug
High ER model drug
High ER test drug
Intermediate ER test drug
Low ER test drug
Prediction error (%)

Figure 4 *The prediction error (PE) of the total (bound and unbound) drug plasma clearance (CLp) predictions for scenarios in which model and test drugs are exclusively metabolized by one isoenzyme (fmA_adult = 100%) and exclusively binding to human serum albumin (Figure 4A) or to alpha-1 acid glycoprotein (Figure 4B). The boxplots represent the minimum, 1st quartile, median, 3rd quartile, and maximum PE and are categorized by low (green), intermediate (blue), and high (pink) adult extraction ratio (ER) of the model drug and low (light color), intermediate (intermediate color), and high (dark color) adult ER of the test drug. For each age, the lowest, intermediate, and highest isoenzyme ontogeny values (percentage of adult $CL_{int,mic}$) reported for the 15 isoenzymes are shown. The intermediate isoenzyme ontogeny was defined as the isoenzyme ontogeny value the closest to the mean of the lowest and highest isoenzyme ontogeny values for a specific age. Low, intermediate, and high ER correspond to $ER \leq 30\%$, $30\% < ER \leq 70\%$ and $ER > 70\%$ respectively. The vertical solid black line indicates a PE of 0. The dotted black and dotted red lines indicate PE intervals of ±30% and ±50% respectively. Note that the x-axes are different for different ages.*

These most discriminative drug properties (i.e., extraction ratio of the model drug, and the difference in extraction ratio and in fraction unbound between model drug and test drug) were used to define model-test drug scenarios systematically leading to accurate CLp predictions in different age ranges, as displayed in the first row of Figure 5A, 5B and of the figures in Supplemental Material 2 and 3. The first row in Figure 5 presents the results for drugs that are exclusively metabolized by CYP3A4 and that bind to HSA (Figure 5A) or AAG (Figure 5B), while Supplementary Material 2 and 3 show the results for substrates of all investigated isoenzymes binding to HSA and AAG respectively. Although the results differ between the different isoenzymes and plasma proteins, they do reveal similar trends.

The between-drug extrapolation potential of pathway-specific pediatric covariate functions generally decreases with decreasing age, with patterns in model-test drug scenarios systematically leading to accurately scaled pediatric CLp being highly dependent on both ontogeny of the system-specific parameters and drug properties. For all ages, the between-drug extrapolation potential increases with decreasing ER values of the model drug, with this effect being most pronounced in younger children (see Supplementary Material 2 and 3). Moreover, the extrapolation potential increases when the difference in ER between model and test drugs decreases. Regarding plasma protein binding, it can be seen that between-drug extrapolation of pathway-specific pediatric covariate functions generally yields more accurately scaled pediatric CLp for drugs binding to HSA compared to drugs binding to AAG. Additionally, the difference in plasma protein binding between model and test drugs was found to mostly impact the method applicability in infants of one month or younger.

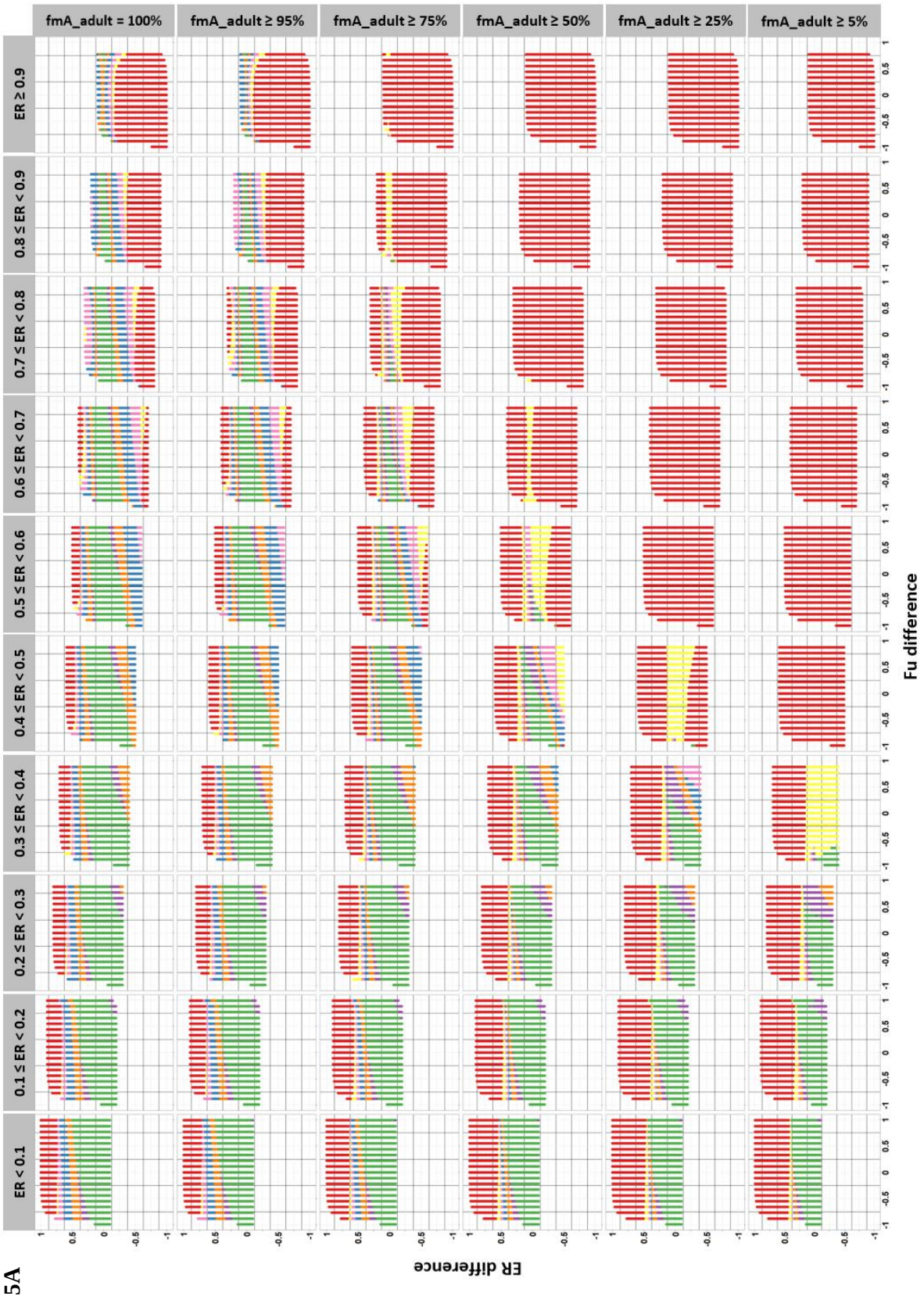
fmA_adult = 100%
fmA_adult ≥ 95%
fmA_adult ≥ 75%
fmA_adult ≥ 50%
fmA_adult ≥ 25%
fmA_adult ≥ 5%
ER ≥ 0.9
0.8 ≤ ER < 0.9
0.7 ≤ ER < 0.8
0.6 ≤ ER < 0.7
0.5 ≤ ER < 0.6
0.4 ≤ ER < 0.5
0.3 ≤ ER < 0.4
0.2 ≤ ER < 0.3
0.1 ≤ ER < 0.2
ER < 0.1
ER difference
Fu difference

5A

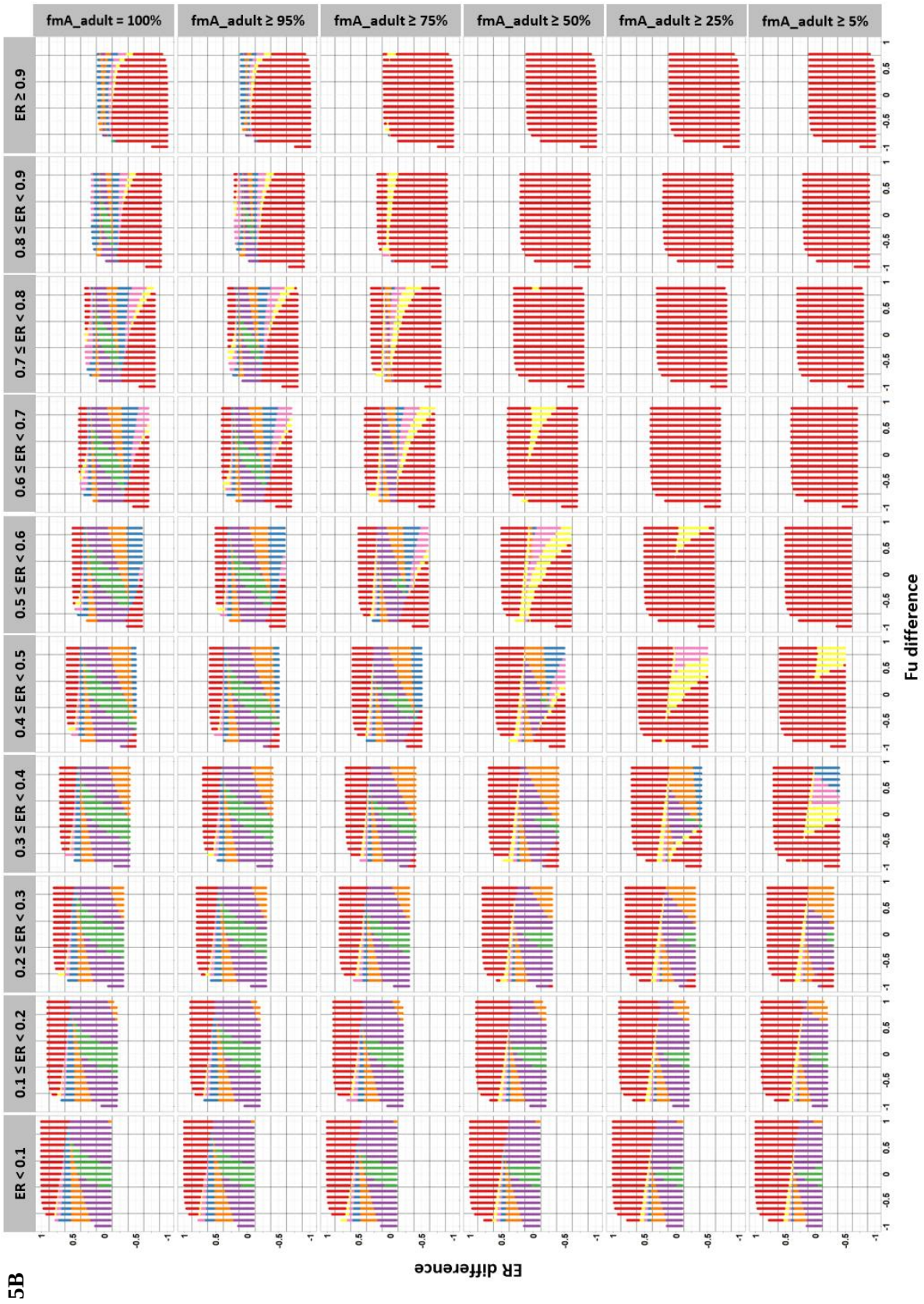
fmA_adult = 100%
fmA_adult ≥ 95%
fmA_adult ≥ 75%
fmA_adult ≥ 50%
fmA_adult ≥ 25%
fmA_adult ≥ 5%
ER ≥ 0.9
0.8 ≤ ER < 0.9
0.7 ≤ ER < 0.8
0.6 ≤ ER < 0.7
0.5 ≤ ER < 0.6
0.4 ≤ ER < 0.5
0.3 ≤ ER < 0.4
0.2 ≤ ER < 0.3
0.1 ≤ ER < 0.2
ER < 0.1
ER difference
Fu difference

5B

Figure 5 *Illustration of model-test drug scenarios that lead to accurate pathway-specific CLp predictions for a test drug after between-drug extrapolation of a pathway-specific pediatric covariate function. Results are presented for drugs that are metabolized by CYP3A4 and that bind to human serum albumin (Figure 5A) or alpha-1 acid glycoprotein (Figure 5B). Each column corresponds to a range of extraction ratio (ER) values for the model drug in adults and each row to a specific range of fraction of drug (model and test drug) that is metabolized by CYP3A4 in adults. For each graph, the y-axis represents the difference in ER between the test drug and the model drug (ER test drug – ER model drug) in adults, and the x-axis represents the difference in fraction unbound (fu) between the test drugs and the model drug in adults (fu test drug – fu model drug). Each dot represents a model-test drug scenario, including multiple model-test drug combinations. A color code is used to indicate systematically accurate CLp predictions for all model-test drug combinations within a model-test drug scenario, for children ≥ 5 years (yellow), ≥ 2 years (pink), ≥ 1 year (blue), ≥ 6 months (orange), ≥ 1 month (purple), and ≥ 1 day term neonates (green). Red dots indicate model-test drug scenarios leading to inaccurate predictions in children older than 5 years for at least one model-test drug combination within the model-test drug scenario. As an example, systematically accurate CLp scaling in children of 6 months and older is represented by the combination of the green, purple and orange dots.*

5.3.2 Results for model drugs and/or test drugs metabolized by several isoenzymes

When the model drug and/or the test drug are metabolized by two isoenzymes, PE increases or decreases, as compared to drugs eliminated by one isoenzyme, depending on the ontogeny of the isoenzyme representing the elimination pathway not accounted for by the covariate model (I_{NA}), and the fmA_adult values of the test drug and model drug. For the specific case in which the isoenzyme representing the elimination pathway accounted for by the covariate model (I_A) and I_{NA} have similar ontogeny, the PEs are similar to the PE for drugs exclusively metabolized by one isoenzyme I_A.

For model drugs and/or test drugs metabolized by several isoenzymes, the most discriminating drug properties to identify systematically accurate CLp predictions were the same as those found when both model and test drugs are metabolized by one unique isoenzyme. However, the larger the contribution of alternative metabolic pathways to the overall CLp in adults, the lower the extrapolation potential of the pathway-specific covariate function will be, as can be seen in the bottom rows of Figure 5 and Supplementary Material 2 and 3.

5.4 Discussion

In this work, for the first time we systematically investigated the applicability of between-drug extrapolation of pathway-specific pediatric covariate functions for CLp of drugs undergoing hepatic metabolism in which CLp stands for total (i.e., bound and unbound) hepatic metabolic plasma clearance. Our results show that pediatric changes in CLp of drugs that are eliminated by the same hepatic elimination pathway will not always follow similar patterns and therefore, in specific cases, these drugs will require a different pediatric PK-based dose adjustment.

CLp ontogeny of a specific elimination pathway was found to mainly depend on the following drug properties: the type of binding plasma protein, the adult fu and ER of the drugs and – in case of multiple elimination pathways - the number and type of isoenzymes responsible for the drug metabolism. This finding disproves the often implicitly made assumption that the ontogeny of CLp is drug-independent [25,26]. Additionally, it highlights the importance of ontogeny processes other than isoenzyme ontogeny alone on CLp scaling from adults to children for drugs undergoing hepatic metabolism (Figure 1). Therefore, the identified drug properties should be taken into account when extrapolating pathway-specific pediatric covariate functions between drugs. Figure 5 and Supplementary Material 2 and 3 were developed to guide the selection of scenarios that will systematically lead to accurate between-drug extrapolation of pediatric covariate functions. These guides can also be interpreted as defining scenarios for which between-drug extrapolation of pediatric covariate functions will approximate PBPK-based predictions with an accepted error of ± 30%. In these scenarios the use of this semi-mechanistic scaling method can be encouraged to expedite pediatric CLp scaling and the development of dosing recommendations.

To illustrate the use of these guides, we can take the example of midazolam (ER = 0.44 [27], fu = 0.022 [28] with binding to HSA [9], fm_A ≈ 93% [28,29]), sildenafil (ER = 0.45 [30], fu ≈ 0.04 with binding to HSA [31], fm_A = 79% [31]), and simvastatin (ER = 0.97 [32], fu = 0.02 [33] with binding to HSA [34], fm_A = 92% [29]), all mainly metabolized by CYP3A4. Based on the results for CYP3A4, we can anticipate that the popPK covariate model describing CYP3A4-mediated clearance ontogeny from adults to neonates of 1 day of midazolam, could be extrapolated to sildenafil, because ER model = 0.44, fu difference = 0.018, ER difference = 0.01, fm_A ≥ 75% corresponds to a green area in Figure 5A. The same plot also shows that this extrapolation from midazolam to simvastatin cannot be performed,

because ER model = 0.44, fu difference = -0.002, ER difference = 0.53, fm_A ≥ 75% corresponds to a red area. Importantly, this scaling method is isoenzyme specific, and one should be careful not to overlook minor pathways in adults which can become major pathways in children when aiming at scaling total clearance.

It should be noted that model-test drug scenarios leading to systematically accurate CLp scaling were defined according to very strict criteria. Each dot in Figure 5 and the accompanying Supplementary Material represents a scenario that summarizes the PEs for many different model-test drug combinations. CLp predictions were defined as not systematically accurate for a scenario if only one model-test drug combination within this scenario and, for drugs metabolized by several isoenzymes, if at least one specific I_{NA} (isoenzyme not accounted for by the covariate model) led to scaled CLp deviating > 30% from its 'true' value. However, it is likely for CLp scaling to be accurate for a (large) number of model-test drug combinations within such scenarios, but in these scenarios the accuracy of the scaling method cannot be easily predicted *a priori* without PBPK modeling.

Overall, our results show that the between-drug extrapolation potential of pathway-specific pediatric covariate functions for CLp increases when the ER of the model drug in adults decreases. The applicability of this method decreases with age and with a decreased adult fraction of the test drug and/or model drug being metabolized by the isoenzyme pathway accounted for by the covariate model (fmA_adult). Moreover, these trends increase with increased ER of the model drug. Plasma protein binding to AAG also limits the between-drug extrapolation potential of pediatric covariate functions for CLp, especially in young children, which can be explained by the more pronounced ontogeny pattern of AAG compared to HSA for these ages [35].

In this work, we discovered that, for drugs metabolized by several isoenzymes, the ontogeny of CLp due to one specific isoenzyme (I_A) is influenced by the ontogeny of the other isoenzymes responsible for the drug clearance (I_{NA}). We also found that this impact increases with increased adult ER and decreased fmA_adult, with fmA_adult standing for adult fraction of drug CLp due to I_A. This is due to changes in ER with age contributed by the ontogeny of all isoenzymes involved in the drug CLp [36], changes which in turn modify each isoenzyme specific CLp ontogenies. This was shown by the reduced applicability of the between-drug extrapolation potential of pathway-specific covariate models for CLp with decreased fmA_adult. This is further supported by the increase of these trends with increased ER of the model drug (see Figure 5 and Supplementary Material 2 and 3).

Although this workflow only investigated drugs undergoing hepatic metabolic CLp, the results on multiple elimination routes also apply to drugs undergoing hepatic metabolism in combination with renal clearance, as renal clearance does not impact the hepatic ER or the ontogeny of hepatic CLp. For these drugs, fmA_adult should be interpreted as the fraction of the total hepatic metabolic CLp in adults due to the isoenzyme pathway accounted for by the covariate model (I_A). Additionally, this workflow can be used to develop guidance on the need for PK-based dose adjustments in clinical situations of reduced plasma protein binding, like for instance uremia and hypoalbuminemia, or drug-drug interactions. In this situation, the model drug properties correspond to the drug properties in normal clinical situations and the test drug properties are changed to fu and ER values adapted to the calculated values for plasma protein binding in adults. If such a model-test drug combination yields an accurate CLp prediction for the test drug, the pediatric dose can be derived by applying the same dose adjustment factor used for maintenance doses in adults with a similar clinical condition.

An important limitation of the PBPK-based simulation workflow is that active influx or efflux of drugs into or out of hepatocytes by transporters is not included, thereby implicitly assuming this process to be passive. The impact of active drug transport in the membranes of hepatocytes on the between-drug extrapolation of pathway-specific pediatric covariate functions requires further investigation.

In conclusion, the developed PBPK-based simulation workflow utilizing mechanistic equations defining hepatic metabolism allowed, for the first time, to unravel the variables most impacting CLp ontogeny and to define scenarios for which extrapolation of pediatric covariate functions from one drug to another systematically leads to accurate isoenzyme specific CLp scaling from adults to pediatric patients for 15 hepatic isoenzymes.

Funding

This study was supported by the Innovational Research Incentives Scheme (Vidi grant, June 2013) of the Netherlands Organization for Scientific Research (NWO) to Catherijne A. J. Knibbe (2013).

Conflict of interest

Trevor Johnson is a paid employee of Simcyp Limited (a Certara company). Amin Rostami-Hodjegan holds shares in Certara, a company focusing on model-informed drug development and also has shares in Diurnal, which focuses on developing high quality products for the life-long treatment of chronic endocrine conditions. As Editor-in-Chief for CPT: Pharmacometrics & Systems Pharmacology, Piet H. van der Graaf was not involved in the review or decision process for this article.

References

1. Manolis, E. *et al.* The role of modeling and simulation in development and registration of medicinal products: output from the EFPIA/EMA Modeling and Simulation Workshop. *CPT pharmacometrics Syst. Pharmacol.* **2,** e31 (2013).

2. Brussee, J. M. *et al.* Children in clinical trials: towards evidence-based pediatric pharmacotherapy using pharmacokinetic-pharmacodynamic modeling. *Expert Rev. Clin. Pharmacol.* **9,** 1235–44 (2016).

3. US Department of Health and Human Services Food and Drug Administration Center for Drug Evaluation and Research (CDER). General considerations for pediatric pharmacokinetic studies for drugs and biological products. (1998). Available at: https://www.fda.gov/ohrms/dockets/ac/03/briefing/3927B1_04_GFI-Pharmacokinetic Guidance.pdf. (Accessed: 27th September 2017)

4. Zisowsky, J., Krause, A. & Dingemanse, J. Drug development for pediatric populations: regulatory aspects. *Pharmaceutics* **2,** 364–388 (2010).

5. Espié, P., Tytgat, D., Sargentini-Maier, M.-L., Poggesi, I. & Watelet, J.-B. Physiologically based pharmacokinetics (PBPK). *Drug Metab. Rev.* **41,** 391–407 (2009).

6. Maharaj, A. R., Barrett, J. S. & Edginton, A. N. A workflow example of PBPK modeling to support pediatric research and development: case study with lorazepam. *AAPS J.* **15,** 455–64 (2013).

7. Maharaj, A. R. & Edginton, A. N. Physiologically based pharmacokinetic modeling and simulation in pediatric drug development. *CPT pharmacometrics Syst. Pharmacol.* **3,** 1–13 (2014).

8. Barrett, J. S., Della Casa Alberighi, O., Läer, S. & Meibohm, B. Physiologically based pharmacokinetic (PBPK) modeling in children. *Clin. Pharmacol. Ther.* **92,** 40–9 (2012).

9. Johnson, T. N., Rostami-Hodjegan, A. & Tucker, G. T. Prediction of the clearance of eleven drugs and associated variability in neonates, infants and children. *Clin. Pharmacokinet.* **45,** 931–56 (2006).

10. Björkman, S. Prediction of drug disposition in infants and children by means of physiologically based pharmacokinetic (PBPK) modelling: theophylline and midazolam as model drugs. *Br. J. Clin. Pharmacol.* **59,** 691–704 (2005).

11. Johnson, T. N. & Rostami-Hodjegan, A. Resurgence in the use of physiologically based pharmacokinetic models in pediatric clinical pharmacology: parallel shift in incorporating the knowledge of biological elements and increased applicability to drug development and clinical practice. *Pediatr. Anesth.* **21,** 291–301 (2011).

12. Joerger, M. Covariate pharmacokinetic model building in oncology and its potential clinical relevance. *AAPS J.* **14,** 119–32 (2012).

13. Patel, K. & Kirkpatrick, C. M. J. Pharmacokinetic concepts revisited--basic and applied. *Curr. Pharm. Biotechnol.* **12,** 1983–90 (2011).

14. Knibbe, C. A. J. *et al.* [Individualized dosing guidelines for children]. *Ned. Tijdschr. Geneeskd.* **157,** A4214 (2013).

15. Krekels, E. H. J. *et al.* From pediatric covariate model to semiphysiological function for maturation: part I-extrapolation of a covariate model from morphine to Zidovudine. *CPT pharmacometrics Syst. Pharmacol.* **1,** e9 (2012).

16. Krekels, E. H. J. *et al.* From Pediatric Covariate Model to Semiphysiological Function for Maturation: Part II-Sensitivity to Physiological and Physicochemical Properties. *CPT pharmacometrics Syst. Pharmacol.* **1,** e10 (2012).

17. Zhao, W., Biran, V. & Jacqz-Aigrain, E. Amikacin maturation model as a marker of renal maturation to predict glomerular filtration rate and vancomycin clearance in neonates. *Clin. Pharmacokinet.* **52,** 1127–34 (2013).

18. De Cock, R. F. W. *et al.* Simultaneous pharmacokinetic modeling of gentamicin, tobramycin and vancomycin clearance from neonates to adults: towards a semi-physiological function for maturation in glomerular filtration. *Pharm. Res.* **31,** 2643–54 (2014).

19. De Cock, R. F. W. *et al.* A neonatal amikacin covariate model can be used to predict ontogeny of other drugs eliminated through glomerular filtration in neonates. *Pharm. Res.* **31,** 754–767 (2014).

20. R Development Core Team. R: A language and environment for statistical computing version 3.3.1. <https://cran.r-project.org/doc/manuals/fullrefman.pdf> (2016).

21. Calvier, E. A. M. *et al.* Allometric scaling of clearance in paediatric patients: when does the magic of 0.75 fade? *Clin. Pharmacokinet.* **56,** 273–285 (2017).

22. Hines, R. N. The ontogeny of drug metabolism enzymes and implications for adverse drug events. *Pharmacol. Ther.* **118,** 250–67 (2008).

23. Naritomi, Y. *et al.* Prediction of human hepatic clearance from in vivo animal experiments and in vitro metabolic studies with liver microsomes from animals and humans. *Drug Metab. Dispos.* **29,** 1316–24 (2001).

24. Izenman, A. J. Cluster analysis. In: *Modern Multivariate Statistical Techniques Regression, Classification, and Manifold Learning* 407–462 (Springer-Verlag, New York, NY, 2013). doi:10.1007/978-0-387-78189-1_12

25. Fernandez, E. *et al.* Factors and mechanisms for pharmacokinetic differences between pediatric population and adults. *Pharmaceutics* **3,** 53–72 (2011).

26. Krekels, E. H. J., Danhof, M., Tibboel, D. & Knibbe, C. a J. Ontogeny of hepatic glucuronidation; methods and results. *Curr. Drug Metab.* **13,** 728–43 (2012).

27. Hohmann, N. *et al.* Midazolam microdose to determine systemic and pre-systemic metabolic CYP3A activity in humans. *Br. J. Clin. Pharmacol.* **79,** 278–285 (2015).

28. Lown, K. S. *et al.* The erythromycin breath test predicts the clearance of midazolam*. *Clin. Pharmacol. Ther.* **57,** 16–24 (1995).

29. Venkatakrishnan, K., Obach, R. S. & Rostami-Hodjegan, A. Mechanism-based inactivation of human cytochrome P450 enzymes: strategies for diagnosis and drug-drug interaction risk assessment. *Xenobiotica.* **37,** 1225–56 (2007).

30. Zhao, P. *et al.* Applications of physiologically based pharmacokinetic (PBPK) modeling and simulation during regulatory review. *Clin. Pharmacol. Ther.* **89,** 259–67 (2011).

31. Mehrotra, N., Gupta, M., Kovar, A. & Meibohm, B. The role of pharmacokinetics and pharmacodynamics in phosphodiesterase-5 inhibitor therapy. *Int. J. Impot. Res.* **19,** 253–264 (2007).

32. Fenneteau, F., Poulin, P. & Nekka, F. Physiologically based predictions of the impact of inhibition of intestinal and hepatic metabolism on human pharmacokinetics of CYP3A substrates. *J. Pharm. Sci.* **99,** 486–514 (2010).

33. Vickers, S., Duncan, C. A., Chen, I. W., Rosegay, A. & Duggan, D. E. Metabolic disposition studies on simvastatin, a cholesterol-lowering prodrug. *Drug Metab. Dispos.* **18,** (1990).

34. Lennernäs, H. & Fager, G. Pharmacodynamics and pharmacokinetics of the HMG-CoA reductase inhibitors. Similarities and differences. *Clin. Pharmacokinet.* **32,** 403–25 (1997).

35. McNamara, P. J. & Alcorn, J. Protein binding predictions in infants. *AAPS PharmSci* **4,** 19–26 (2002).

36. Salem, F., Abduljalil, K., Kamiyama, Y. & Rostami-Hodjegan, A. Consideringage variation when coining drugs as high versus low hepatic extraction ratio. *Drug Metab. Dispos.* **44,** 1099–1102 (2016).

Supplementary material 1 Methodology

PBPK-based simulation workflow

Variables in the PBPK-based simulation workflow

System-specific parameters

PBPK simulations were performed for typical pediatric individuals of various ages and for a typical 25 years old adult. Demographic values (average for males and females) were taken from the CDC growth charts [1] for the typical pediatric individuals and from the Simcyp® (Simcyp Ltd, Sheffield, UK) V15.R1 library for a typical adult (see table below). Body surface area (BSA) was estimated using the equations of Dubois and Dubois [2] for children weighing > 15kg, and of Haycock *et al.* [3] for those weighing ≤ 15kg, as implemented in Simcyp® V15.R1.

	1 day	1 month	6 months	1 year	2 years	5 years	15 years	25 years
Bodyweight (kg)	3.45	4.30	7.55	9.90	12.35	18.25	54.25	72.65
Height (cm)	49.75	54.25	66.00	74.75	86.00	108.25	166.00	172.30

PBPK parameters were taken from the Simcyp® V15.R1 library as were ontogeny patterns in the hepatic blood flow (Qh), plasma protein concentrations for human serum albumin (HSA) and alpha-1 acid glycoprotein (AAG), haematocrit, liver size, milligram protein per gram of liver (MPPGL) and isoenzyme abundance, excepted for the isoenzyme ontogeny of SULT1A1 for which maturity was taken to have been reached at birth [4].

Drug-specific properties of the model drugs and test drugs

Hypothetical drugs were generated to serve as model and test drugs in the PBPK-based simulation workflow. For each individual drug-specific property, a realistic range of values was selected.

The model parameters to calculate hepatic plasma clearance (CLp) in this workflow which are based on a combination of drug-specific and system-specific parameters are: the unbound drug fraction in plasma (fu), the blood to plasma ratio (B:P), and the intrinsic metabolic clearance in the liver based on unbound drug concentration (CLint). These parameters therefore reflect drug properties in a population of a specific age. In this analysis, fu and CLint in adults were used as surrogates of their contributing drug-specific parameters (i.e., affinity to plasma proteins and affinity to isoenzymes respectively), since they are most often reported.

To derive the affinity to plasma proteins from the unbound drug fraction in plasma (fu) and the concentration of the binding plasma protein in adults, equations by Rodgers and Rowland [5,6] were used. The hypothetical drugs were assumed to be exclusively bound to either HSA or AAG. The fu in adults ranged from 1% to 100%, with 8 equidistant intermediate values. Values for the blood to plasma partitioning coefficient (Kp) of 0.35, 1, 2, 3, 4, 5, 10, 20, and 40 were selected, reflecting different extents of drug diffusion into the red blood cells. $CL_{int,mic,total}$ in adults ranged between $0.56.10^{-6}$ and $0.209.10^{-3}$ L. $min^{-1}.mg^{-1}$ microsomal protein [7], with 40 equidistant intermediate values. These different values reflect difference in both affinities for and abundances of isoenzymes in adults. Equations 3 to 6 below were used to calculate the extraction ratio (ER) of each hypothetical drug in adults.

Step 1 of the PBPK-based simulation workflow

'True' total hepatic plasma clearance (CLp) values were computed using the dispersion model (Equations 1 to 6). The dispersion model was selected as it has been reported to more accurately predict hepatic CLp than the well-stirred model for highly cleared drugs, while both models lead to equivalent clearance predictions for other drugs [8].

$$\mathrm{CLp} = \mathrm{CL_B} \times \mathrm{B{:}\,P} \quad (1)$$

$$\mathrm{CL_B} = \mathrm{Qh} \times \mathrm{ER} \quad (2)$$

$$\mathrm{ER} = 1 - \mathrm{F_H} \quad (3)$$

$$\mathrm{F_H} = \frac{4a}{(1+a)^2 \exp\{(a-1)/2D_N\} - (1-a)^2 \exp\{-(a+1)/2D_N\}} \quad (4)$$

$$a = (1 + 4R_N \times D_N)^{1/2} \quad (5)$$

$$R_N = (fu/B{:}\,P) \times CLint/Qh \quad (6)$$

In these equations, CLp is the overall total (i.e., bound and unbound) hepatic plasma clearance, CL_B is the total whole blood clearance, B:P is the blood to plasma ratio, Qh is the hepatic blood flow, ER is the hepatic extraction ratio, fu is the unbound drug fraction in plasma, CLint is the total hepatic intrinsic clearance, R_N is the efficiency number and D_N is the axial dispersion number. For the axial dispersion number (D_N) a value of 0.17 was used [9].

For each hypothetical drugs, CLint in adults was computed as the product of $CL_{int,mic,total}$, the MPPGL, and the liver weight. B:P in adults was derived from the adult haematocrit, from the Kp value, and the value of fu in adults [10]. Values of adult $CL_{int,mic,total}$, Kp, and adult fu were taken from the values defined to generate the hypothetical drugs (see under Hypothetical drugs). Qh, CLint, fu, and B:P in pediatric patients were scaled using the ontogeny functions of the relevant system-specific parameters. The R model code for the CLp simulations is provided in the Model Code Supplementary Material.

Conditions leading to accurate CLp predictions

In order to identify the drug-specific properties allowing to best discriminate between accurate and inaccurate scaled pediatric CLp, the prediction errors (PEs) obtained in step 4 of the PBPK-based simulation workflow were first split into different groups. A group was defined as containing PEs for all ages for one combination of model and test drugs eliminated by the same isoenzyme and binding to the same plasma protein (both including drugs not binding to plasma proteins). Then, the PEs within each group were transformed into a binary outcome according to the following definitions:

- Positive outcome: all CLp predictions within the defined group are accurate (absolute PE $\leq$ 30%).
- Negative outcome: at least one CLp prediction within the defined group is inaccurate (absolute PE >30%).

Then, for each isoenzyme and type of binding plasma protein, drug-specific parameters were tested for their discriminative power between positive and negative outcome using a hierarchical tree method with a penalty function. The hierarchical tree method used was the recursive partitioning and regression tree from the rpart R package [11]. The penalty function was implemented in order to obtain variables best discriminating positive outcomes, while accepting a decreased discriminative power for negative outcomes. The drug specific parameters tested were Kp, and fu, CLint, and B:P in adults of the model drug and of the test

drug, as well as the difference in these parameters between the model drug and test drug. The most discriminatory variables were defined as the variables allowing to discriminate the maximum of positive outcomes from negative outcomes. A maximum of 3 most discriminatory variables was set in order to allow for readability of the results.

Multiple elimination pathways

For model drugs metabolized by several isoenzymes, the CLp_A corresponds to the part of the overall drug CLp due to isoenzyme A (I_A), this is the isoenzyme for which ontogeny is accounted for by the covariate function. Likewise, for test drugs metabolized by several isoenzymes, CLp_A corresponds to the part of the overall CLp due to I_A and the adult CLp_A is scaled to pediatric patients using the covariate function describing the changes in CLp_A from adults to pediatric patients of a model drug. This is equivalent to scaling part of the drug clearance responsible for the formation of a specific metabolite due to a specific isoenzyme. An isoenzyme that was not accounted for (I_{NA}) in the pediatric covariate function was included in the simulations since it impacts the extraction ratio of the drug which in turn might impact the ontogeny of CLp_A.

In this part of our investigation, the same steps of the PBPK-based simulation workflow were performed as for the case described for only one metabolizing isoenzyme, with thereinafter adaptations.

All 15 isoenzymes that were included in the simulation workflow were included as I_A and I_{NA} in all possible combinations. For the fraction metabolized by I_A in adults (fmA_adult), values of 5, 25, 50, 75, and 95% were selected and the remaining fraction was assumed to be metabolized by I_{NA}. fmA_adult was included in the PBPK-based simulation workflow as a drug property, leading to a greater set of hypothetical model drug and test drugs to be investigated compared to the investigation of drugs only eliminated by one isoenzyme. Equations 7 to 9 were used to determine intrinsic microsomal clearance for each isoenzyme.

$$CL_{int,mic,A} = CL_{int,mic,total} \times fmA \quad (7)$$

$$CL_{int,mic,NA} = CL_{int,mic,total} \times fmNA \quad (8)$$

$$\text{With } CL_{int,mic,A} + CL_{int,mic,NA} = CL_{int,mic,total} \quad (9)$$

In step 1 of the workflow, 'true' CLp_A were derived from the $'true'\ total\ CLp$ using equation 10.

$$\text{'true' } CLp_A = \text{'true' total } CLp \times fmA \quad (10)$$

Adult 'true' total CLp_A was derived as described for drugs eliminated by one isoenzymes, using the adult $CL_{int,mic,total}$ (to obtain the adult 'true' total CLp),and adult fmA (fmA _adults), both defined as a drug property.

Pediatric 'True' total CLp from Eq. 10 was computed as described earlier, by scaling $CL_{int,mic,total}$ from adult to pediatric values. Since for drugs metabolized by several isoenzymes, $CL_{int,mic,total}$ corresponds to the sum of $CL_{int,mic,A}$ and $CL_{int,mic,NA}$ (Eq. 9), adult values of $CL_{int,mic,A}$, and $CL_{int,mic,NA}$ were scaled to pediatric values by accounting for the isoenzyme ontogeny of I_A (IO_A) and I_{NA} (IO_{NA}) respectively and then summed up to derive pediatric $CL_{int,mic,total}$. The fmA in pediatric patients (fmA_pediatrics) was derived according to Eq.11.

$$\text{fmA\_pediatrics} = \frac{\text{fmA\_adult} \times IO_A}{\text{fmA\_adult} \times IO_A + \text{fmNA\_adult} \times IO_{NA}} \quad (11)$$

In this equation, IO_A and IO_{NA} are the isoenzyme ontogeny defined as the ratio of pediatric $CL_{int,mic}$ and adults $CL_{int,mic}$ of I_A and I_{NA} respectively, and fmA_adult and fmNA_adult are the fraction metabolized in adults by I_A and I_{NA} respectively. The R model code for the CLp_A simulations is provided in the Model Code Supplementary Material.

In step 2 and 3 of the workflow the pediatric covariate function is developed for the elimination of model drug M via I_A only and is extrapolated to predict the elimination of the test drug T via I_A only. The isoenzyme that is not accounted for (I_{NA}) in the pediatric covariate function is responsible for CLp_{NA}. While I_{NA} is contributing to the overall CLp of the model and/or test drugs and thereby influencing the extraction ratio of these drugs, CLp_{NA} is not part of the pediatric covariate function that is extrapolated between the model and the test drug.

In step 4, the PE is only calculated for CLp_A, the plasma clearance by I_A.

The identification of drug properties allowing to best discriminate between accurate and inaccurate scaled pediatric CLp_A was done by defining PEs groups similarly as for drugs eliminated by one isoenzyme, but drugs contained in each group take all possible values of fmA_adult, and are co-metabolized by all possible I_{NA}.

Finally, to define model-test drug scenarios systematically leading to accurate scaled pediatric CLp, PE not only were grouped based on the most discriminative drug properties (similarly as for drug eliminated by one isoenzymes), but also were grouped per fmA-adult category, disregarding the I_{NA} involved in drug clearance. FmA_adult categories were: fmA_adult = 100%, fmA_adult ≥ 95%, ≥ 75%, ≥ 50%, ≥ 25% and ≥ 5%.

References

1. Centers for Disease Control and Prevention NCHS. Length-for-age and weight-for-age percentiles. (2000).

2. Du Bois, D. & Du Bois, E. F. A formula to estimate the approximate surface area if height and weight be known. 1916. *Nutrition* **5,** 303-11; discussion 312–3

3. Haycock, G. B., Schwartz, G. J. & Wisotsky, D. H. Geometric method for measuring body surface area: a height-weight formula validated in infants, children, and adults. *J. Pediatr.* **93,** 62–6 (1978).

4. Hines, R. N. The ontogeny of drug metabolism enzymes and implications for adverse drug events. *Pharmacol. Ther.* **118,** 250–67 (2008).

5. Rodgers, T. & Rowland, M. Physiologically based pharmacokinetic modelling 2: predicting the tissue distribution of acids, very weak bases, neutrals and zwitterions. *J. Pharm. Sci.* **95,** 1238–57 (2006).

6. Johnson, T. N., Rostami-Hodjegan, A. & Tucker, G. T. Prediction of the clearance of eleven drugs and associated variability in neonates, infants and children. *Clin. Pharmacokinet.* **45,** 931–56 (2006).

7. Nikolic, K. & Agababa, D. Prediction of hepatic microsomal intrinsic clearance and human clearance values for drugs. *J. Mol. Graph. Model.* **28,** 245–52 (2009).

8. Ridgway, D., Tuszynski, J. A. & Tam, Y. K. Reassessing models of hepatic extraction. *J. Biol. Phys.* **29,** 1–21 (2003).

9. Naritomi, Y. *et al.* Prediction of human hepatic clearance from in vivo animal experiments and in vitro metabolic studies with liver microsomes from animals and humans. *Drug Metab. Dispos.* **29,** 1316–24 (2001).

10. Maharaj, A. R., Barrett, J. S. & Edginton, A. N. A workflow example of PBPK modeling to support pediatric research and development: case study with lorazepam. *AAPS J.* **15,** 455–64 (2013).

11. Terry Therneau, B. A. and B. R. rpart: Recursive Partitioning and Regression Trees. (2017).

Supplementary material 2 Model-test drug scenarios, for drugs binding to human serum albumin, that lead to accurate pathway specific CLp predictions for a test drug after between-drug extrapolation of a pathway specific pediatric covariate function.

Figures A to O display model-test drug scenarios that lead to accurate pathway specific CLp predictions for a test drug after between-drug extrapolation of a pathway specific pediatric covariate function. Results are displayed for drugs binding to human serum albumin (HSA) and eliminated through CYP1A2 (A), CYP2A6 (B), CYP2B6 (C), CYP2C8 (D), CYP2C9 (E), CYP2C18_19 (F), CYP2D6 (G), CYP2E1 (H), CYP3A4 (I), SULT1A1 (J), UGT1A1 (K), UGT1A4 (L), UGT1A6 (M), UGT1A9 (N) and UGT2B7 (O) hepatic metabolism. Each column corresponds to a range of extraction ratio (ER) values for the model drug in adults and each row to a specific range of fraction of drug (model and test drug) that is metabolized by CYP1A2 in adults (fmA_adult). For each graph, the y-axis represents the difference in ER between the test drug and the model drug (ER test drug – ER model drug) in adults, and the x-axis represents the difference in fraction unbound (fu) between the test drugs and the model drug in adults (fu test drug – fu model drug). Each dot represents a model-test drug scenario, including multiple model-test drug combinations. A color code is used to indicate systematically accurate CLp predictions for all model-test drug combinations within a model-test drug scenario, for children ≥ 5 years (yellow), ≥ 2 years (pink), ≥ 1 year (blue), ≥ 6 months (orange), ≥ 1 month (purple), and ≥ 1 day term neonates (green). Red dots indicate model-test drug scenarios leading to inaccurate predictions in children older than 5 years for at least one model-test drug combination within the model-test drug scenario. As an example, systematically accurate CLp scaling in children of 6 months and older is represented by the combination of the green, purple and orange dots. The table below summarizes the color code used to indicate systematically accurate scaled pediatric CLp (+) and inaccurate scaled pediatric CLp (-) in the different ages studied.

1 day	1 month	6 months	1 year	2 years	≥ 5 years	
+	+	+	+	+	+	**green**
-	+	+	+	+	+	**purple**
-	-	+	+	+	+	**orange**
-	-	-	+	+	+	**blue**
-	-	-	-	+	+	**pink**
-	-	-	-	-	+	**Yellow**
-	-	-	-	-	-	**Red**

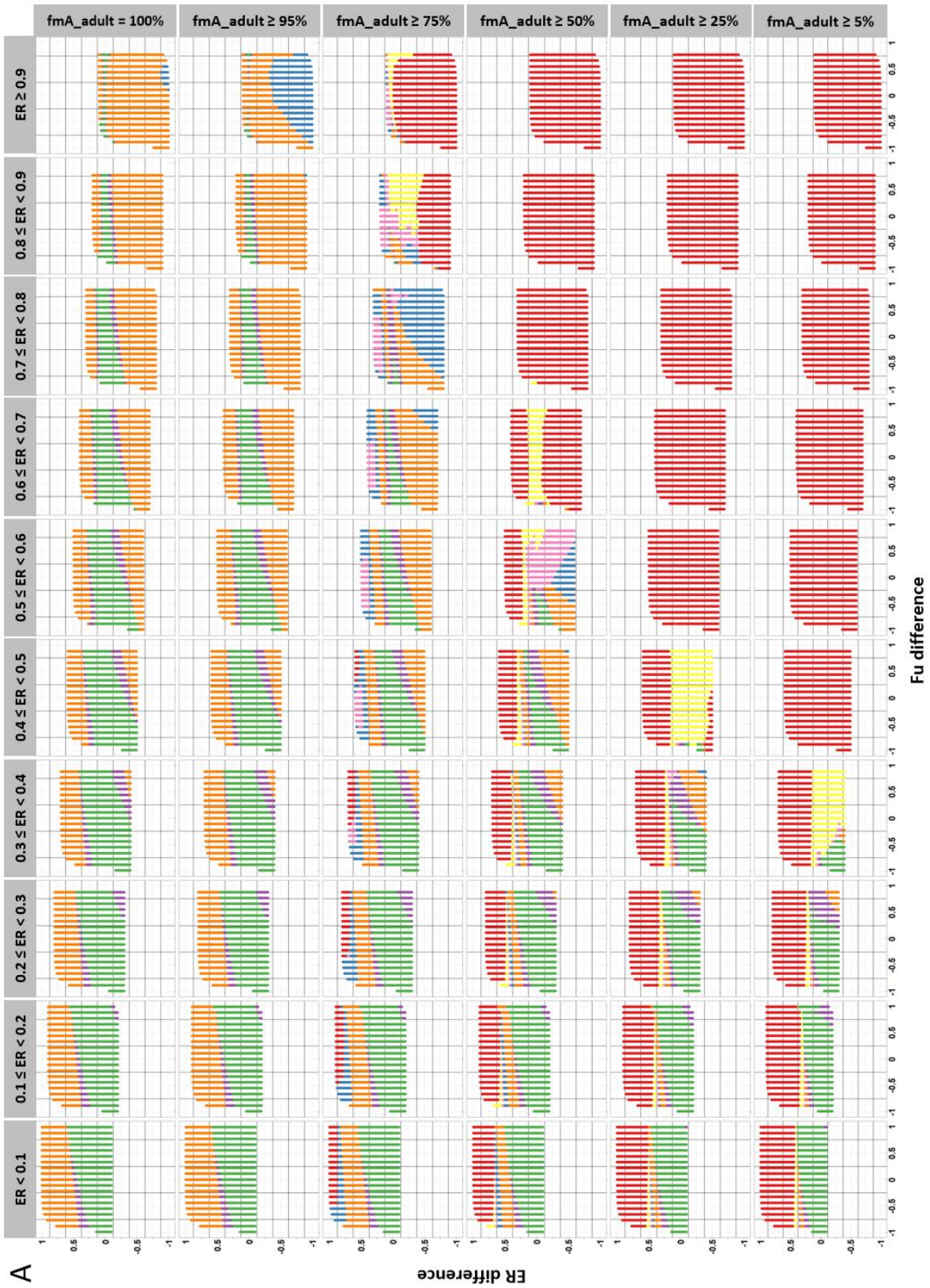
A
fmA_adult = 100%
fmA_adult ≥ 95%
fmA_adult ≥ 75%
fmA_adult ≥ 50%
fmA_adult ≥ 25%
fmA_adult ≥ 5%
ER ≥ 0.9
0.8 ≤ ER < 0.9
0.7 ≤ ER < 0.8
0.6 ≤ ER < 0.7
0.5 ≤ ER < 0.6
0.4 ≤ ER < 0.5
0.3 ≤ ER < 0.4
0.2 ≤ ER < 0.3
0.1 ≤ ER < 0.2
ER < 0.1
ER difference
Fu difference

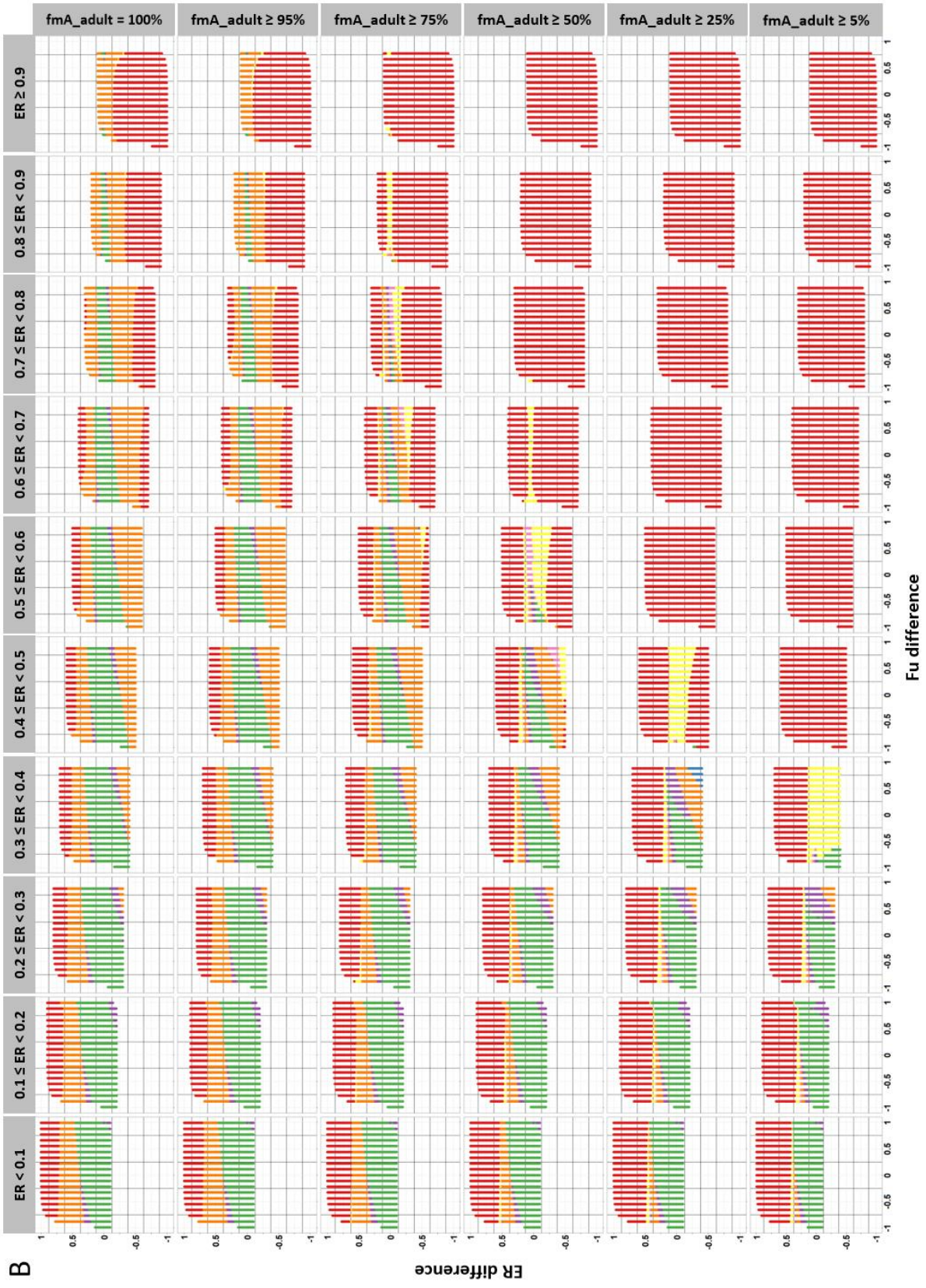
B
fmA_adult = 100%
fmA_adult ≥ 95%
fmA_adult ≥ 75%
fmA_adult ≥ 50%
fmA_adult ≥ 25%
fmA_adult ≥ 5%
ER ≥ 0.9
0.8 ≤ ER < 0.9
0.7 ≤ ER < 0.8
0.6 ≤ ER < 0.7
0.5 ≤ ER < 0.6
0.4 ≤ ER < 0.5
0.3 ≤ ER < 0.4
0.2 ≤ ER < 0.3
0.1 ≤ ER < 0.2
ER < 0.1
ER difference
Fu difference

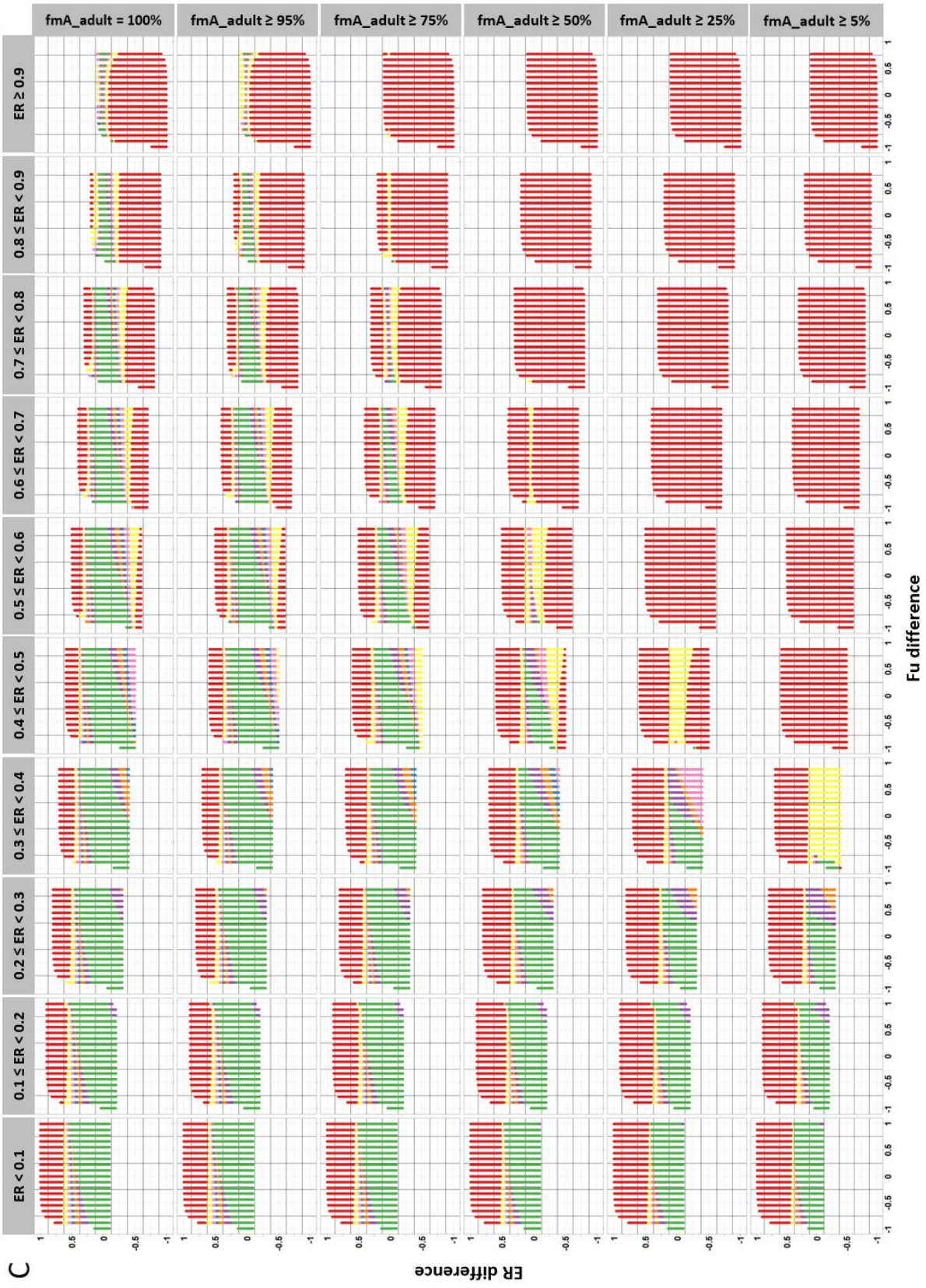
C
fmA_adult = 100%
fmA_adult ≥ 95%
fmA_adult ≥ 75%
fmA_adult ≥ 50%
fmA_adult ≥ 25%
fmA_adult ≥ 5%
ER ≥ 0.9
0.8 ≤ ER < 0.9
0.7 ≤ ER < 0.8
0.6 ≤ ER < 0.7
0.5 ≤ ER < 0.6
0.4 ≤ ER < 0.5
0.3 ≤ ER < 0.4
0.2 ≤ ER < 0.3
0.1 ≤ ER < 0.2
ER < 0.1
ER difference
Fu difference

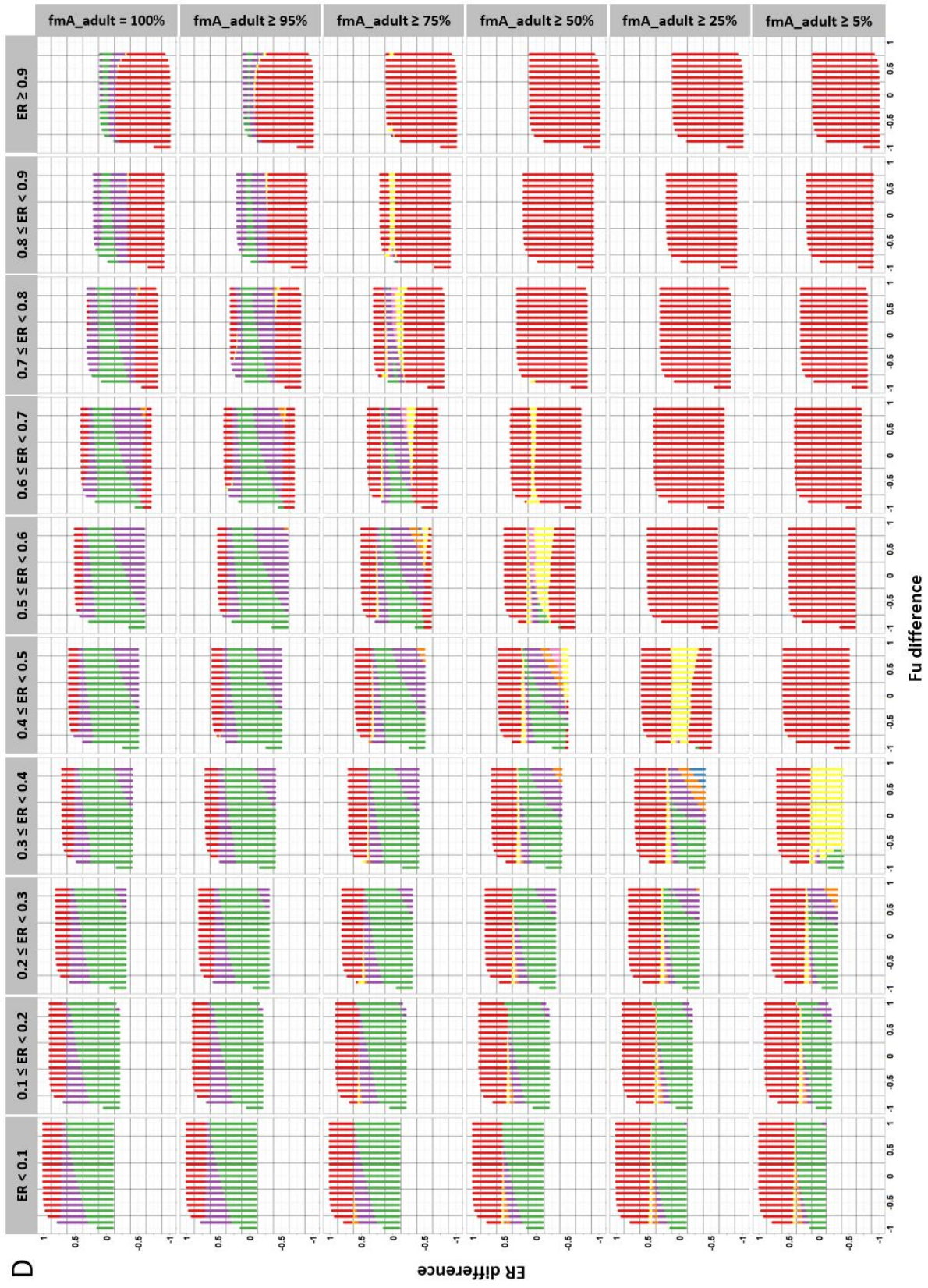
D
fmA_adult = 100%
fmA_adult ≥ 95%
fmA_adult ≥ 75%
fmA_adult ≥ 50%
fmA_adult ≥ 25%
fmA_adult ≥ 5%
ER ≥ 0.9
0.8 ≤ ER < 0.9
0.7 ≤ ER < 0.8
0.6 ≤ ER < 0.7
0.5 ≤ ER < 0.6
0.4 ≤ ER < 0.5
0.3 ≤ ER < 0.4
0.2 ≤ ER < 0.3
0.1 ≤ ER < 0.2
ER < 0.1
ER difference
Fu difference

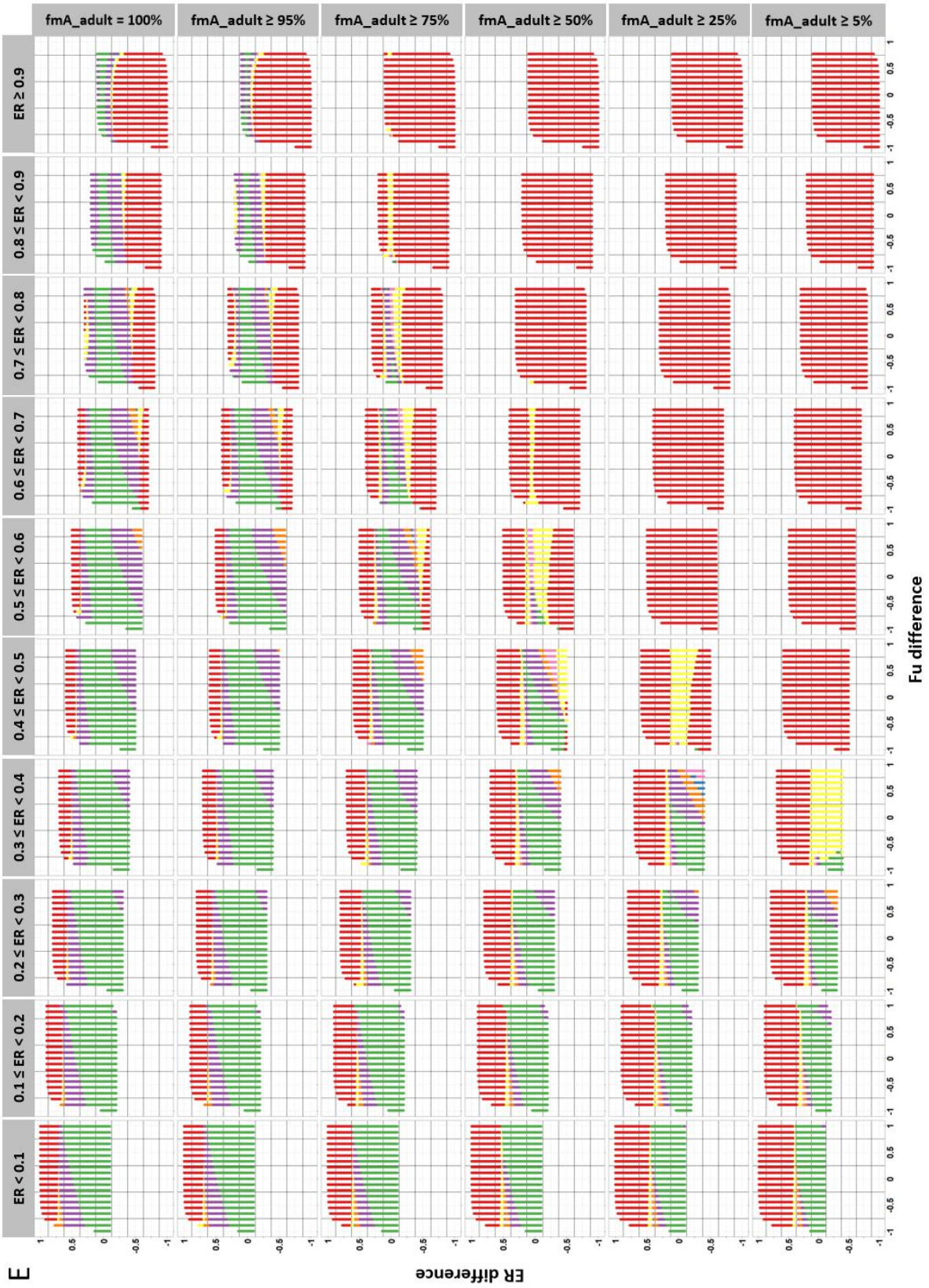
fmA_adult = 100%
fmA_adult ≥ 95%
fmA_adult ≥ 75%
fmA_adult ≥ 50%
fmA_adult ≥ 25%
fmA_adult ≥ 5%
ER ≥ 0.9
0.8 ≤ ER < 0.9
0.7 ≤ ER < 0.8
0.6 ≤ ER < 0.7
0.5 ≤ ER < 0.6
0.4 ≤ ER < 0.5
0.3 ≤ ER < 0.4
0.2 ≤ ER < 0.3
0.1 ≤ ER < 0.2
ER < 0.1
Fu difference
ER difference
E

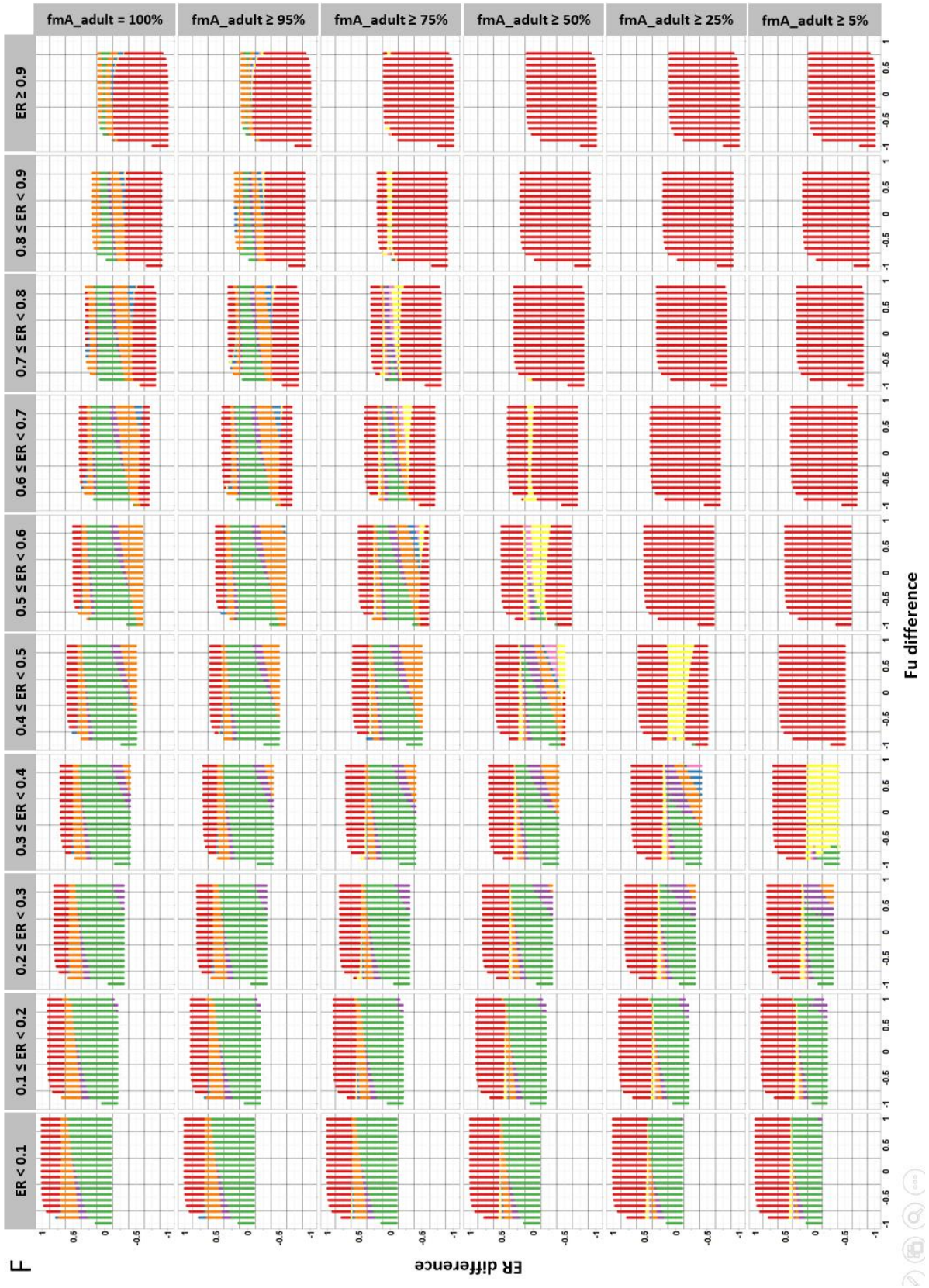
fmA_adult = 100%
fmA_adult ≥ 95%
fmA_adult ≥ 75%
fmA_adult ≥ 50%
fmA_adult ≥ 25%
fmA_adult ≥ 5%
ER ≥ 0.9
0.8 ≤ ER < 0.9
0.7 ≤ ER < 0.8
0.6 ≤ ER < 0.7
0.5 ≤ ER < 0.6
0.4 ≤ ER < 0.5
0.3 ≤ ER < 0.4
0.2 ≤ ER < 0.3
0.1 ≤ ER < 0.2
ER < 0.1
Fu difference
ER difference
F

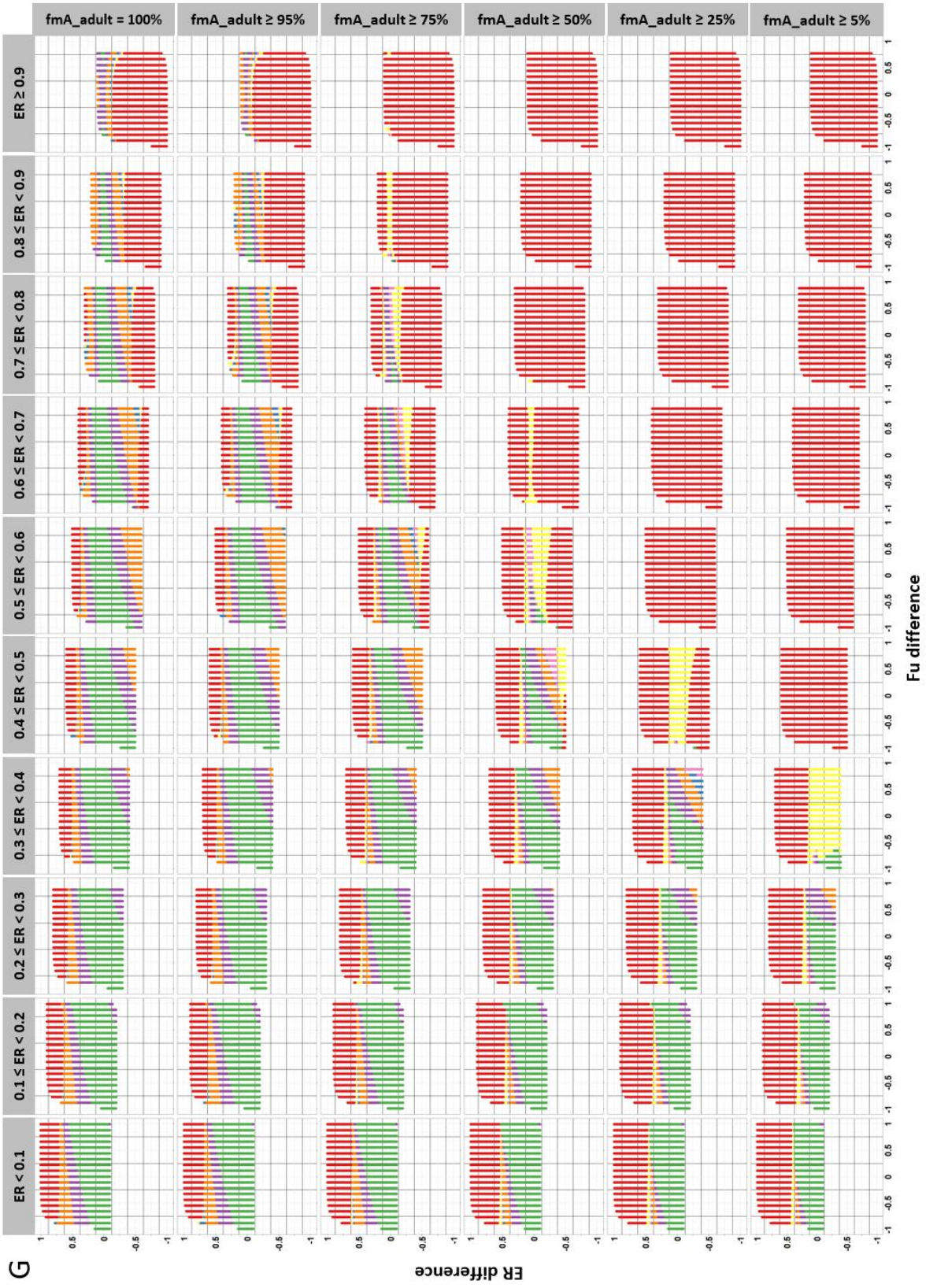
fmA_adult = 100%
fmA_adult ≥ 95%
fmA_adult ≥ 75%
fmA_adult ≥ 50%
fmA_adult ≥ 25%
fmA_adult ≥ 5%
ER ≥ 0.9
0.8 ≤ ER < 0.9
0.7 ≤ ER < 0.8
0.6 ≤ ER < 0.7
0.5 ≤ ER < 0.6
0.4 ≤ ER < 0.5
0.3 ≤ ER < 0.4
0.2 ≤ ER < 0.3
0.1 ≤ ER < 0.2
ER < 0.1
Fu difference
ER difference
G

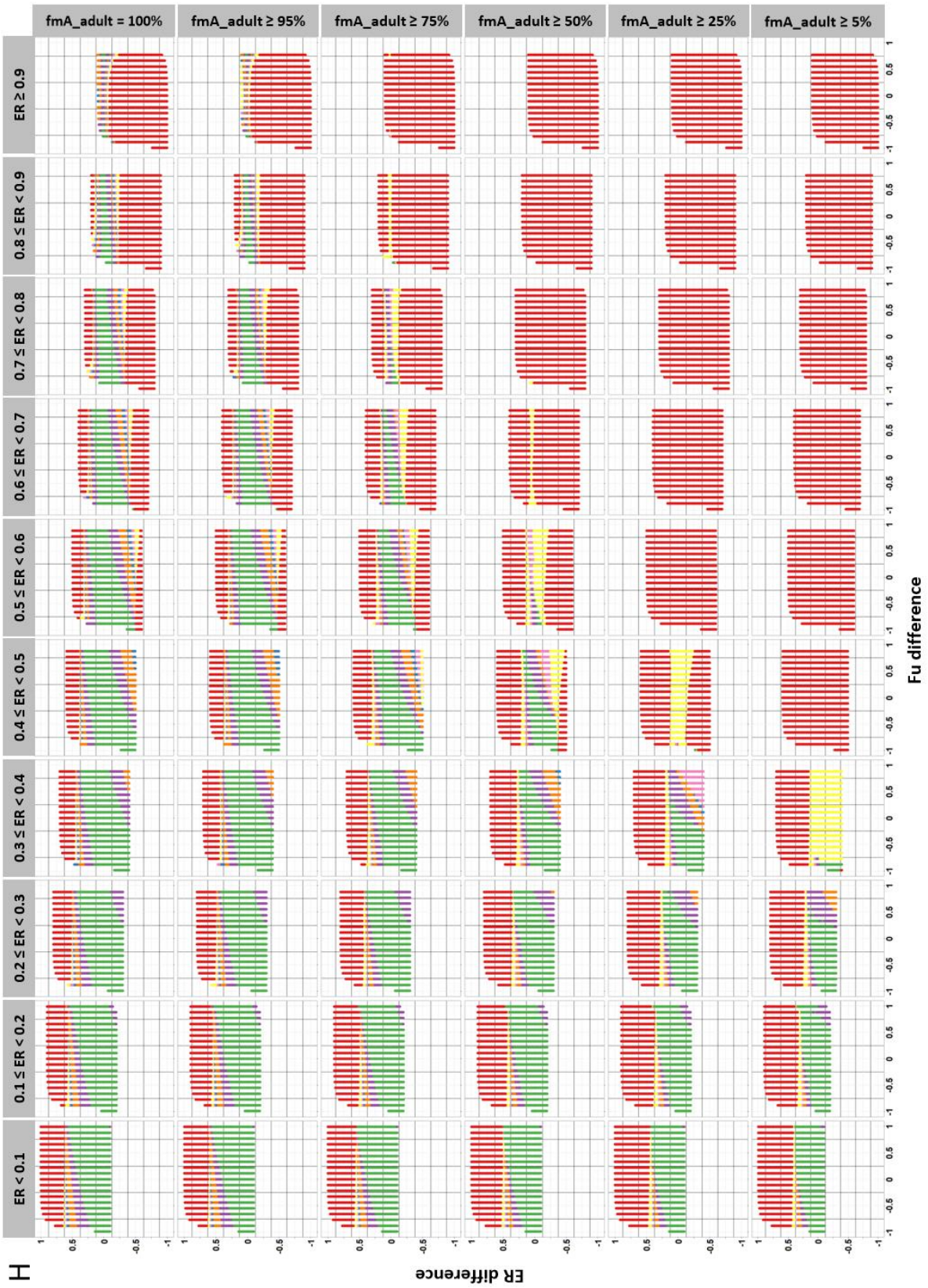
fmA_adult = 100%
fmA_adult ≥ 95%
fmA_adult ≥ 75%
fmA_adult ≥ 50%
fmA_adult ≥ 25%
fmA_adult ≥ 5%
ER ≥ 0.9
0.8 ≤ ER < 0.9
0.7 ≤ ER < 0.8
0.6 ≤ ER < 0.7
0.5 ≤ ER < 0.6
0.4 ≤ ER < 0.5
0.3 ≤ ER < 0.4
0.2 ≤ ER < 0.3
0.1 ≤ ER < 0.2
ER < 0.1
Fu difference
ER difference
H

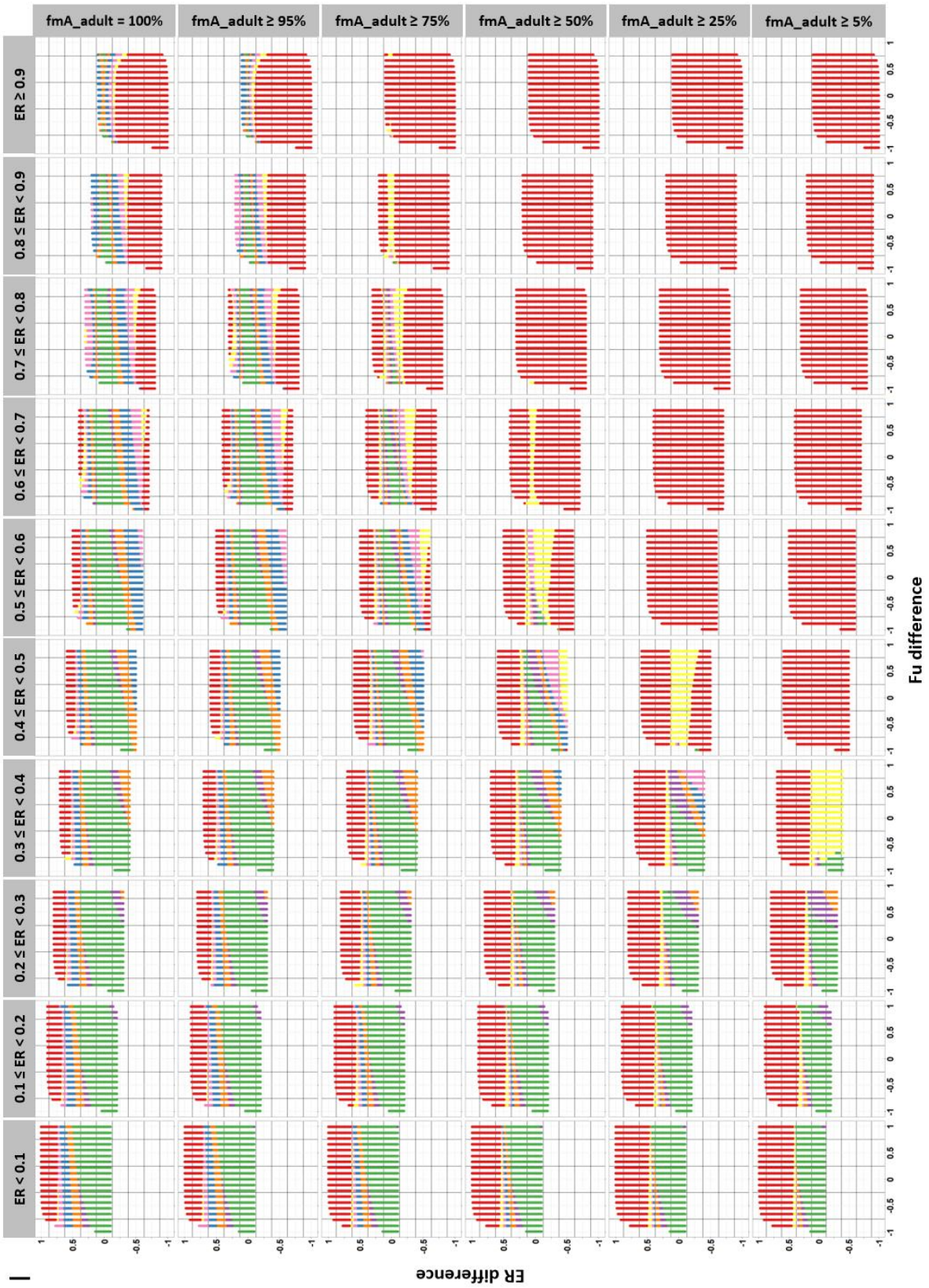
fmA_adult = 100%
fmA_adult ≥ 95%
fmA_adult ≥ 75%
fmA_adult ≥ 50%
fmA_adult ≥ 25%
fmA_adult ≥ 5%
ER ≥ 0.9
0.8 ≤ ER < 0.9
0.7 ≤ ER < 0.8
0.6 ≤ ER < 0.7
0.5 ≤ ER < 0.6
0.4 ≤ ER < 0.5
0.3 ≤ ER < 0.4
0.2 ≤ ER < 0.3
0.1 ≤ ER < 0.2
ER < 0.1
ER difference
Fu difference

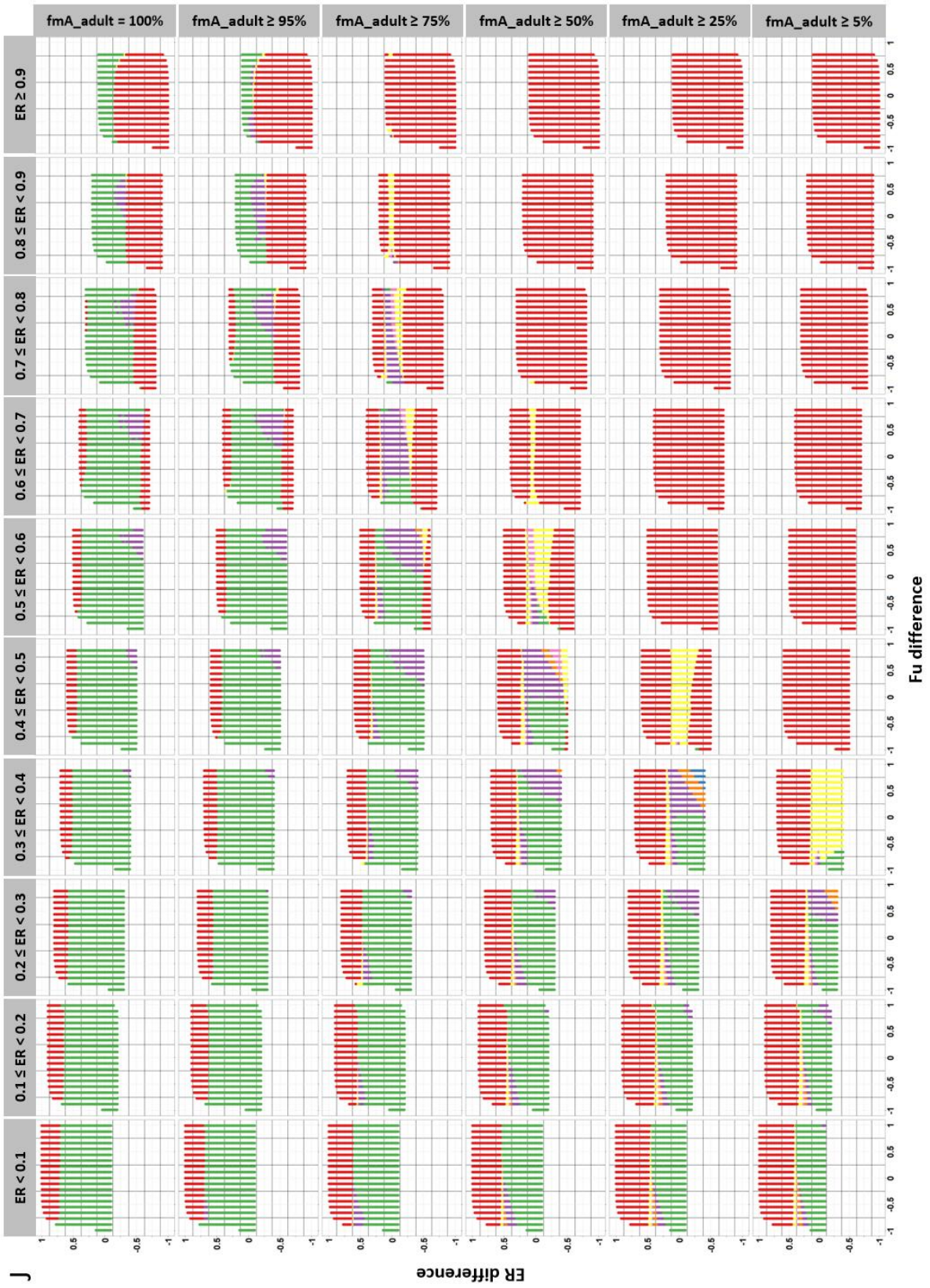
fmA_adult = 100%
fmA_adult ≥ 95%
fmA_adult ≥ 75%
fmA_adult ≥ 50%
fmA_adult ≥ 25%
fmA_adult ≥ 5%
ER ≥ 0.9
0.8 ≤ ER < 0.9
0.7 ≤ ER < 0.8
0.6 ≤ ER < 0.7
0.5 ≤ ER < 0.6
0.4 ≤ ER < 0.5
0.3 ≤ ER < 0.4
0.2 ≤ ER < 0.3
0.1 ≤ ER < 0.2
ER < 0.1
J
ER difference
Fu difference

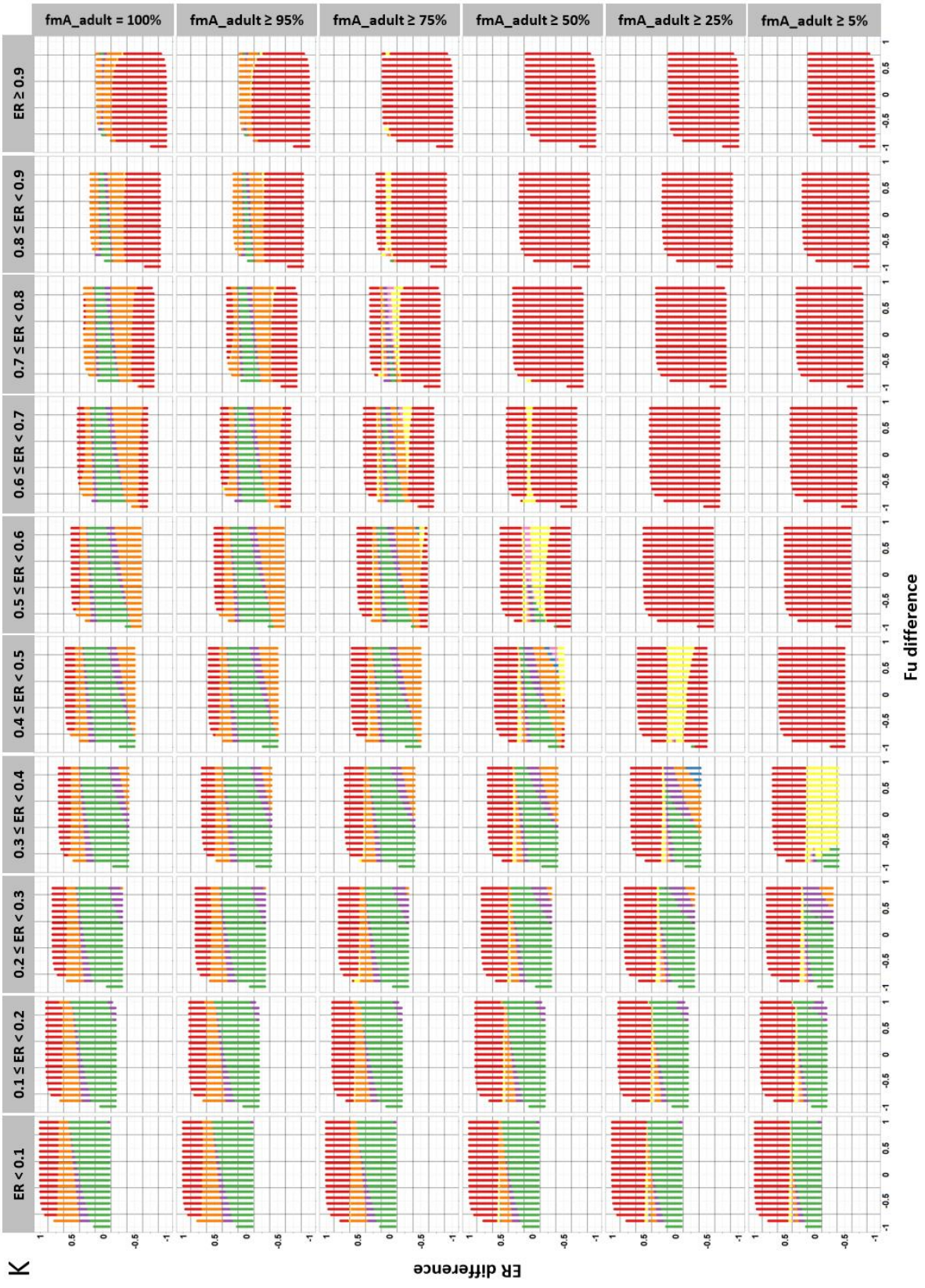
fmA_adult = 100%
fmA_adult ≥ 95%
fmA_adult ≥ 75%
fmA_adult ≥ 50%
fmA_adult ≥ 25%
fmA_adult ≥ 5%
ER ≥ 0.9
0.8 ≤ ER < 0.9
0.7 ≤ ER < 0.8
0.6 ≤ ER < 0.7
0.5 ≤ ER < 0.6
0.4 ≤ ER < 0.5
0.3 ≤ ER < 0.4
0.2 ≤ ER < 0.3
0.1 ≤ ER < 0.2
ER < 0.1
K
ER difference
Fu difference

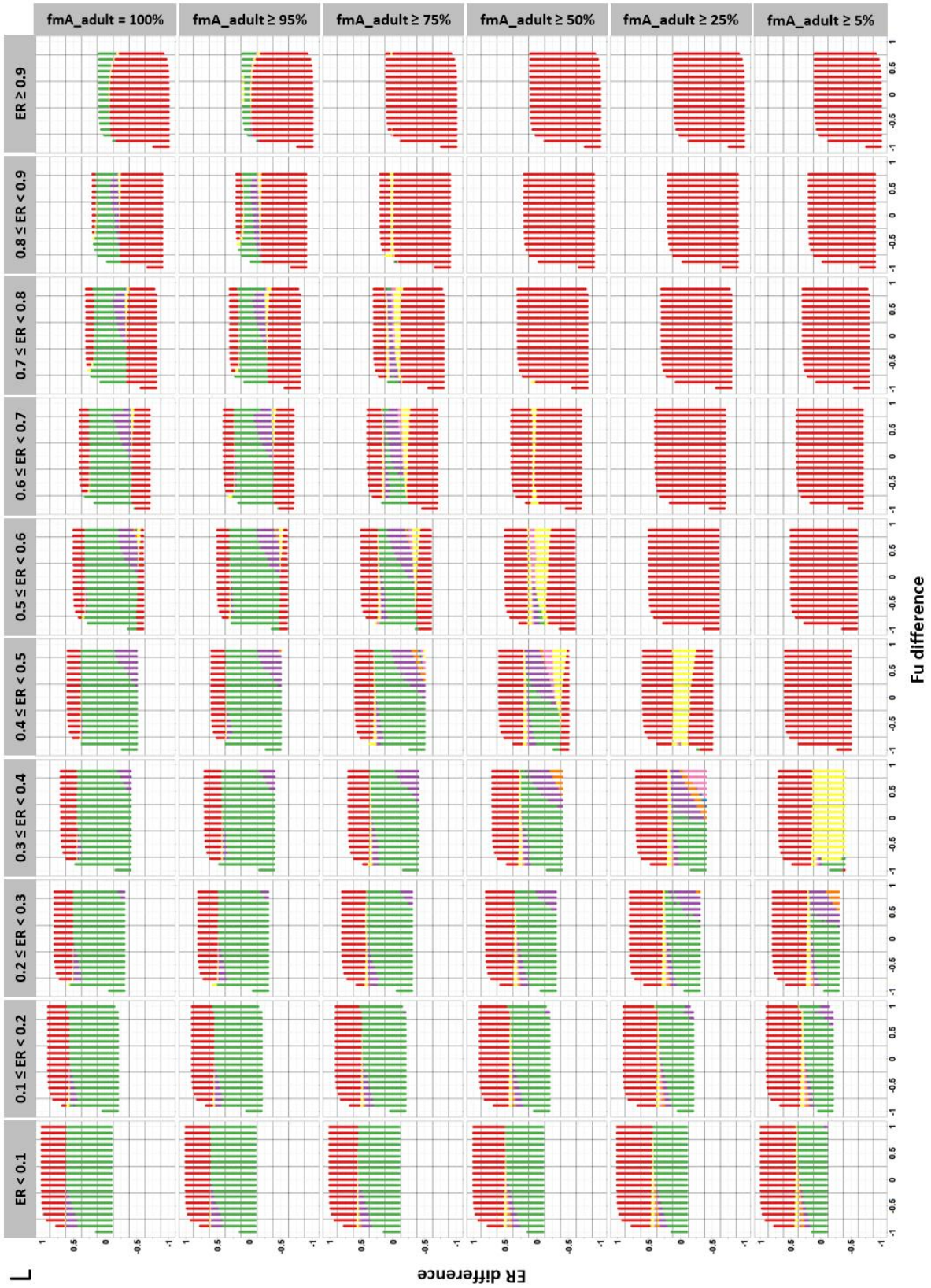
fmA_adult = 100%
fmA_adult ≥ 95%
fmA_adult ≥ 75%
fmA_adult ≥ 50%
fmA_adult ≥ 25%
fmA_adult ≥ 5%
ER ≥ 0.9
0.8 ≤ ER < 0.9
0.7 ≤ ER < 0.8
0.6 ≤ ER < 0.7
0.5 ≤ ER < 0.6
0.4 ≤ ER < 0.5
0.3 ≤ ER < 0.4
0.2 ≤ ER < 0.3
0.1 ≤ ER < 0.2
ER < 0.1
Fu difference
ER difference
1
0.5
0
-0.5
-1

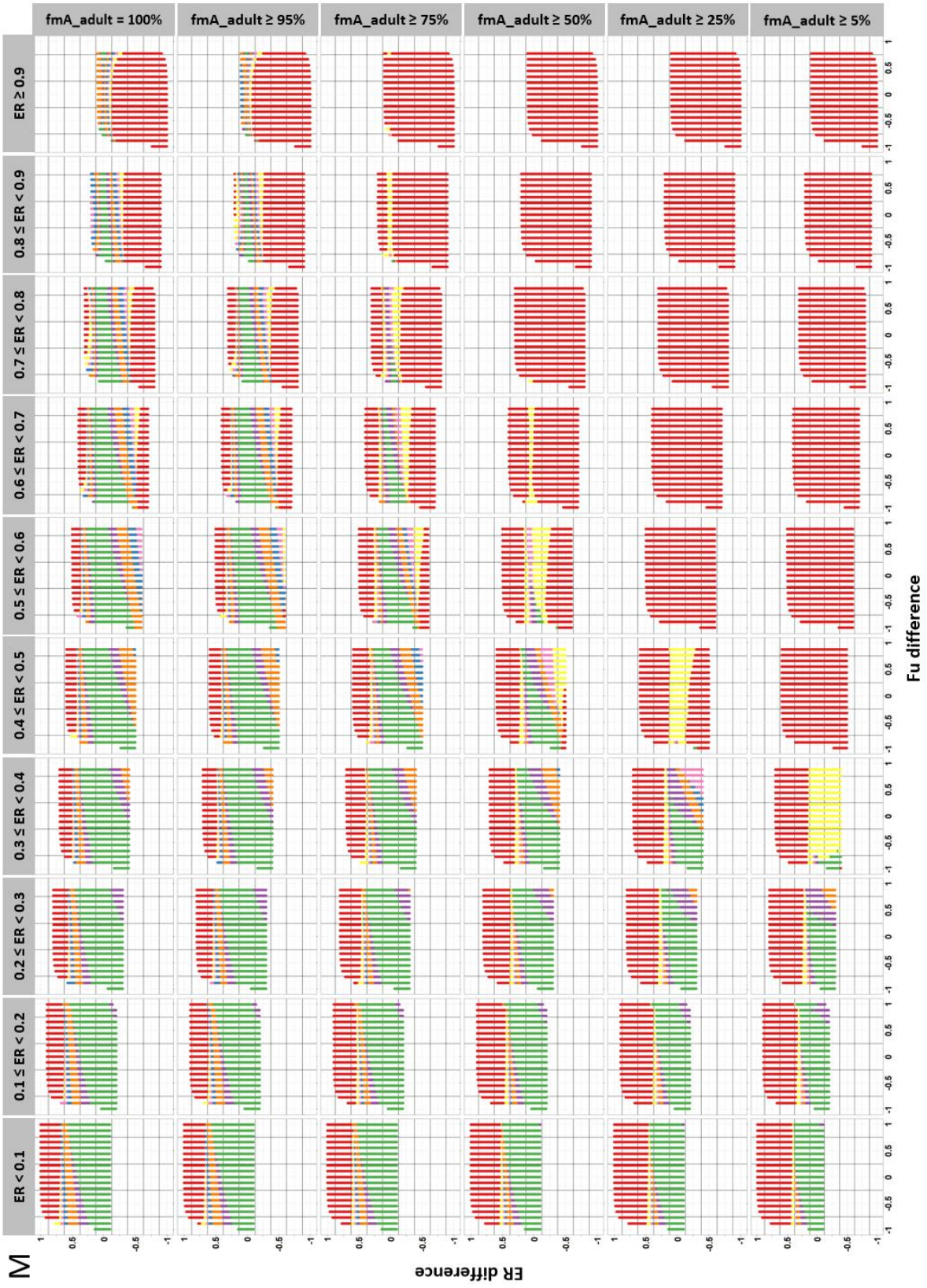
fmA_adult = 100%
fmA_adult ≥ 95%
fmA_adult ≥ 75%
fmA_adult ≥ 50%
fmA_adult ≥ 25%
fmA_adult ≥ 5%
ER ≥ 0.9
0.8 ≤ ER < 0.9
0.7 ≤ ER < 0.8
0.6 ≤ ER < 0.7
0.5 ≤ ER < 0.6
0.4 ≤ ER < 0.5
0.3 ≤ ER < 0.4
0.2 ≤ ER < 0.3
0.1 ≤ ER < 0.2
ER < 0.1
Fu difference
ER difference
M

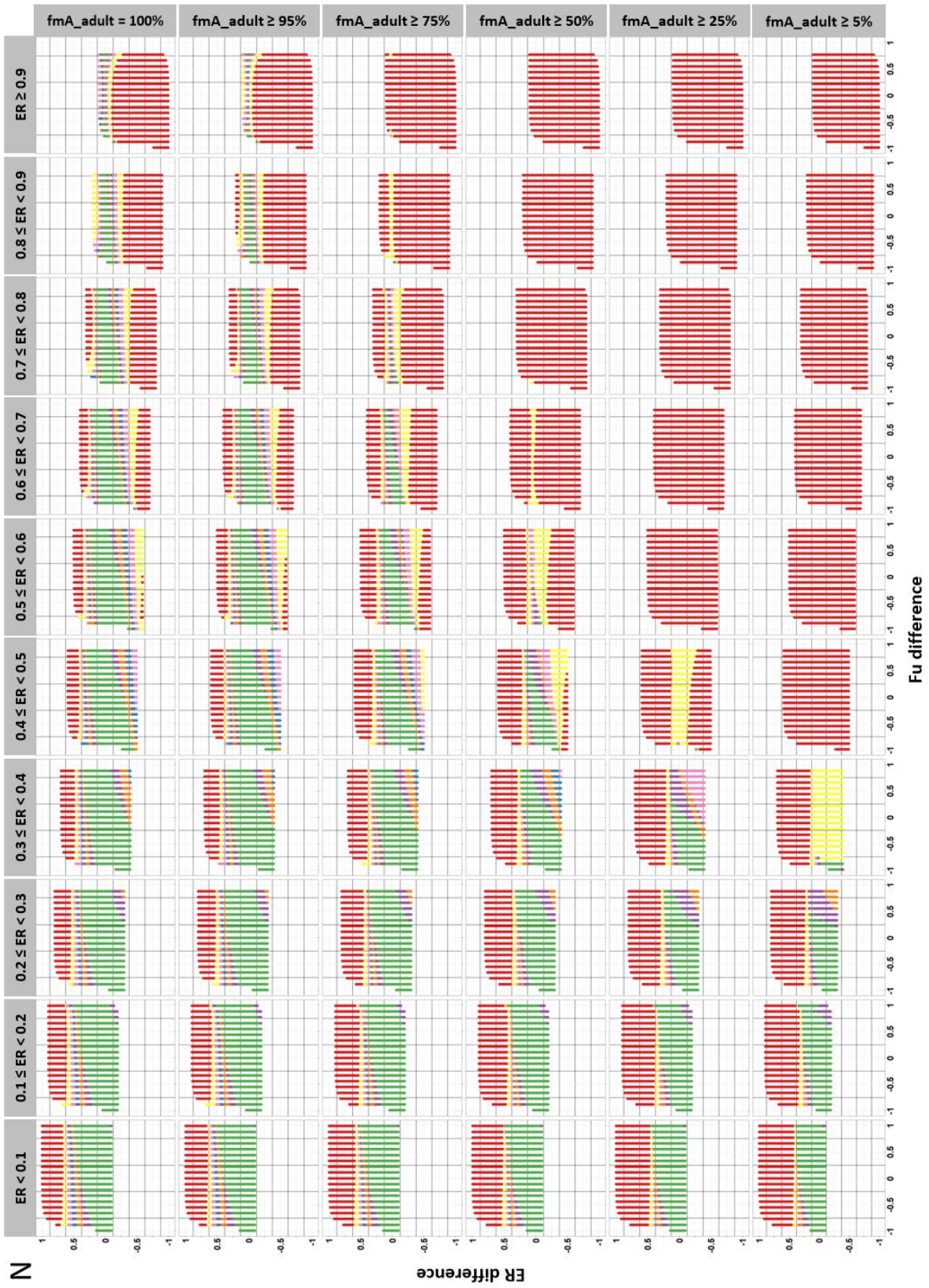
fmA_adult = 100%
fmA_adult ≥ 95%
fmA_adult ≥ 75%
fmA_adult ≥ 50%
fmA_adult ≥ 25%
fmA_adult ≥ 5%
ER ≥ 0.9
0.8 ≤ ER < 0.9
0.7 ≤ ER < 0.8
0.6 ≤ ER < 0.7
0.5 ≤ ER < 0.6
0.4 ≤ ER < 0.5
0.3 ≤ ER < 0.4
0.2 ≤ ER < 0.3
0.1 ≤ ER < 0.2
ER < 0.1
Fu difference
ER difference
N

fmA_adult = 100%
fmA_adult ≥ 95%
fmA_adult ≥ 75%
fmA_adult ≥ 50%
fmA_adult ≥ 25%
fmA_adult ≥ 5%
ER ≥ 0.9
0.8 ≤ ER < 0.9
0.7 ≤ ER < 0.8
0.6 ≤ ER < 0.7
0.5 ≤ ER < 0.6
0.4 ≤ ER < 0.5
0.3 ≤ ER < 0.4
0.2 ≤ ER < 0.3
0.1 ≤ ER < 0.2
ER < 0.1
Fu difference
ER difference

Supplementary material 3 Model-test drug scenarios, for drugs binding to alpha-1 acid glycoprotein, that lead to accurate pathway specific CLp predictions for a test drug after between-drug extrapolation of a pathway specific pediatric covariate function.

Figures A to O display model-test drug scenarios that lead to accurate pathway specific CLp predictions for a test drug after between-drug extrapolation of a pathway specific pediatric covariate function. Results are displayed for drugs binding to alpha-1 acid glycoprotein (AAG) and eliminated through CYP1A2 (A), CYP2A6 (B), CYP2B6 (C), CYP2C8 (D), CYP2C9 (E), CYP2C18_19 (F), CYP2D6 (G), CYP2E1 (H), CYP3A4 (I), SULT1A1 (J), UGT1A1 (K), UGT1A4 (L), UGT1A6 (M), UGT1A9 (N) and UGT2B7 (O) hepatic metabolism. Each column corresponds to a range of extraction ratio (ER) values for the model drug in adults and each row to a specific range of fraction of drug (model and test drug) that is metabolized by CYP1A2 in adults (fmA_adult). For each graph, the y-axis represents the difference in ER between the test drug and the model drug (ER test drug – ER model drug) in adults, and the x-axis represents the difference in fraction unbound (fu) between the test drugs and the model drug in adults (fu test drug – fu model drug). Each dot represents a model-test drug scenario, including multiple model-test drug combinations. A color code is used to indicate systematically accurate CLp predictions for all model-test drug combinations within a model-test drug scenario, for children ≥ 5 years (yellow), ≥ 2 years (pink), ≥ 1 year (blue), ≥ 6 months (orange), ≥ 1 month (purple), and ≥ 1 day term neonates (green). Red dots indicate model-test drug scenarios leading to inaccurate predictions in children older than 5 years for at least one model-test drug combination within the model-test drug scenario. As an example, systematically accurate CLp scaling in children of 6 months and older is represented by the combination of the green, purple and orange dots. The table below summarizes the color code used to indicate systematically accurate scaled pediatric CLp (+) and inaccurate scaled pediatric CLp (-) in the different ages studied.

1 day	1 month	6 months	1 year	2 years	≥ 5 years	
+	+	+	+	+	+	**green**
-	+	+	+	+	+	**purple**
-	-	+	+	+	+	**orange**
-	-	-	+	+	+	**blue**
-	-	-	-	+	+	**pink**
-	-	-	-	-	+	**Yellow**
-	-	-	-	-	-	**Red**

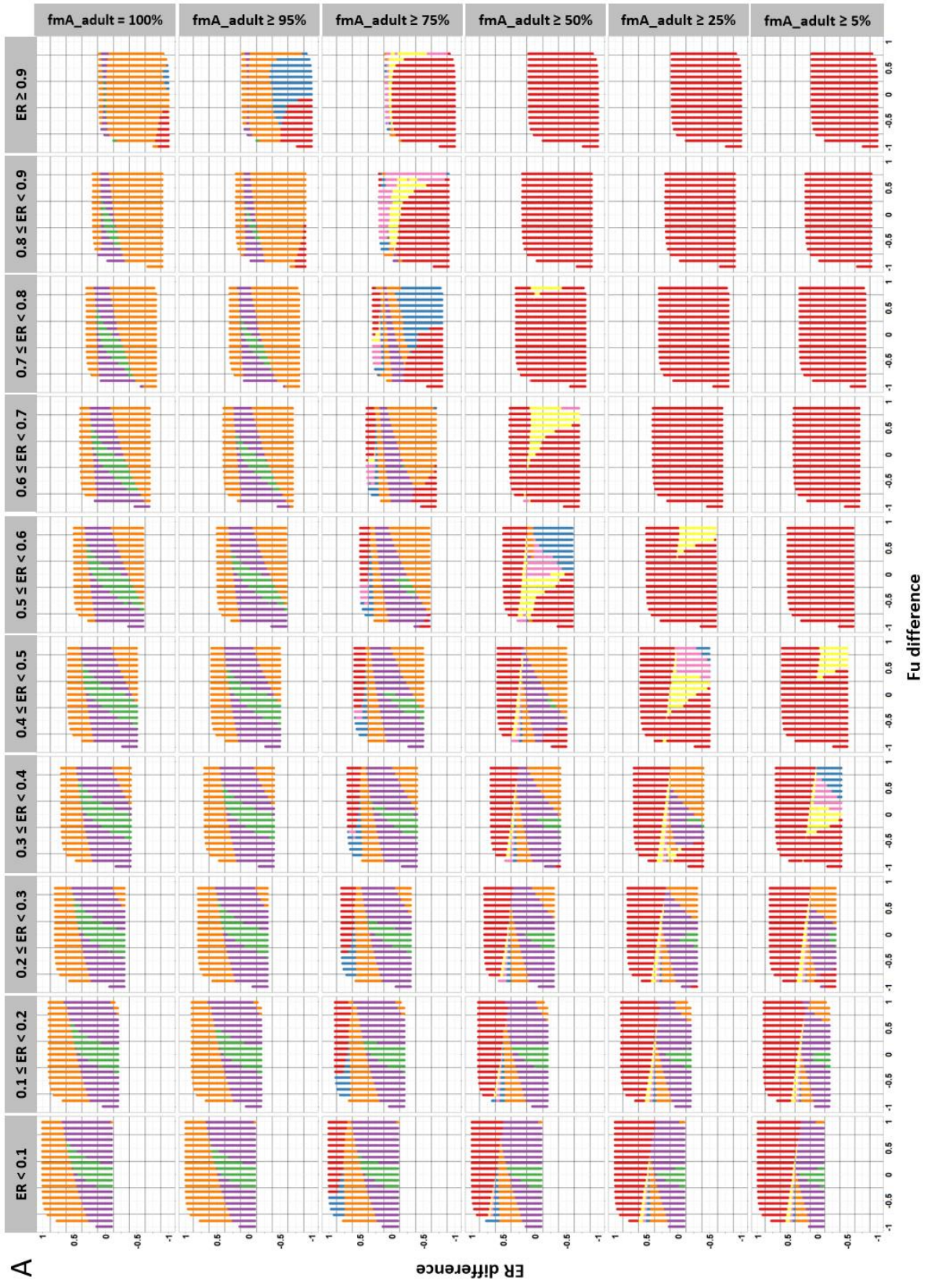
A
fmA_adult = 100%
fmA_adult ≥ 95%
fmA_adult ≥ 75%
fmA_adult ≥ 50%
fmA_adult ≥ 25%
fmA_adult ≥ 5%
ER ≥ 0.9
0.8 ≤ ER < 0.9
0.7 ≤ ER < 0.8
0.6 ≤ ER < 0.7
0.5 ≤ ER < 0.6
0.4 ≤ ER < 0.5
0.3 ≤ ER < 0.4
0.2 ≤ ER < 0.3
0.1 ≤ ER < 0.2
ER < 0.1
ER difference
Fu difference

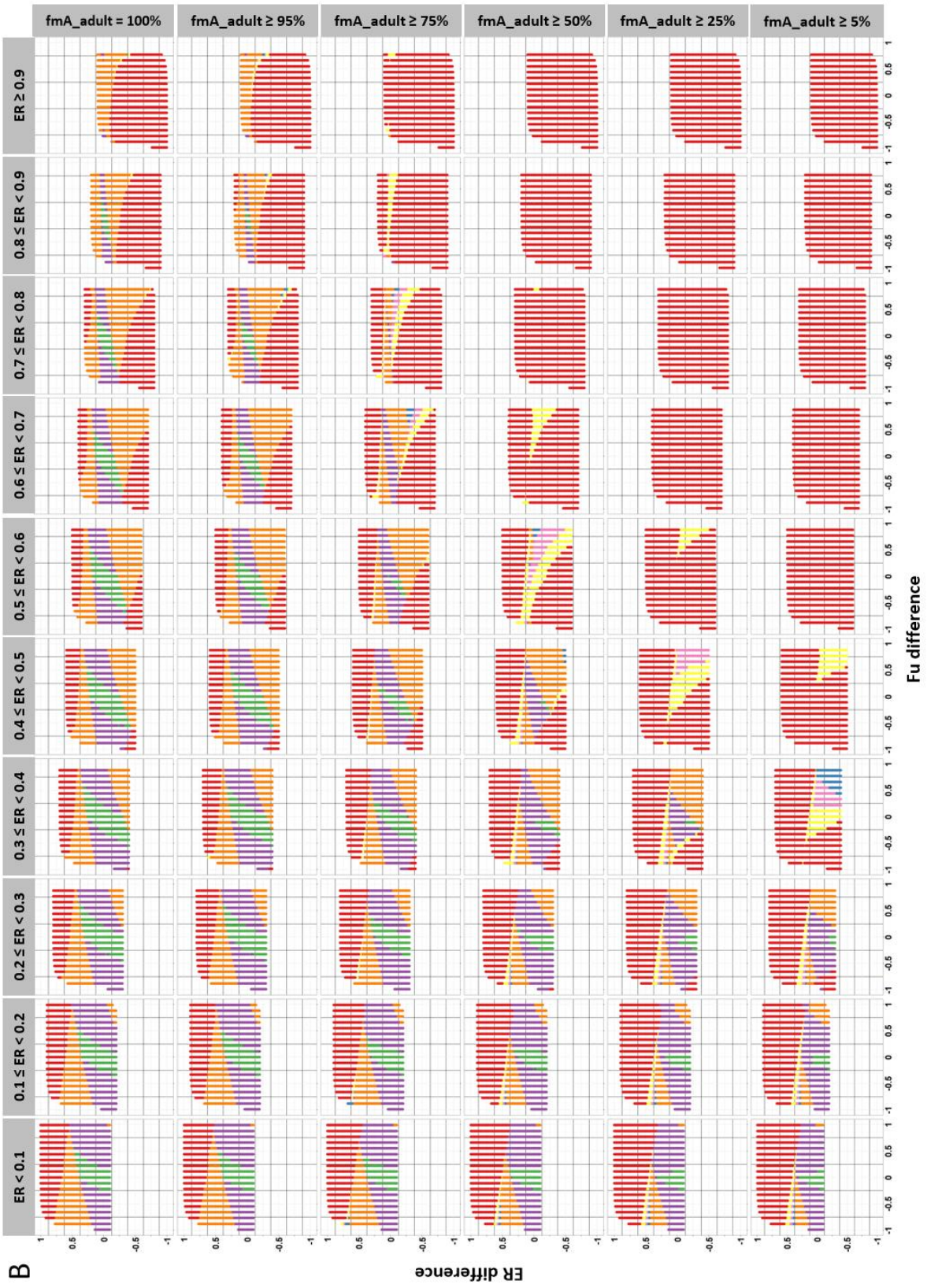
B
fmA_adult = 100%
fmA_adult ≥ 95%
fmA_adult ≥ 75%
fmA_adult ≥ 50%
fmA_adult ≥ 25%
fmA_adult ≥ 5%
ER ≥ 0.9
0.8 ≤ ER < 0.9
0.7 ≤ ER < 0.8
0.6 ≤ ER < 0.7
0.5 ≤ ER < 0.6
0.4 ≤ ER < 0.5
0.3 ≤ ER < 0.4
0.2 ≤ ER < 0.3
0.1 ≤ ER < 0.2
ER < 0.1
ER difference
Fu difference

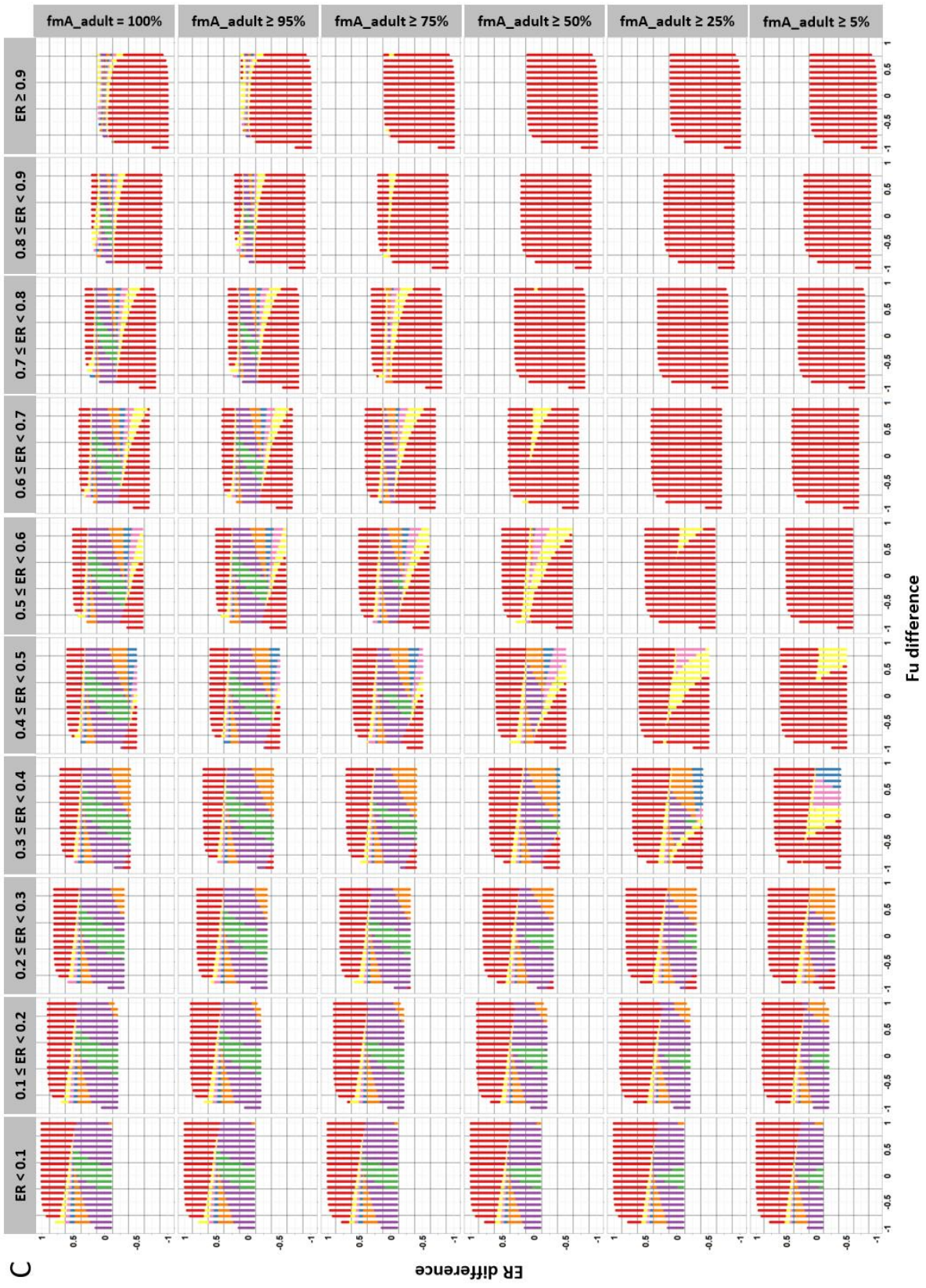
fmA_adult = 100%
fmA_adult ≥ 95%
fmA_adult ≥ 75%
fmA_adult ≥ 50%
fmA_adult ≥ 25%
fmA_adult ≥ 5%
ER ≥ 0.9
0.8 ≤ ER < 0.9
0.7 ≤ ER < 0.8
0.6 ≤ ER < 0.7
0.5 ≤ ER < 0.6
0.4 ≤ ER < 0.5
0.3 ≤ ER < 0.4
0.2 ≤ ER < 0.3
0.1 ≤ ER < 0.2
ER < 0.1
ER difference
Fu difference
C

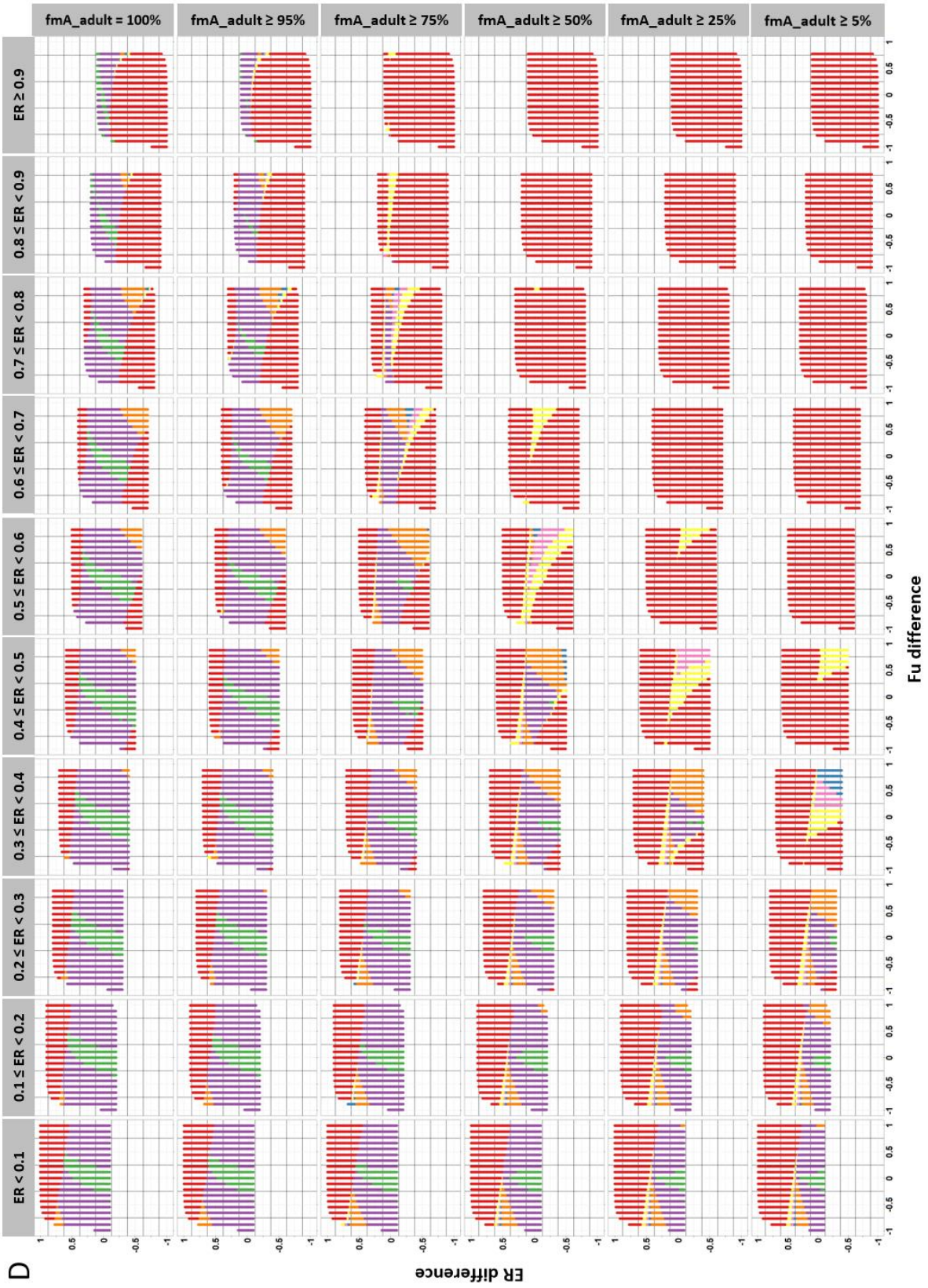
D
fmA_adult = 100%
fmA_adult ≥ 95%
fmA_adult ≥ 75%
fmA_adult ≥ 50%
fmA_adult ≥ 25%
fmA_adult ≥ 5%
ER ≥ 0.9
0.8 ≤ ER < 0.9
0.7 ≤ ER < 0.8
0.6 ≤ ER < 0.7
0.5 ≤ ER < 0.6
0.4 ≤ ER < 0.5
0.3 ≤ ER < 0.4
0.2 ≤ ER < 0.3
0.1 ≤ ER < 0.2
ER < 0.1
ER difference
Fu difference

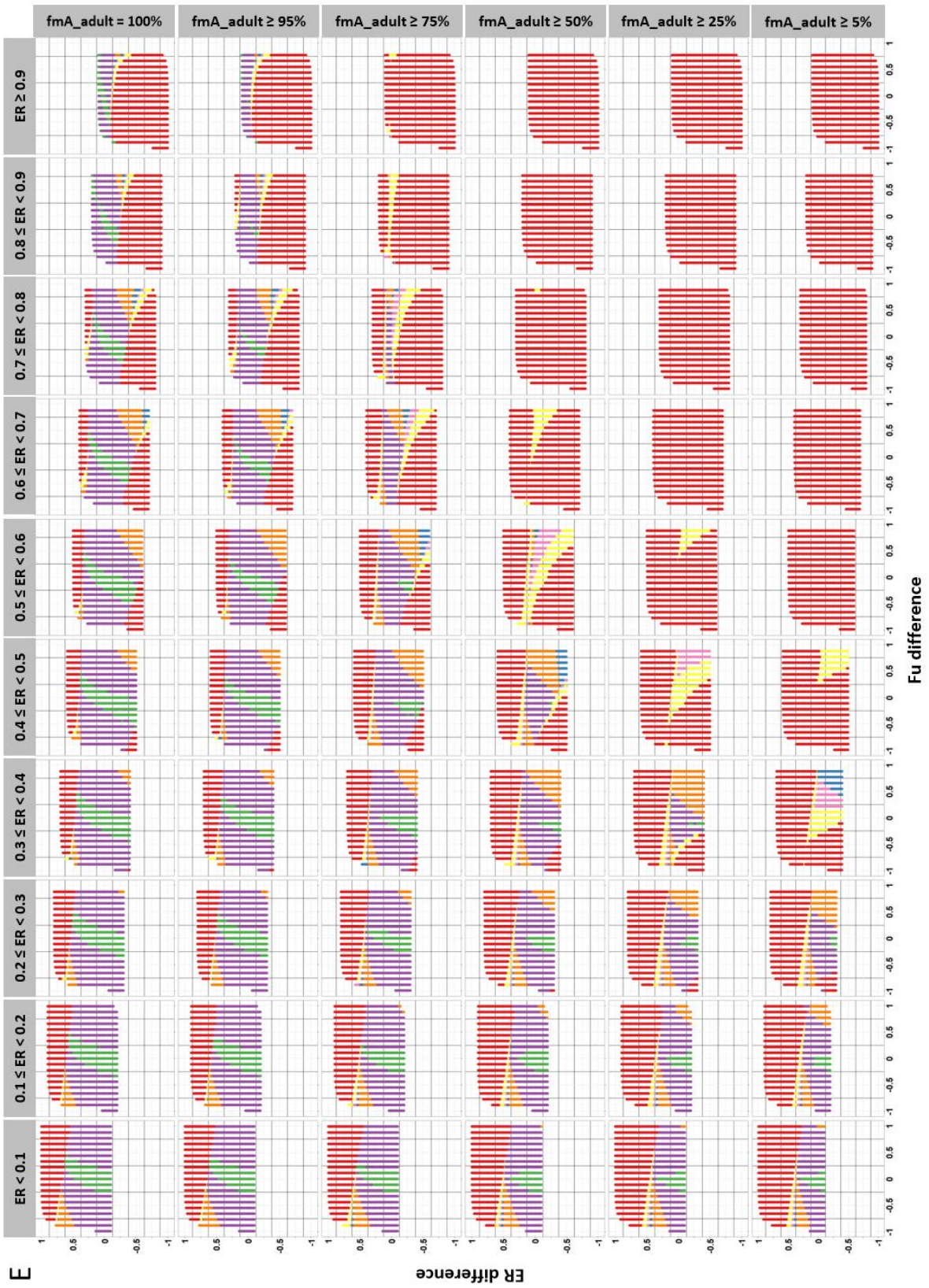
fmA_adult = 100%
fmA_adult ≥ 95%
fmA_adult ≥ 75%
fmA_adult ≥ 50%
fmA_adult ≥ 25%
fmA_adult ≥ 5%
ER ≥ 0.9
0.8 ≤ ER < 0.9
0.7 ≤ ER < 0.8
0.6 ≤ ER < 0.7
0.5 ≤ ER < 0.6
0.4 ≤ ER < 0.5
0.3 ≤ ER < 0.4
0.2 ≤ ER < 0.3
0.1 ≤ ER < 0.2
ER < 0.1
ER difference
Fu difference

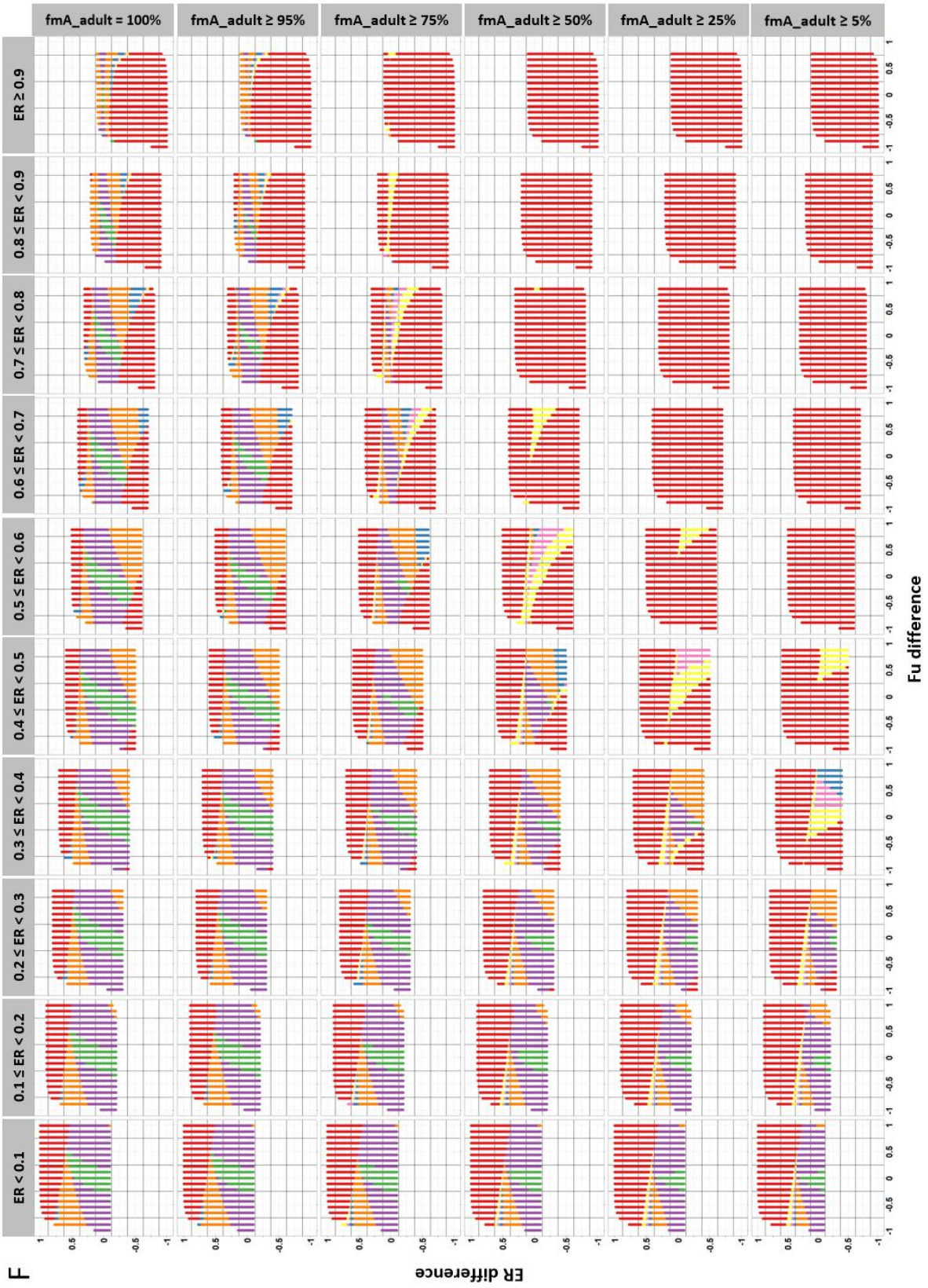
fmA_adult = 100%
fmA_adult ≥ 95%
fmA_adult ≥ 75%
fmA_adult ≥ 50%
fmA_adult ≥ 25%
fmA_adult ≥ 5%
ER ≥ 0.9
0.8 ≤ ER < 0.9
0.7 ≤ ER < 0.8
0.6 ≤ ER < 0.7
0.5 ≤ ER < 0.6
0.4 ≤ ER < 0.5
0.3 ≤ ER < 0.4
0.2 ≤ ER < 0.3
0.1 ≤ ER < 0.2
ER < 0.1
Fu difference
ER difference
1
0.5
0
-0.5
-1

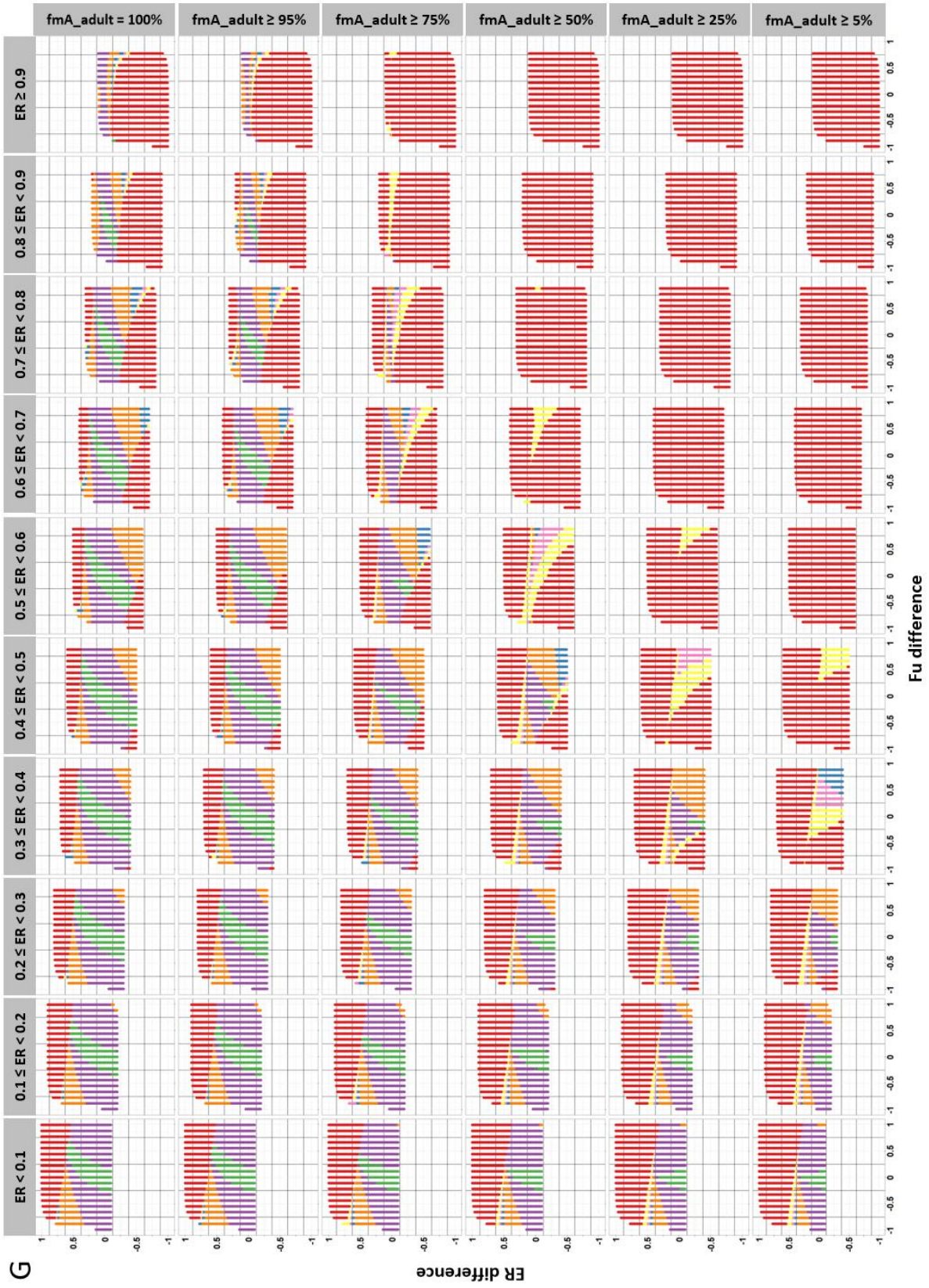
fmA_adult = 100%
fmA_adult ≥ 95%
fmA_adult ≥ 75%
fmA_adult ≥ 50%
fmA_adult ≥ 25%
fmA_adult ≥ 5%
ER ≥ 0.9
0.8 ≤ ER < 0.9
0.7 ≤ ER < 0.8
0.6 ≤ ER < 0.7
0.5 ≤ ER < 0.6
0.4 ≤ ER < 0.5
0.3 ≤ ER < 0.4
0.2 ≤ ER < 0.3
0.1 ≤ ER < 0.2
ER < 0.1
Fu difference
ER difference
G

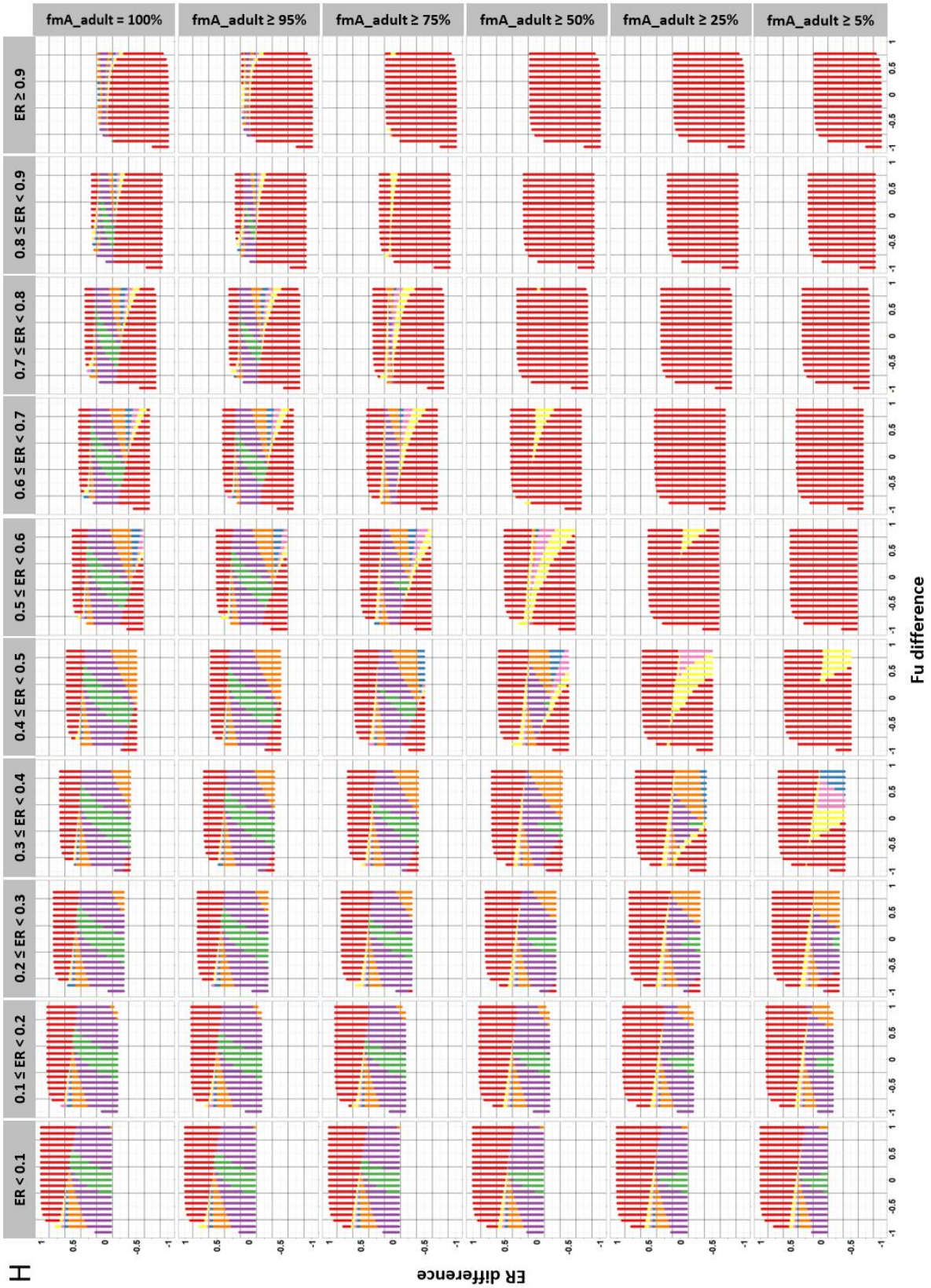
H
ER difference
Fu difference
fmA_adult = 100%
fmA_adult ≥ 95%
fmA_adult ≥ 75%
fmA_adult ≥ 50%
fmA_adult ≥ 25%
fmA_adult ≥ 5%
ER ≥ 0.9
0.8 ≤ ER < 0.9
0.7 ≤ ER < 0.8
0.6 ≤ ER < 0.7
0.5 ≤ ER < 0.6
0.4 ≤ ER < 0.5
0.3 ≤ ER < 0.4
0.2 ≤ ER < 0.3
0.1 ≤ ER < 0.2
ER < 0.1

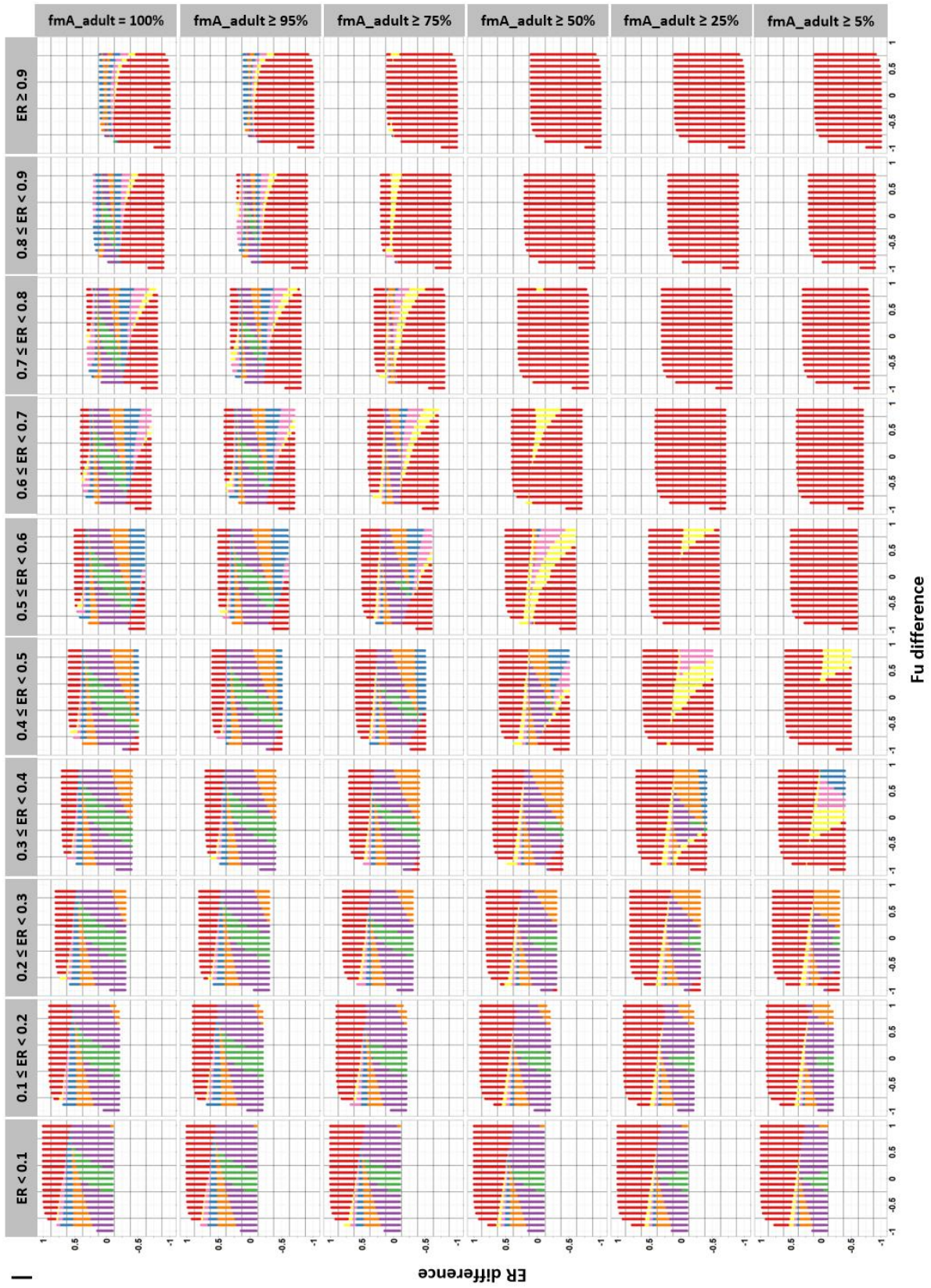
fmA_adult = 100%
fmA_adult ≥ 95%
fmA_adult ≥ 75%
fmA_adult ≥ 50%
fmA_adult ≥ 25%
fmA_adult ≥ 5%
ER ≥ 0.9
0.8 ≤ ER < 0.9
0.7 ≤ ER < 0.8
0.6 ≤ ER < 0.7
0.5 ≤ ER < 0.6
0.4 ≤ ER < 0.5
0.3 ≤ ER < 0.4
0.2 ≤ ER < 0.3
0.1 ≤ ER < 0.2
ER < 0.1
ER difference
Fu difference

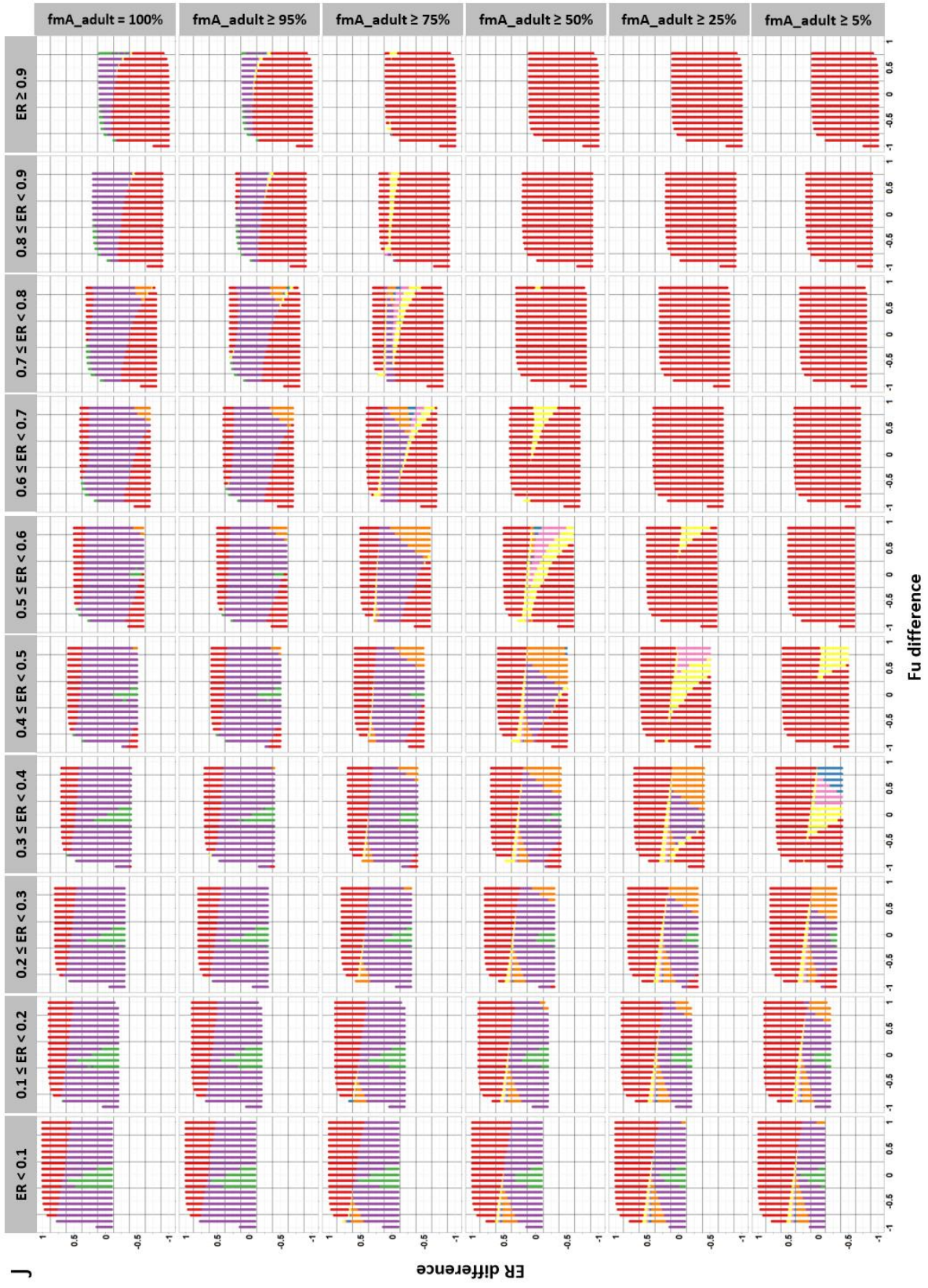
fmA_adult = 100%
fmA_adult ≥ 95%
fmA_adult ≥ 75%
fmA_adult ≥ 50%
fmA_adult ≥ 25%
fmA_adult ≥ 5%
ER ≥ 0.9
0.8 ≤ ER < 0.9
0.7 ≤ ER < 0.8
0.6 ≤ ER < 0.7
0.5 ≤ ER < 0.6
0.4 ≤ ER < 0.5
0.3 ≤ ER < 0.4
0.2 ≤ ER < 0.3
0.1 ≤ ER < 0.2
ER < 0.1
J
ER difference
Fu difference

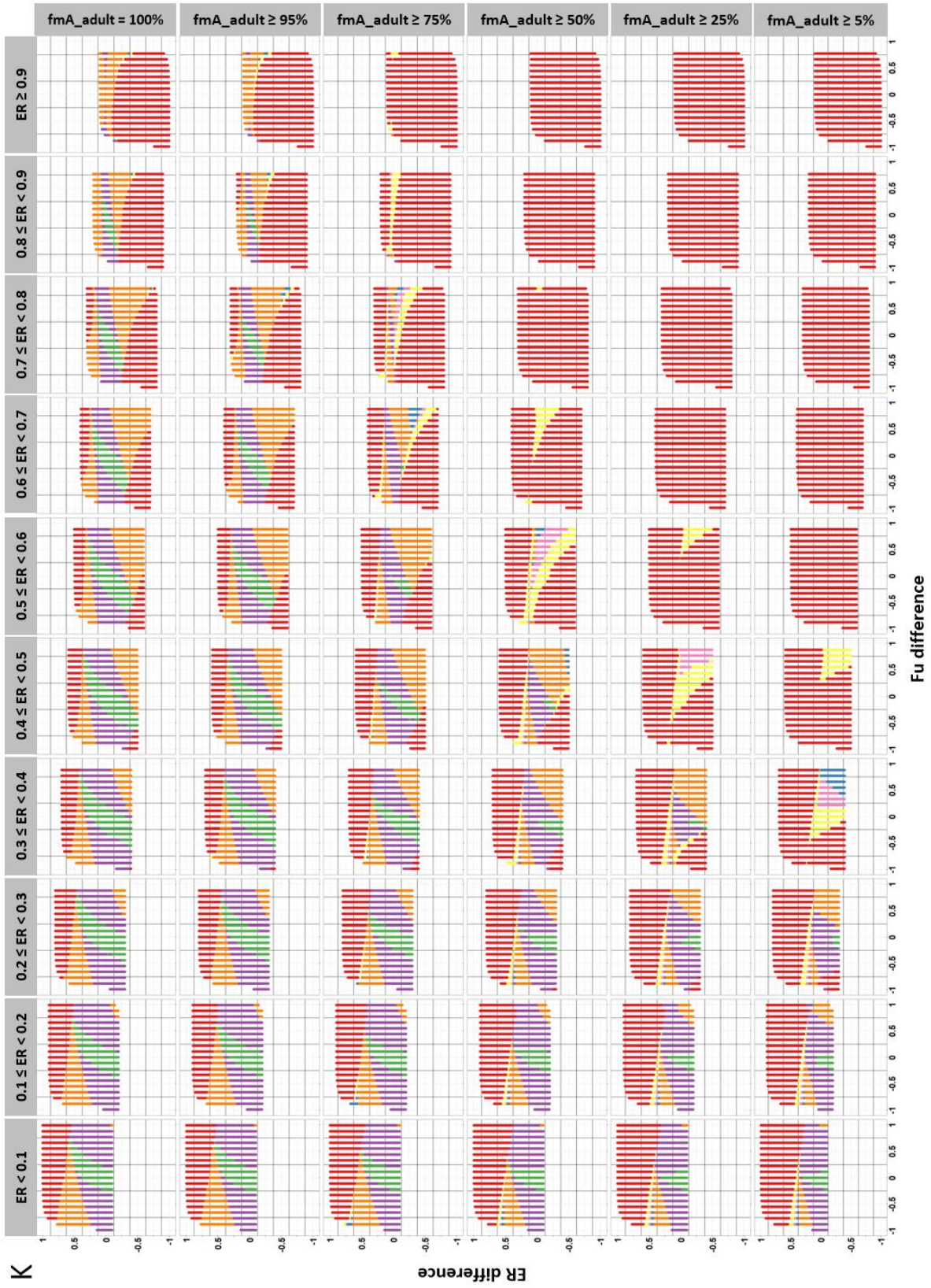
fmA_adult = 100%
fmA_adult ≥ 95%
fmA_adult ≥ 75%
fmA_adult ≥ 50%
fmA_adult ≥ 25%
fmA_adult ≥ 5%
ER ≥ 0.9
0.8 ≤ ER < 0.9
0.7 ≤ ER < 0.8
0.6 ≤ ER < 0.7
0.5 ≤ ER < 0.6
0.4 ≤ ER < 0.5
0.3 ≤ ER < 0.4
0.2 ≤ ER < 0.3
0.1 ≤ ER < 0.2
ER < 0.1
K
ER difference
Fu difference

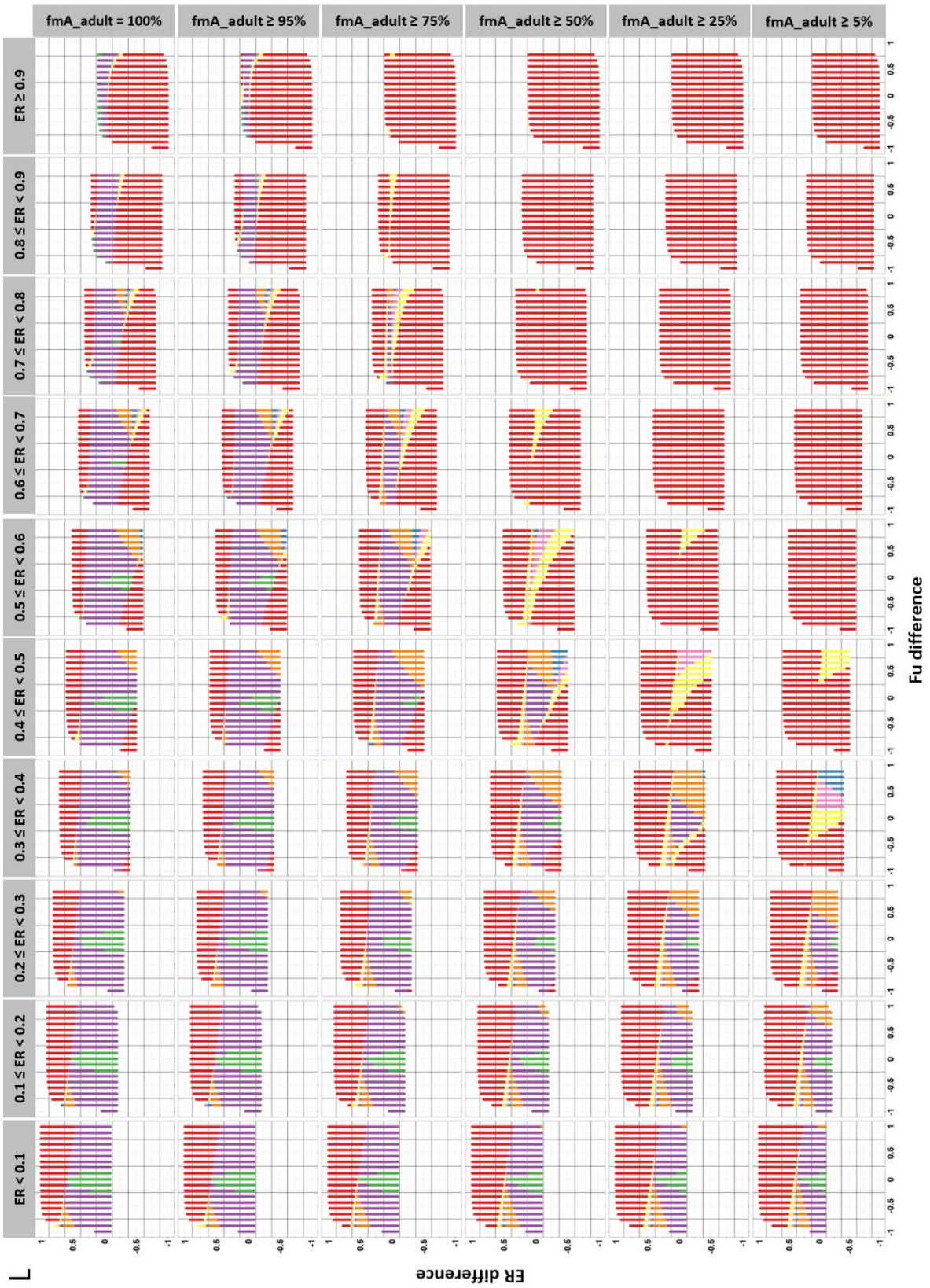
fmA_adult = 100%
fmA_adult ≥ 95%
fmA_adult ≥ 75%
fmA_adult ≥ 50%
fmA_adult ≥ 25%
fmA_adult ≥ 5%
ER ≥ 0.9
0.8 ≤ ER < 0.9
0.7 ≤ ER < 0.8
0.6 ≤ ER < 0.7
0.5 ≤ ER < 0.6
0.4 ≤ ER < 0.5
0.3 ≤ ER < 0.4
0.2 ≤ ER < 0.3
0.1 ≤ ER < 0.2
ER < 0.1
Fu difference
ER difference
1
0.5
0
-0.5
-1

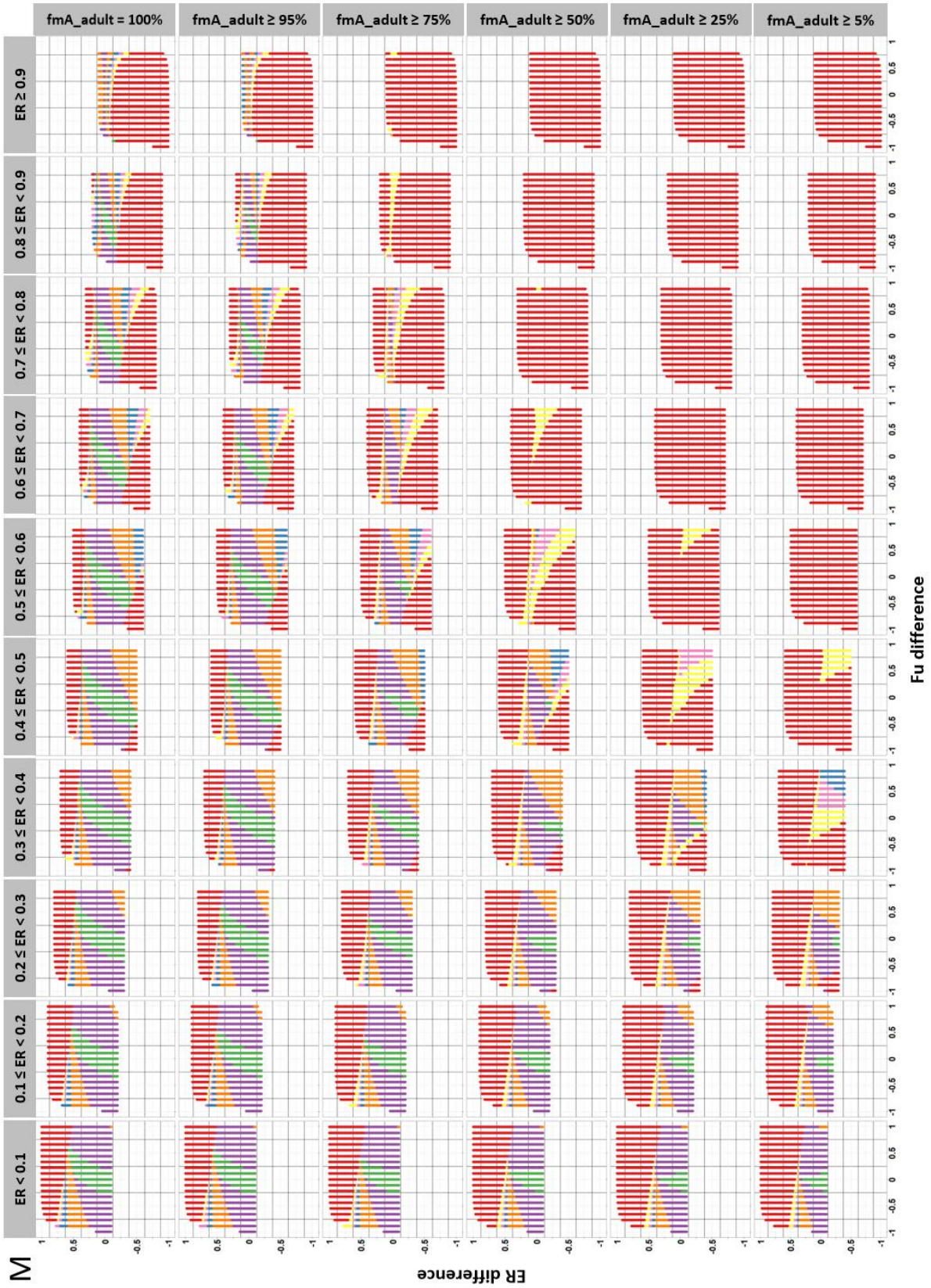
fmA_adult = 100%
fmA_adult ≥ 95%
fmA_adult ≥ 75%
fmA_adult ≥ 50%
fmA_adult ≥ 25%
fmA_adult ≥ 5%
ER ≥ 0.9
0.8 ≤ ER < 0.9
0.7 ≤ ER < 0.8
0.6 ≤ ER < 0.7
0.5 ≤ ER < 0.6
0.4 ≤ ER < 0.5
0.3 ≤ ER < 0.4
0.2 ≤ ER < 0.3
0.1 ≤ ER < 0.2
ER < 0.1
M
ER difference
Fu difference

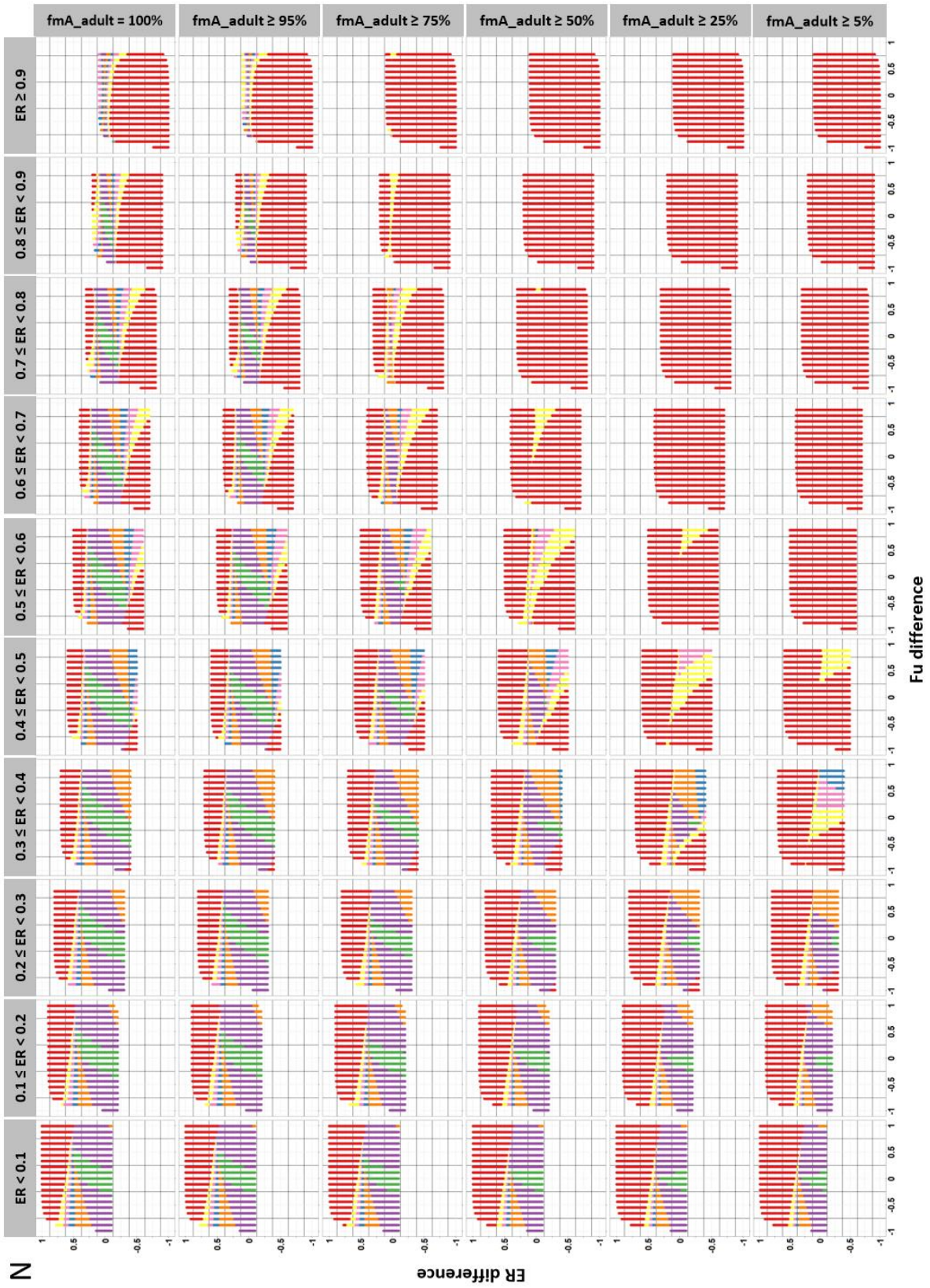
fmA_adult = 100%
fmA_adult ≥ 95%
fmA_adult ≥ 75%
fmA_adult ≥ 50%
fmA_adult ≥ 25%
fmA_adult ≥ 5%
ER ≥ 0.9
0.8 ≤ ER < 0.9
0.7 ≤ ER < 0.8
0.6 ≤ ER < 0.7
0.5 ≤ ER < 0.6
0.4 ≤ ER < 0.5
0.3 ≤ ER < 0.4
0.2 ≤ ER < 0.3
0.1 ≤ ER < 0.2
ER < 0.1
Fu difference
ER difference
N

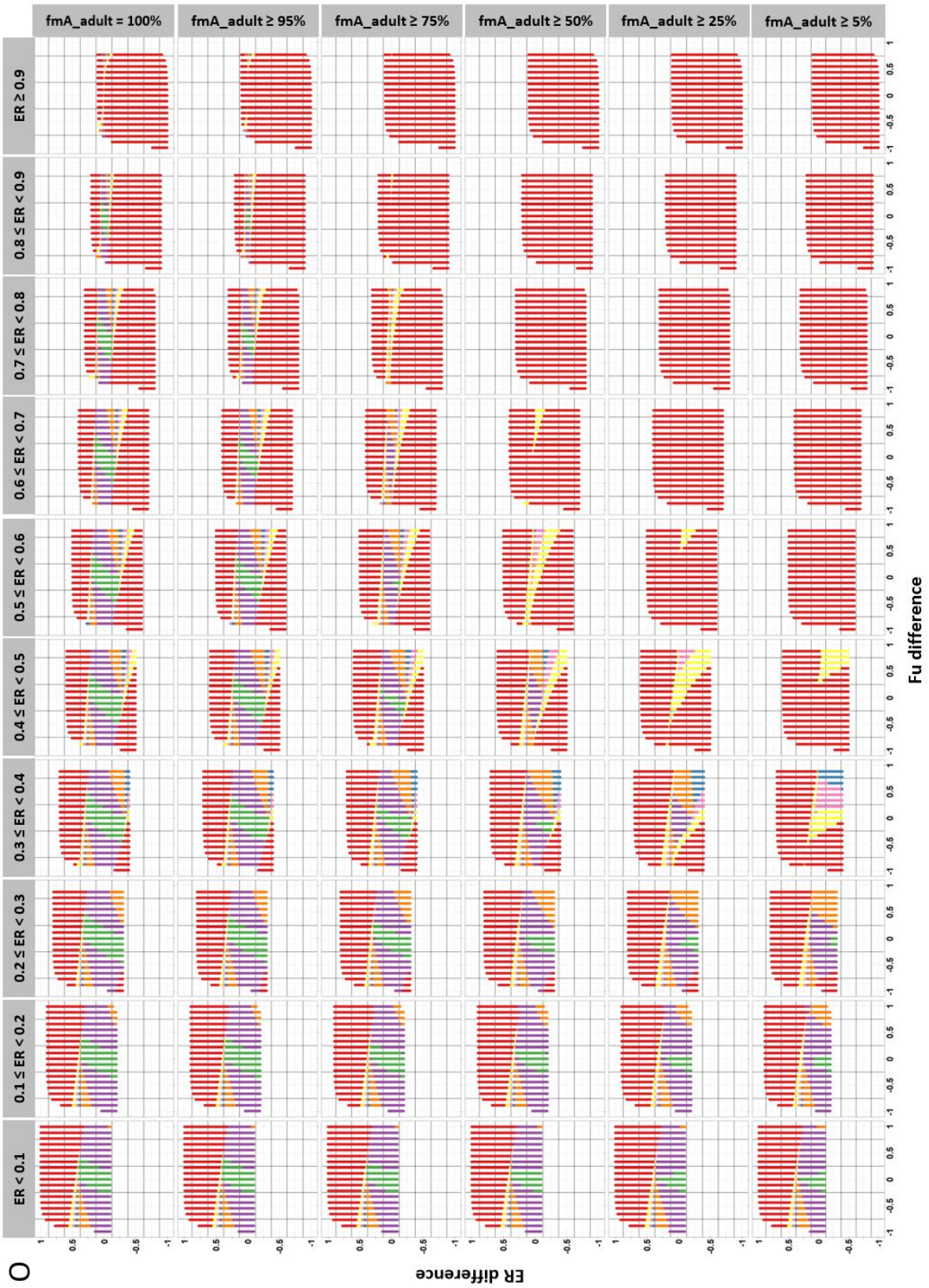
fmA_adult = 100%
fmA_adult ≥ 95%
fmA_adult ≥ 75%
fmA_adult ≥ 50%
fmA_adult ≥ 25%
fmA_adult ≥ 5%
ER ≥ 0.9
0.8 ≤ ER < 0.9
0.7 ≤ ER < 0.8
0.6 ≤ ER < 0.7
0.5 ≤ ER < 0.6
0.4 ≤ ER < 0.5
0.3 ≤ ER < 0.4
0.2 ≤ ER < 0.3
0.1 ≤ ER < 0.2
ER < 0.1
ER difference
Fu difference

Model Code Supplementary Material

R model code for CLp, ER and CLpA simulations

```
################################################################################
############################## Demographic values ##############################
################################################################################

# Typical individuals are characterized by a specific post-natal age, bodyweight and height
# AGE: post-natal age (years)
# BW: bodyweight (kg)
# HT: height (cm)
# BSA: body surface area (square meters), derived based on HT and BW

# Vector of investigated post-natal ages (years)
AGE_vector<- c(1/365,30/365,0.5,1,2,5,15,25)

# Vector of investigated bodyweights (kg)
BW_vector <- c(3.45,4.3,7.55,9.9,12.35,18.25,54.25,72.65)

# Vector of investigated heights (cm)
HT_vector<- c(49.75,54.25,66,74.75,86,108.25,166,172.30)

# Selection of the age of the typical pediatric patient for which simulations are performed (1 for
neonates of 1 day, 2 and 3 for infants of 1 and 6 months respectively, 4, 5 and 6 for for children
of 1, 2 and 5 years respectively, 7 for adolescent of 15 years and 8 for adults of 25 years)
Age_index <- 1

# Post-natal age (years) for the selected typical individual
AGE<- AGE_vector[Age_index]

# Bodyweight (kg) for the selected typical individual
BW<- BW_vector[Age_index]

# Height (cm) for the selected typical individual
HT<- HT_vector[Age_index]


# Body surface area for children of 15kg or less, formula from Haycock et al.
BSA_Haycock <- function(HT,BW){
BSA <- 0.024265 * HT**0.3964 * BW**0.5378
BSA
}

# Body surface area for children >15kg and adults, formula from Dubois and Dubois
BSA_Dubois <- function(HT,BW){
BSA <- 0.007184 * HT**0.725 * BW**0.425
BSA
}

# Selection of the BSA formula according to the bodyweight of the selected typical individual
(BW) for which simulations are performed
```

```
BSA <- ifelse(BW>15,BSA_Dubois(HT,BW),BSA_Haycock(HT,BW))

################################################################################
########################### Drug-specific parameters ###########################
################################################################################

### Selection of drug specific parameters using the index of the selected values within each
vector (value between square brackets)

# Adult total unbound intrinsic microsomal clearance (L/min/mg microsome)
CLintmictotal_adult <- seq(from=0.56/1000000, to=0.209/1000, length.out= 42) [4]

# Adult unbound drug fraction in plasma (similar for HSA bound drugs and AAG bound drugs).
fu_adult <- seq(from=0.01,to=1, by=0.11)[10]

# Blood to plasma partition coefficient.
Kp <- c(0.35,1,2,3,4,5,10,20,40)[2]

# Fraction of the drug metabolized by IA in adults. For drugs metabolized by one
isoennzyme,fmA_adult = 1
fmA_adult <- c(1,0.95,0.75,0.5,0.25,0.05) [2]


################################################################################
########################### System-specific parameters #########################
################################################################################

### Hepatic blood flow (QH)

# Cardiac output (L/min)
CO <- (BSA*(110 + 184.974*(exp(-0.0378*AGE)-exp(-0.24477*AGE)))/60)

# QH: hepatic blood flow (L/min), expressed as a fraction of the cardiac output (CO). 26.75% is
the average between males (25.5%) and females (28%).
QH <- CO * 0.2675


### Human serum albumin (HSA) concentration (g/L). HSA concentration changes with age (age
dependent)

# HSA concentration (g/L) for the different investigated post-natal ages (AGE)
HSA_vector <- c(35.78,39.94,42.07,42.90,43.73,44.82,44.68,43.94)
# HSA concentration (g/L) in adults
HSA_adult <- HSA_vector[8]

# HSA concentration (g/L) for a selected post-natal age
HSA <- HSA_vector[Age_index]
### Alpha-1-acid glycoprotein concentration (g/L). AAG concentration changes with age (age
dependent)

# AAG concentration (g/L) for the different investigated post-natal ages (AGE)
AAG_vector <- c(0.2678,0.5497,0.6774,0.7172,0.7512,0.7877,0.6711,0.6847)
```

```
# AAG concentration (g/L) in adults
AAG_adult <- AAG_vector[8]

# AAG concentration (g/L) for a selected post-natal age
AAG <- AAG_vector[Age_index]


### Hematocrit

# Vector of investigated hematocrit values for the different investigated post-natal ages
Hematocrit_vector <- c(51.93,38.14,35.11,35.78,36.79,38.29,40.01,40.74)/100

# Hematocrit value for a selected post natal age
Hematocrit <- Hematocrit_vector[Age_index]


### Microsomal Protein Per Gram of Liver (mg/g)
# Microsomal Protein Per Gram of Liver (mg/g) for a selected postnatal age
MPPGL <- 10**(1.407+0.01579*AGE-0.0003824*AGE**2+0.00000237*AGE**3)

### Isoenzyme ontogeny values
CYP1A2 <- c(24.03,35.14,118.15,149.64,163.82,161.05,125.83,100)/100
CYP2A6 <- ifelse(AGE_vector<=1,1*AGE_vector**5.68/(0.21**5.68+AGE_vector**5.68),1)
CYP2B6 <- ifelse(AGE_vector<=16,(1.1-
0.15)*AGE_vector**1/(2**1+AGE_vector**1)+0.15,1)
CYP2C8 <- ifelse(AGE_vector<=2,(1-0.3)*AGE_vector**1/(0.02**1+AGE_vector**1)+0.3,1)
CYP2C9 <- ifelse(AGE_vector<=3,(0.98-
0.17)*AGE_vector**0.53/(0.0157**0.53+AGE_vector**0.53)+0.17,1)
CYP2C18_19 <- ifelse(AGE_vector<=5,(0.98-
0.3)*AGE_vector**2.44/(0.29**2.44+AGE_vector**2.44)+0.3,1)
CYP2D6 <- ifelse(AGE_vector<=10,(1-
0.036)*AGE_vector**1/(0.1**1+AGE_vector**1)+0.036,1)
CYP2E1 <- ifelse(AGE_vector<=18,0.99*AGE_vector**0.5/(0.23**0.5+AGE_vector**0.5),1)
CYP3A4_5 <- ifelse(AGE_vector<=25,(1.06-
0.11)*AGE_vector**1.91/(0.64**1.91+AGE_vector**1.91)+0.11,1)
UGT1A1 <- ifelse(AGE_vector<=1,(1.064-
0.0015)*AGE_vector**2.07/(0.154**2.07+AGE_vector**2.07)+0.0015,1)
UGT1A4 <- 0.7354 + AGE_vector*0.0157
UGT1A6 <- ifelse(AGE_vector<=15,(1.025-
0.142)*AGE_vector**0.97/(0.411**0.97+AGE_vector**0.97)+0.142,1)
UGT1A9 <- ifelse(AGE_vector<=15,(1.041-
0.086)*AGE_vector**1.2/(1.16**1.2+AGE_vector**1.2)+0.086,1)
UGT2B7 <- 0.0846 + AGE_vector*0.0472
SULT1A1 <- c(100,100,100,100,100,100,100,100)/100
Isoenzyme_Ontogeny <-
data.frame(rbind(CYP1A2,CYP2A6,CYP2B6,CYP2C8,CYP2C9,CYP2C18_19,CYP2D6,
CYP2E1,CYP3A4_5,UGT1A1,UGT1A4,UGT1A6,UGT1A9,UGT2B7,SULT1A1))
names(Isoenzyme_Ontogeny) <- AGE_vector

# All isoenzymes are mature in adults
Isoenzyme_Ontogeny[,8] <- 1
```

```
# Selection of a specific iosenzyme A (IA), the value corresponds to the row number of the relevant isoenzyme in the table Isoenzyme_Ontogeny. 1 for instance selects CYP1A2
IsoenzymeA_index <- 1

# Selection of a specific iosenzyme B (IB), the value corresponds to the row number of the relevant isoenzyme in the table Isoenzyme_Ontogeny. 2 for instance selects CYP2A6
IsoenzymeB_index <- 2

# IOA: isoenzyme ontogeny value for a specific isoenzyme A (IA) and age, expressed as the pediatric to adult CLintmicA (CLintmic due to IA) ratio. In adults, IOA=1 (IA mature in adults)
IOA <- Isoenzyme_Ontogeny[IsoenzymeA_index,Age_index]

# IOB: isoenzyme ontogeny value for a specific isoenzyme B (IB) and age, expressed as the pediatric to adult CLintmicB (CLintmic due to IB) ratio. In adults, IOB=1 (IB mature in adults)
IOB <- Isoenzyme_Ontogeny[IsoenzymeB_index,Age_index]


################################################################################
################### Drug and system-specific parameters ####################
################################################################################

####################### Unbound drug fraction in plasma (fu) ###################
nKa_HSA <- (1/fu_adult-1)/HSA_adult
fu_HSA <- 1/(1+nKa_HSA*HSA)
# nKa_HSA: drug affinity to HSA dervied from the adult unbound drug fraction in plasma (fu_adult) and HSA concentration in adults (HSA_adult) using the equations by Rodgers and Rowland
# fu_adult: unbound plasmatic drug fraction in adults (identical between HSA bound drugs and AAG bound drugs in the simulations, considered as a drug_specific parameter)
# HSA_adult and HSA: human serum albumin (HSA) concentration in adult and for a specific post-natal age respectively (g/L). HSA changes with age.
# fu_HSA: unbound drug fraction for drugs binding to HSA for a specific typical individual
nKa_AAG <- (1/fu_adult-1)/AAG_adult
fu_AAG<- 1/(1+nKa_AAG*AAG)
# nKa_AAG: drug affinity to AAG dervied from the adult unbound drug fraction in plasma (fu_adult) and AAG concentration in adults (AAG_adult) using the equations by Rodgers and Rowland
# fu_adult: unbound plasmatic drug fraction in adults (identical between HSA bound drugs and AAG bound drugs in the simulations, considered as a drug_specific parameter)
# AAG_adult and AAG_pediatric: alpha-1 acid glycoprotein (AAG) concentration in adult and and for a specific post-natal age respectively (g/L). AAG changes with age.
# fu_AAG: unbound drug fraction for drugs binding to AAG for a specific typical individual


############################ Blood to plasma ratio (BP) ########################
# B:P for drugs binding to HSA
BP_HSA <- 1+(Hematocrit*(fu_HSA*Kp-1))

# B:P for drugs binding to AAG
BP_AAG <- 1+(Hematocrit*(fu_AAG*Kp-1))
# Hematocrit is the hematocrit for a specific age (age dependent)
```

```
# Kp is the blood to plasma partition coefficient (drug-specific property)


################### Total intrinsic metabolic clearance in the liver ##################
################### based on unbound drug concentration (CLint)###################

### CLint (L/min)

CLint_function <- function(CLintmictotal_adult,BSA,AGE,IOA,IOB,fmA_adult){

# LIVER_VOLUME: liver volume (L), dependent on BSA
LIVER_VOLUME <- 0.722 * BSA**1.176

# LIVER_DENSITY: Liver density (g/L), identical for all ages
LIVER_DENSITY <- 1080

# LIVERWT: liver weight  (g)
LIVERWT <- LIVER_VOLUME * LIVER_DENSITY
# CLint: total intrinsic metabolic clearance in the liver based on unbound drug concentration
(L/min)

CLint <- (CLintmictotal_adult*fmA_adult*IOA+CLintmictotal_adult*(1-fmA_adult)*IOB) *
LIVERWT*MPPGL

CLint
}

# CLint: total intrinsic metabolic clearance in the liver based on unbound drug concentration
(L/min). CLint is a function of CLintumictotal_adult, BSA, AGE, IOA, IOB and fmA_adult

CLint <- CLint_function(CLintmictotal_adult,BSA,AGE,IOA,IOB,fmA_adult)

# CLintumictotal_adult: adult total unbound intrinsic microsomal clearance (L/min/mg
microsome)
# BSA: bodysurface area (square meters)
# AGE: post natale age (years)
# IOA: isoenzyme ontogeny value for a specific isoenzyme A (IA) and age, expressed as the
pediatric to adult CLintmicA (CLintmic due to IA) ratio. In adults, IOA=1 (IA mature in adults)
# IOB: isoenzyme ontogeny value for a specific isoenzyme B (IB) and age, expressed as the
pediatric to adult CLintmicB (CLintmic due to IB) ratio. In adults, IOB=1 (IB mature in adults)
# fmA_adult: fraction of the drug metabolized by IA. For drugs metabolized by one
isoennzyme,fmA_adult = 100%
# (1-fmA_adult): fraction of the drug metabolized by IB (fmB_adult). For drugs metabolized by
one isoennzyme,fmB_adult = 0%


##########################################################################
#################### Plasma clearance and extraction ratio ###################
##########################################################################

### Overall total (bound and unbound) hepatic metabolic plasma clearance (CLp) based on the
dispersion model, with a dispersion number (Dn) of 0.17
```

```
dispersionmodelCLp <- function(CLint,fu,BP,QH){
Rn <- fu*CLint/BP/QH
Dn <- 0.17
a <- sqrt(1+4*Rn*Dn)
CLp <- (QH*(1-(4*a/((1+a)**2*exp((a-1)/(2*Dn))-(1-a)**2*exp(-(a+1)/(2*Dn))))))*BP
CLp
}


#### Extraction ratio (ER) based on the dispersion model, with a dispersion number (Dn) of 0.17

dispersionmodelER <- function(CLint,fu,BP,QH){
Rn <- fu*CLint/BP/QH
Dn <- 0.17
a <- sqrt(1+4*Rn*Dn)
ER <- 1-(4*a/((1+a)**2*exp((a-1)/(2*Dn))-(1-a)**2*exp(-(a+1)/(2*Dn))))
ER
}

# CLp for HSA bound drugs
CLp_HSA <- dispersionmodelCLp(CLint,fu_HSA,BP_HSA,QH)

# CLp for AAG bound drugs
CLp_AAG <- dispersionmodelCLp(CLint,fu_AAG,BP_HSA,QH)

# ER for HSA bound drugs
ER_HSA <- dispersionmodelER(CLint,fu_HSA,BP_HSA,QH)

# CLp for AAG bound drugs
ER_AAG <- dispersionmodelER(CLint,fu_AAG,BP_HSA,QH)


### Total (bound and unbound) hepatic metabolic plasma clearance due to isoenzyme A (CLpA)

# CLpA for HSA bound drugs
CLpA_HSA <- CLp_HSA*fmA_adult*IOA/(fmA_adult*IOA+((1-fmA_adult)*IOB))

# CLpA for AAG bound drugs
CLpA_AAG <- CLp_AAG*fmA_adult*IOA/(fmA_adult*IOA+((1-fmA_adult)*IOB))

# fmA_adult*IOA/(fmA_adult*IOA+((1-fmA_adult)*IOB)) corresponds to the fmA of the
selected typical individual
```